NASA/TM—2013-216610

Investigation of Sideband Index Response to Prototype Gear Tooth Damage

Paula J. Dempsey
Glenn Research Center, Cleveland, Ohio

November 2013

NASA STI Program . . . in Profile

Since its founding, NASA has been dedicated to the advancement of aeronautics and space science. The NASA Scientific and Technical Information (STI) program plays a key part in helping NASA maintain this important role.

The NASA STI Program operates under the auspices of the Agency Chief Information Officer. It collects, organizes, provides for archiving, and disseminates NASA's STI. The NASA STI program provides access to the NASA Aeronautics and Space Database and its public interface, the NASA Technical Reports Server, thus providing one of the largest collections of aeronautical and space science STI in the world. Results are published in both non-NASA channels and by NASA in the NASA STI Report Series, which includes the following report types:

- TECHNICAL PUBLICATION. Reports of completed research or a major significant phase of research that present the results of NASA programs and include extensive data or theoretical analysis. Includes compilations of significant scientific and technical data and information deemed to be of continuing reference value. NASA counterpart of peer-reviewed formal professional papers but has less stringent limitations on manuscript length and extent of graphic presentations.

- TECHNICAL MEMORANDUM. Scientific and technical findings that are preliminary or of specialized interest, e.g., quick release reports, working papers, and bibliographies that contain minimal annotation. Does not contain extensive analysis.

- CONTRACTOR REPORT. Scientific and technical findings by NASA-sponsored contractors and grantees.

- CONFERENCE PUBLICATION. Collected papers from scientific and technical conferences, symposia, seminars, or other meetings sponsored or cosponsored by NASA.

- SPECIAL PUBLICATION. Scientific, technical, or historical information from NASA programs, projects, and missions, often concerned with subjects having substantial public interest.

- TECHNICAL TRANSLATION. English-language translations of foreign scientific and technical material pertinent to NASA's mission.

Specialized services also include creating custom thesauri, building customized databases, organizing and publishing research results.

For more information about the NASA STI program, see the following:

- Access the NASA STI program home page at *http://www.sti.nasa.gov*

- E-mail your question to *help@sti.nasa.gov*

- Fax your question to the NASA STI Information Desk at 443–757–5803

- Phone the NASA STI Information Desk at 443–757–5802

- Write to:
  STI Information Desk
  NASA Center for AeroSpace Information
  7115 Standard Drive
  Hanover, MD 21076–1320

NASA/TM—2013-216610

Investigation of Sideband Index Response to Prototype Gear Tooth Damage

Paula J. Dempsey
Glenn Research Center, Cleveland, Ohio

National Aeronautics and
Space Administration

Glenn Research Center
Cleveland, Ohio 44135

November 2013

Acknowledgments

The author would like to thank the NASA Rotary Wing Project and Traci Stadtmueller and Paul Swindell of the FAA Technical Center for their assistance and support of this work.

This work was sponsored by the Fundamental Aeronautics Program at the NASA Glenn Research Center.

Level of Review: This material has been technically reviewed by technical management.

Available from

NASA Center for Aerospace Information
7115 Standard Drive
Hanover, MD 21076–1320

National Technical Information Service
5301 Shawnee Road
Alexandria, VA 22312

Available electronically at http://www.sti.nasa.gov

Investigation of Sideband Index Response to Prototype Gear Tooth Damage

Paula J. Dempsey
National Aeronautics and Space Administration
Glenn Research Center
Cleveland, Ohio 44135

Abstract

The objective of this analysis was to evaluate the ability of gear condition indicators (CI) to detect contact fatigue damage on spiral bevel gear teeth. Tests were performed in the NASA Glenn Spiral Bevel Gear Fatigue Rig on eight prototype gear sets (pinion/gear). Damage was initiated and progressed on the gear and pinion teeth. Vibration data was measured during damage progression at varying torque values while varying damage modes to the gear teeth were observed and documented with inspection photos. Sideband indexes (SI) and root mean square (RMS) CIs were calculated from the time synchronous averaged vibration data. Results found that both CIs respond differently to varying torque levels, damage levels and damage modes.

Background

Helicopter transmission health is important because helicopters depend on the power train for transmission of torque required for lift and flight maneuvering. Health Usage Monitoring Systems (HUMS) capable of predicting impending transmission component failure for "on-condition" maintenance have the potential to decrease operating and maintenance costs and increase safety and aircraft availability. "On-condition" refers to replacing time-based maintenance intervals with planned maintenance when HUMS "condition indicators" indicate decreased system performance. These HUMS "condition indicators" (CI) are typically vibration signatures or trends that develop when a fault occurs on a component and interacts with its operational environment. The CI must be correlated to a known failure mode to reliably detect the health of the system.

A "seeded fault test," in support of a rotorcraft condition based maintenance program (CBM), is an experiment in which a component is tested with a known fault while health monitoring data is collected. These tests are performed at operating conditions comparable to operating conditions the component would be exposed to while installed on the aircraft. Performance of seeded fault tests is one method used to provide evidence that a HUMS can replace current maintenance practices required for "on-condition" maintenance.

Previous analyses were performed on rotorcraft spiral bevel gear condition indicator performance in support of the U.S. Army's Condition-Based Maintenance (CBM) program (Refs. 1 and 2). CI performance was evaluated using helicopter datasets recorded when damage occurred on spiral bevel gear (pinion/gear) teeth. The type of damage was also tied to available Army Tear-Down Analyses in which tooth damage was documented through descriptions and photographs. The CI referred to as SI performed the best at detecting contact fatigue failure modes.

The objective of this analysis was to gain a better understanding why gear vibration based CI trend with damage under some conditions and poorly for others. The focused objective was to evaluate the ability of the gear CI, sideband index, to detect contact fatigue damage on spiral bevel gear teeth of prototype gears. A second objective was to study the trends of the RMS CI as a function of the condition of the gears and operating conditions of the test rig. A third objective was to use the results of these tests to define analyses to be applied to tests of the gear final design. Tests were performed in the

NASA Glenn Spiral Bevel Gear Fatigue Rig. The eight gear sets (pinion/gear) tested during four tests and evaluated within this analysis were prototypes of 42 newly designed spiral bevel gears. The results of these initial tests will be used to define analysis methods for the remaining 42 tests.

Test Facility

Tests were performed in the Spiral Bevel Gear Test Rig at NASA Glenn Research Center. A detailed description of this test facility can be found in References 3 and 4. The Spiral Bevel Gear Fatigue Rig is illustrated in Figure 1. In addition to developing gear health monitoring tools, the test facility has been used to study the effects of gear material, gear tooth design, and lubrication on the fatigue strength of gears. Two sets of spiral bevel gears are installed in the test rig and tested simultaneously. Facing the gearboxes per Figure 1, the left gear set (pinion/gear) is referenced as left and the right gear set (pinion/gear) is referenced as right within the paper.

Figure 2 shows the cross-sectional view of the rig. The facility operates in a closed-loop arrangement where the load is locked into the loop via a split shaft and a thrust piston on the slave side of the rig. This forces a helical gear into mesh per Figure 2. Rotation is obtained using a drive motor connected through v-belts to the helical gear. The spiral bevel gears on the left side operate where the pinion drives the gear. The right side of the facility acts as a speed increaser where the gear drives the pinion. The concave side of the pinion is always in contact with the convex side of the gear on both the left and right side of the gearbox. Load and speed are monitored by torque and speed sensors.

Data Acquisition and Instrumentation

Vibration data was collected using accelerometers mounted on the left and right housing of the test rig. Further studies, outside the scope of this paper, are underway relating transfer paths between the gear mesh and accelerometer locations (Ref. 5). Data was collected at sample rates that provided sufficient vibration data for calculating time synchronous averaged data (TSA). TSA refers to techniques for averaging vibration signals over several revolutions of the shaft, in the time domain, to improve signal-to-noise ratio (Ref. 6). Using a once per revolution signal, the vibration signal is interpolated into a fixed number of points per shaft revolution. Signals synchronous with the shaft speed, will intensify relative to the non-periodic signals.

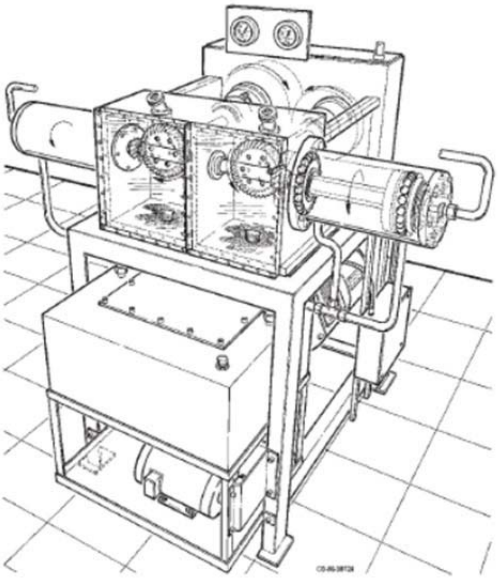

Figure 1.—Spiral bevel gear fatigue rig.

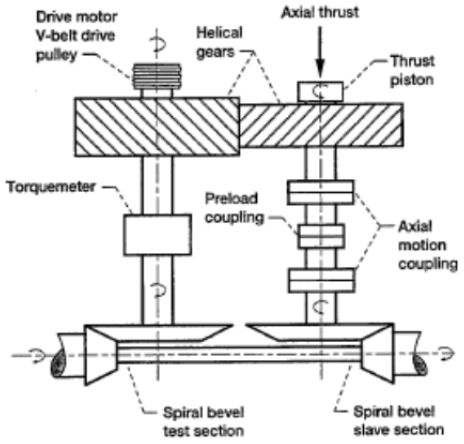

Figure 2.—Cross section of spiral bevel gear fatigue rig.

Since helicopter gears generate vibration signals synchronous with speed, all helicopter gear condition indicators are calculated from TSA data. Gear vibration condition indicators are indexes calculated from vibration signal information. Many are based on statistical measurements of vibration energy. Signal processing techniques used to extract useful information to calculate a gear CI from the vibration signal are discussed in detail in Reference 7. Some gear CI's are calculated from the time domain TSA signal, such as RMS. Some are calculated from the TSA converted to the frequency domain, such as SI. Some convert the TSA signal to the frequency domain, filter specific frequencies, convert it back to the time domain, then calculate a statistical parameter from this data with examples shown in References 6 to 8.

Figure 3 illustrates the information used to calculate the TSA for the right gear and pinion. Using the sample rate of 200 KHz for 1 sec duration and the speed of both shafts, the number of TSA averages for each acquisition is determined. Each average consists of 1 revolution of the shaft. Each average is made up of the number of linearly interpolated points rounded down to a power of two. A power of two is used because it eases the future use of the Fast Fourier Transform (FFT) to transform the time domain signal for the time domain to the frequency domain. Per Figure 3, the top figure displays the right accelerometer data sampled for one second at 200,000 samples/second. The green and blue lines are pulses from the gear and pinion 1/rev signal measured for each shaft rotation during this one second period. Only the right accelerometer is plotted in the next figure with an expanded y-axis scale. The two lowest plots are the TSA signal calculated from the 1/rev and vibration data for the right gear and pinion. Pulses from the 41 tooth gear and the 19 tooth pinion can easily be seen within these two plots.

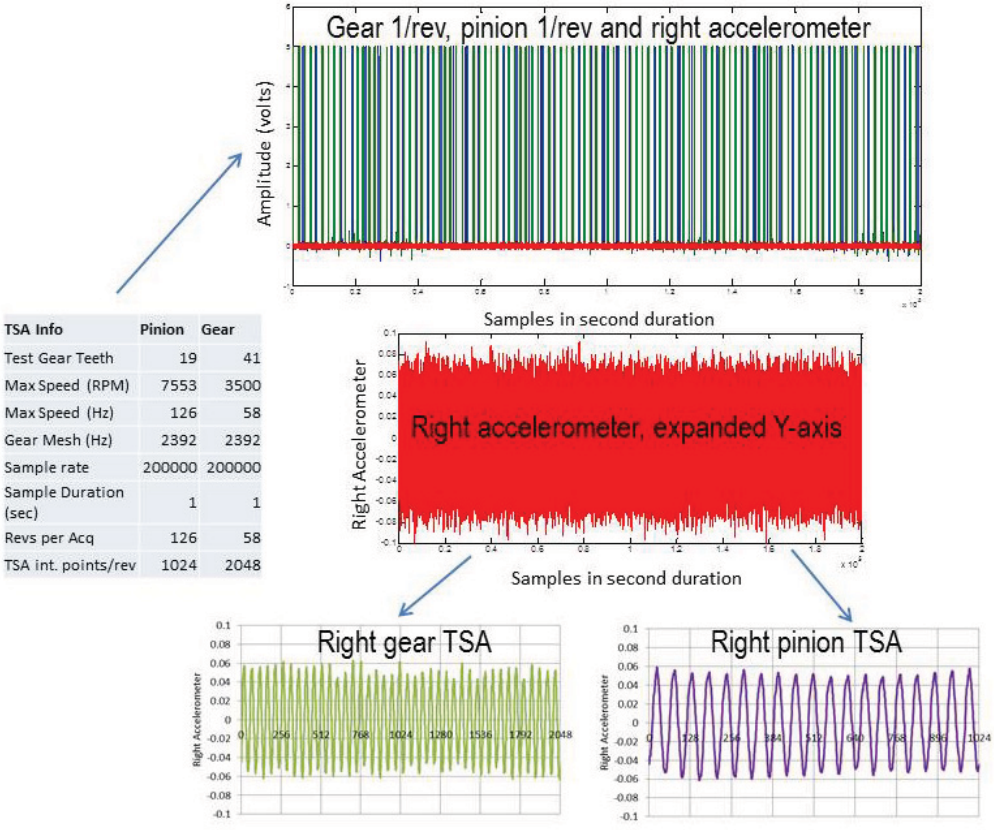

TSA Info	Pinion	Gear
Test Gear Teeth	19	41
Max Speed (RPM)	7553	3500
Max Speed (Hz)	126	58
Gear Mesh (Hz)	2392	2392
Sample rate	200000	200000
Sample Duration (sec)	1	1
Revs per Acq	126	58
TSA int. points/rev	1024	2048

Figure 3.—Information used to calculate TSA.

During these tests, three data acquisition systems were used. Vibration, oil debris, torque and speed data were collected once every minute with the NASA Glenn research data acquisition system, referred to as Mechanical Diagnostic System Software (MDSS). Vibration and speed data were collected from a second set of sensors with a helicopter Health Usage Monitoring System referred to as Modern Signal Processing Unit (MSPU). Operational parameters were collected with a third system referred to as Daytronic. These operational parameters included torque, speed, right and left gearbox oil inlet and outlet temperatures and oil system pressures.

Turbine engine oil that meets DOD-L-87354 specifications is used in the test rig. Both gear sets are lubricated with oil jets pumped from an oil reservoir. The lubrication from the gearbox then exits the gearbox and flows through an inductance type in-line oil debris sensor then past a magnetic chip detector. A strainer and a three micron filter are located downstream of the oil debris (OD) sensor to capture any debris before returning to the sensor and gearbox.

A non-contact rotary transformer shaft mounted torque sensor was used to measure torque during testing. Thermocouples were used to measure inlet and outlet oil temperatures. The inductance type oil debris sensor was used to measure the debris generated during fatigue damage to the gear teeth. For the sensor, the MDSS records the particle counts measured by the oil debris sensor, their approximate size and an approximate mass. The sensor measures the number of particles and their approximate size based on user defined particle size ranges or bins. Based on the bin configuration, the average particle size for each bin is used to calculate the cumulative mass for the experiment by assuming the average particle size as a diameter spherical in shape and multiplying it by the density of steel. Chip indications from the chip detector, when the gap was closed with debris, were also measured.

For the MDSS system, accelerometers were installed on the right and left side of the test rig housing. Accelerometer frequency range is 0.7 to 20 KHz with a resonant frequency of ≥70 KHz. The MDSS accelerometers were mounted on the housing, radially and vertically with respect to the pinion, as shown in Figure 4. Facing the gearboxes, the left gear set (pinion/gear) and right gear set (pinion/gear) accelerometers were referenced as such in the MDSS system. Speed was measured with optical tachometers mounted on the left pinion shaft and right gear shaft to produce a separate once-per-rev tach pulse for the pinion and gears. Time synchronous averaging of the vibration data collected from the left and right accelerometer is performed in the MDSS system for the pinions via the pinion tach pulse and the gears via the gear tach pulse.

For the MSPU system, accelerometers are also installed on the right and left side of the test rig. Accelerometer frequency range is 0.5 to 5 KHz with a resonant frequency of 26 KHz. A magnetic tachometer is installed on the right pinion and measures pinion pulses per tooth pass. This is used to calculate the TSA for both the pinion and the gear. The gear ratio is used to process the data at the correct speed for the gear.

For the first test, the MSPU accelerometers were mounted on the housing, axially and horizontally with respect to the pinion. At completion of the test it was determined that this location had a poor response to the gear mesh vibration signatures through analysis of the TSA data. For the remaining three tests, the accelerometers were mounted on the housing, in close proximity to the MDSS accelerometers, radially and vertically with respect to the pinion, as shown in Figure 4. The TSA data had a good response to the gear mesh vibration and correlated well with the MDSS data at this location. The thrust and tangential forces at the mesh of the spiral bevel gear design were also calculated from the gear set operating conditions and found the tangential force in the radial direction significantly larger than the thrust force in the radial direction indicating a larger amplitude in the radial vertical orientation. This is illustrated in Figure 4.

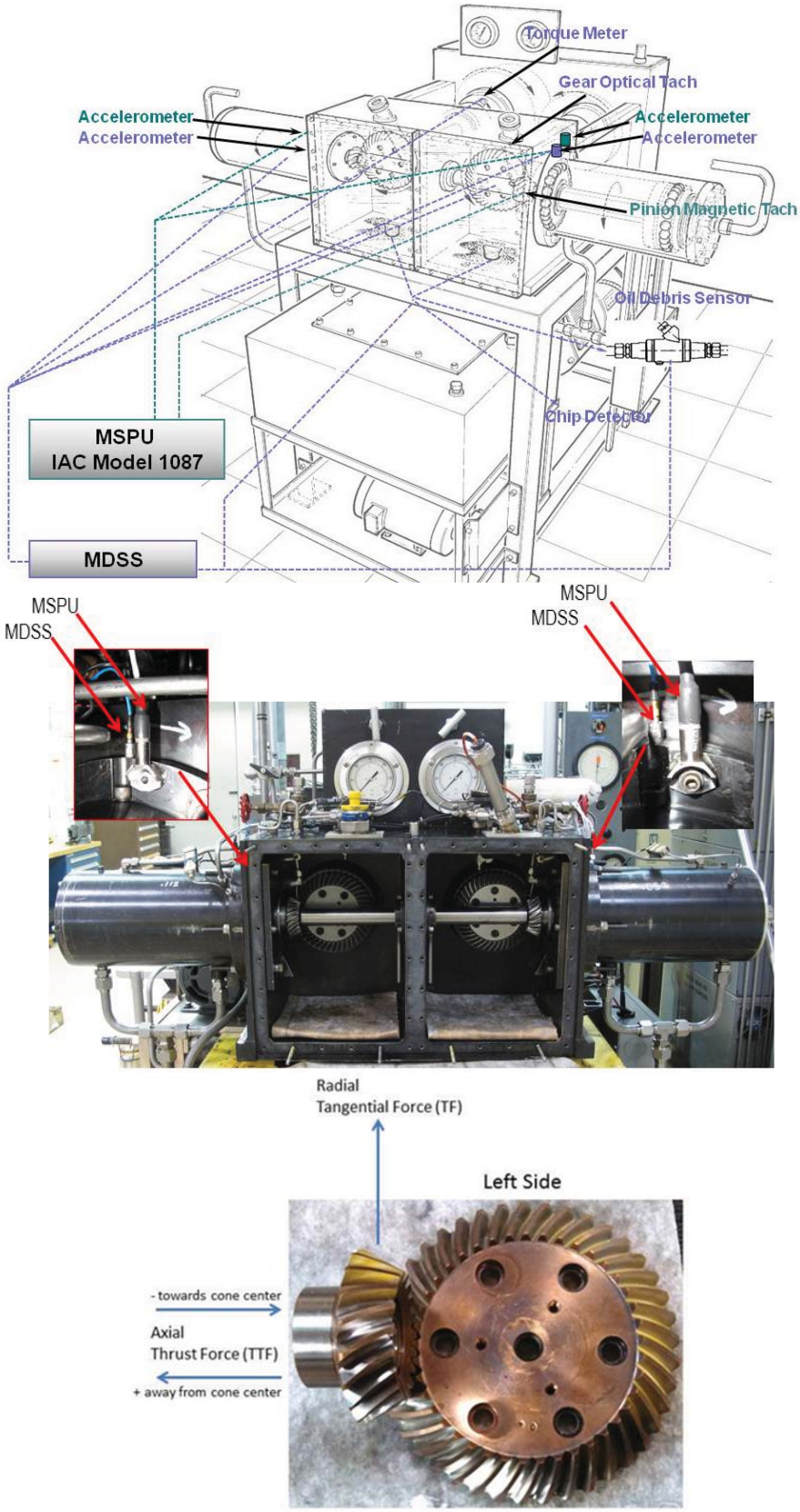

Figure 4.—Location of accelerometers.

Test Gear Sets

The gears tested were prototypes of gears designed and specified to represent a rotorcraft drive system gear mesh and fit within the space available in the spiral bevel gear fatigue rig gearboxes. The gears were made from a steel alloy CEVM 9310, carburized, hardened and ground. However, the eight gear sets tested differed from the final design in that they were not shot peened and the surface roughness varied. The surface roughness on the pinions tested ranged from 11 to 15 μin. and the surface roughness on the gears tested ranged from 26 to 35 μin. In addition, two of the sets tested, referred to as test 1, had pinion teeth slightly thicker than the final design due to incorrectly performing the final grind on the sets per the soft tooth finish. The other six sets tested also differed from the final design in that copper plating used for masking parts of the gear during carburization was not removed from the edge of the gear teeth and the edges were not broken to design specifications.

The prototype gear sets tested have 6.4 in. diametral pitch, 20° pressure angle, 25° spiral angle, 0.94 in. face width and 2.15 gear ratio. The gears have 41 teeth and the pinions have 19 teeth. The test gears were designed to operate at a gear speed of 3500 rpm and torque of 8000 in.-lbs, pinion speed of 7553 rpm and torque of 3707 in.-lbs and 240 to 265 °F inlet oil temperatures with an American Gear Manufacturers Association (AGMA) calculated contact stress of 237 ksi.

Test Description

For this study, eight gear sets were tested at a gear speed of 3500 rpm and pinion speed of 7553 rpm, except for the run-in of the test 1 gear set. Gear torque varied from 4000 to 8000 in.-lbs and pinion torque varied from 1854 to 3707 in.-lbs. At the start of each test, a run-in was performed for a minimum of 1 hr at 4000 in.-lbs gear torque/3500 rpm gear speed and 1854 in.-lbs pinion torque/7553 rpm pinion speed. Contact cycles accumulated at a rate of 210,000 per hour for the gear and 453,180 per hour for the pinion. At completion of the run-in, inspection photos were taken of the left and right gear and pinion teeth. Inspection photos were then taken throughout the test to document damage progression to the gear teeth.

The failure modes to be investigated for this study were defined by class (contact fatigue), general mode (macro pitting) and degree (progressive) per American Gear Manufacturers Association (AGMA) standards for gear wear terminology outlined in Reference 9. However, additional failure modes were observed during each test. Using Reference 9 for tooth damage terminology, a numbering scheme per Reference 1 was developed to streamline the identification of gear damage. Table 1 illustrates this numbering scheme for the types of damage observed during these tests. Tables 2 to 5 summarize the observed failure modes observed on the gear teeth during each inspection interval. Note that the 3rd column in the tables labeled “MDSS Rdg (min)” is the time in operation of the rig in minutes.

TABLE 1.—NUMBERING SCHEME FOR NOMENCLATURE OF GEAR FAILURE MODES (REF. 1)

Class	General Mode	Specific Mode or Degree
2.0 Scuffing	2.1 Scuffing	2.1.1 Mild
		2.1.2 Moderate
		2.1.3 Severe
4.0 Contact Fatigue	4.1 Subcase Fatigue	
	4.2 Micropitting	
	4.3 Macropitting	4.3.1 Initial
		4.3.2 Progressive
		4.3.3 Flake
		4.3.4 Spall
6.0 Fracture	6.0 Fracture	

TABLE 2.—FAILURE MODES DURING TEST 1

Test LWW9_RXX10		MDSS					
	Date	Rdg(Min)	Torque	Gear Left	Pinion Left	Gear Right	Pinion Right
Start	12/14/2011	0	0				
Run-in	12/14/2011	60	4000				
Inspection	12/14/2011	186	4000				
Inspection	12/14/2011	269	8000				4.2 at, 2.1.2 at
Inspection	12/15/2012	553	8000		4.3.1 1t	4.2 at	4.2 at, 2.1.2 at
Inspection	12/20/2011	1862	8000		4.3.1 1t, 4.3.4 1t, 4.2 at	4.2 at, 2.1.2 at, 6.0 at et	4.2 at, 2.1.2 at
Inspection	12/23/2011	4814	8000	4.3.4 3t	4.3.4 2t, 4.2 at	4.2 at, 2.1.2 at, 6.0 at et	4.2 at, 2.1.2 at*
Inspection	1/10/2012	6065	8000	4.3.4 5t, 4.3.2 3t	4.3.4 2t, 4.3.2 2t, 4.2 at	4.2 at, 4.3.1/4.3.4 19t, 6.0 at et	4.3.1 6t, 4.3.2/4.3.4 3t*
Key: xt=number of teeth; at=all teeth; et=edges of teeth; *=add preceding damage to inspection interval							

TABLE 3.—FAILURE MODES DURING TEST 2

Test L0505R0606		MDSS					
	Date	Rdg(Min)	Torque	Gear Left	Pinion Left	Gear Right	Pinion Right
Start	9/4/2012	0	0				
Run-in	9/4/2012	60	4000				
Inspection	9/4/2012	108	4000				
	9/14/2012	202	4000				
Inspection	9/14/2012	379	8000	6.0 at et	4.2 2t	6.0 at et, 2.1.2 at	4.2 at, 2.1.3 at
	9/18/2012	468	4000				
Inspection	9/18/2012	559	8000	6.0 at et	4.3.2 3t, 4.3.4 2t	6.0 at et, 2.1.2 at	4.2 at, 2.1.3 at
	9/19/2012	632	4000				
Inspection	9/19/2012	662	8000	6.0 at et	4.3.4 5t	6.0 at et, 2.1.2 at	4.2 at, 2.1.3 at
Key: xt=number of teeth; at=all teeth; et=edges of teeth							

TABLE 4.—FAILURE MODES DURING TEST 3

Test L0701R0802		MDSS					
	Date	Rdg(Min)	Torque	Gear Left	Pinion Left	Gear Right	Pinion Right
Start	11/27/2012	0	4000				
Run-in	11/27/2012	69	4000				
Inspection	11/27/2012	184	6000	6.0 at et			
	11/28/2012	367	6000				
Inspection	11/28/2012	520	8000	6.0 at et	4.3.2 at	6.0 at et, 2.1.2 at	6.0 at et, 2.1.2 at, 4.3.4 1t
Inspection	11/29/2012	686	8000	6.0 at et	4.3.2 at, 4.3.4 1t	6.0 at et, 2.1.2 at	6.0 at et, 2.1.2 at, 4.3.4 5t, 4.3.2 4t
Key: xt=number of teeth; at=all teeth; et=edges of teeth							

TABLE 5.—FAILURE MODES DURING TEST 4

TestL1103R1204		MDSS					
	Date	Rdg(Min)	Torque	Gear Left	Pinion Left	Gear Right	Pinion Right
Start	12/4/2012	0	4000				
Run-in	12/4/2012	60	4000				
Inspection	12/5/2012	489	6000	6.0 at et		6.0 at et, 2.1.2 at	4.3.1 at, 2.1.2 at
Inspection	12/6/2012	901	6000	6.0 at et	6.0 at et, 4.3.1 at	6.0 at et, 2.1.2 at	4.3.1 at, 2.1.2 at
Inspection	12/7/2012	1196	6000	6.0 at et	6.0 at et, 4.3.1 at	6.0 at et, 2.1.2 at	4.3.1 at, 2.1.2 at
Inspection	12/10/2012	1829	6000	6.0 at et	6.0 at et, 4.3.1 at	6.0 at et, 2.1.2 at	4.3.1 at, 2.1.2 at
Inspection	12/13/2012	4034	6000	6.0 at et, 4.3.4 5t, 4.3.2 6t	6.0 at et, 4.3.1 at	6.0 at et, 2.1.2 at	4.3.1 at, 2.1.2 at
Key: xt=number of teeth; at=all teeth; et=edges of teeth							

The tests ran until macro pitting/spalling (4.3.4) larger than one mm in diameter covered a significant area of two or more gear or pinion tooth surfaces. Definitions for pitting modes per Reference 9 are summarized as follows:

- Initial—Pits less than 1 mm in diameter in localized areas removing high asperities.
- Progressive—Pits in different shapes/sizes greater than 1 mm in diameter covering a large area of the tooth contact surface.
- Flake—Pits that are shallow but cover large areas that consist of thin flakes.
- Spalling—Progressive pitting where smaller pits combine to form irregular craters that cover an area of the tooth contact surface that exceeds progressive pitting.

Since the focus for this analysis was CI performance when macro pitting/spalling was observed, this type of failure mode is highlighted in green in Tables 2 to 5. Other common failure modes observed for the four tests are also highlighted with the same color within each table.

The reader should note that damage mode 6.0, fracture, was a failure mode observed due to the prototype gear design. In the prototype design, the edges of the teeth were not broken per design specifications and the copper masking was left on the edge of the teeth. This caused copper edges to fracture during testing. Since the oil debris sensor does not measure non-ferrous particles, this type of debris was not measured by the sensor.

Due to the storage limitation of the MSPU system, data could only be recorded automatically every 30 min during testing. Manual acquisitions were also performed periodically throughout the test. Sometimes, the system recorded the data for the pinion and did not record the data for the gear when manual acquisitions were performed due to storage and speed limitations. Since the timestamps and frequency of the data acquisition varied with both systems, the inspection intervals were used to correlate the time periods between both systems. Tables 6 to 9 list the MSPU reading that corresponds with the MDSS reading. Note the Index(in) refers to the pinion and the Index(out) refers to the gear.

TABLE 6.—MSPU INDEXED TO MDSS FOR TEST 1

LWW9_RXX10		MDSS	MSPU		
	Date	Rdg(Min)	Index(in)	Index(out)	Torque
Start	12/14/2011	0			0
Run-in	12/14/2011	60	1	1	4000
Inspection	12/14/2011	186	10	3	4000
Inspection	12/14/2011	269	17	10	8000
Inspection	12/15/2012	553	30	23	8000
Inspection	12/20/2011	1862	82	75	8000
Inspection	12/23/2011	4814	200	193	8000
Inspection	1/10/2012	6065	221	213	8000

TABLE 7.—MSPU INDEXED TO MDSS FOR TEST 2

L0505R0606		MDSS	MSPU		
	Date	Rdg(Min)	Index(in)	Index(out)	Torque
Start	9/4/2012	0			0
Run-in	9/4/2012	60	10	10	4000
Inspection	9/4/2012	108	12	12	4000
	9/14/2012	202	21	21	4000
Inspection	9/14/2012	379	32	32	8000
	9/18/2012	468	40	40	4000
Inspection	9/18/2012	559	49	49	8000
	9/19/2012	632	56	56	4000
Inspection	9/19/2012	662	59	59	8000

TABLE 8.—MSPU INDEXED TO MDSS FOR TEST 3

L0701R0802		MDSS	MSPU		
	Date	Rdg(Min)	Index(in)	Index(out)	Torque
Start	11/27/2012	0			4000
Run-in	11/27/2012	69	4	3	4000
Inspection	11/27/2012	184	13	12	6000
	11/28/2012	367	27	26	6000
Inspection	11/28/2012	520	37	36	8000
Inspection	11/29/2012	686	46	45	8000

TABLE 9.—MSPU INDEXED TO MDSS FOR TEST 4

L1103R1204		MDSS	MSPU		
	Date	Rdg(Min)	Index(in)	Index(out)	Torque
Start	12/4/2012	0			4000
Run-in	12/4/2012	60	2	2	4000
Inspection	12/5/2012	489	31	31	6000
Inspection	12/6/2012	901	54	54	6000
Inspection	12/7/2012	1196	69	69	6000
Inspection	12/10/2012	1829	100	100	6000
Inspection	12/13/2012	4034	188	188	6000

Analysis of Test Operational Conditions

When detecting rotorcraft component damage, a data driven approach is traditionally used to identify damage within the transmission. Data from "healthy" transmission components are used to define healthy vibration signatures. Significant changes in these or signatures comparable to those historically measured on damaged components are used to indicate damage. A model based approach for assessment of CI response to damage has an advantage in that it does not require validation data from all types and modes of damage. Randall (Ref. 10) presented a model based on changes of the gear vibration signature caused by changes in the tooth profile caused by tooth wear or damage. He noted measuring gear mesh signatures at the same load due sensitivities of the signature to changes in the tooth profile caused by its deflection under load. To date, a model based approach has not been implemented. This is mainly due to the dynamic characteristics unique to each system, under varying operational conditions that can affect CI response (Ref. 11).

Typically, within a helicopter HUMS system, the CI and operational data are acquired, stored, tracked, trended and monitored separately (Ref. 12). Limited work has been performed evaluating gear CI performance under varying load, speed and operational conditions (Refs. 13 to 17). Passing key information between both systems and integrating this information can improve the performance and reliability of both systems to indicate progression of damage and remaining time in operation.

Operational parameters were collected during testing and are included within this discussion. Gear speed of 3500 rpm was maintained for each test. Torque was maintained at 3 levels: 4000, 6000, and 8000 in.-lbs. Inlet oil temperatures ranged from 183 to 225 °F, oil jet inlet temperatures ranged from 38 to 79 psi. Often, the vibration signatures respond to significant changes in conditions. Although a complete data set of all the varying conditions was unavailable to statistically assess these differences a simple model will be applied to this dataset for future use when additional gear tests are completed.

Table 10 provides a causal model that was presented in References 18 and 19 for use in the analysis of in-flight maneuvering effects on transmission vibration. Although our test rig does not simulate flight maneuvers, the framework can be applied to understand the affects inputs have on the measured outputs based on the internal response of the test gearbox to its inputs. These inputs are the test conditions that include torque, speed, oil temperatures and oil jet pressures. The internal response changes with these conditions when gear or pinion teeth are undamaged and is measured with the output sensors. When tooth damage occurs, the internal response will be affected causing changes in the output response. This response must differ from the undamaged gear output response and be reflected in the condition indicator.

TABLE 10.—MODEL FOR CAUSAL RELATIONSHIPS (REFS. 18 AND 19)

Flight Maneuver {M} →	Aircraft Attitude {A} →	Physical Input {I} →	Internal Response {R} →	Measured Output {O}
		Torque	Tooth contact	Vibration
		Speed	Friction	Oil Debris
		Oil Temperatures	Heat	Temperature
		Oil Pressures	Transmission Error	Noise
			Backlash	
			Tooth Damage	

Several condition indicators exist to detect gear tooth damage. The referenced analysis (Refs. 18 and 19) used the time domain CI, RMS of the time synchronous averaged vibration data (a), as the measured output of the internal response.

$$\mathrm{RMS} = \sqrt{\frac{1}{n}\sum_{i=1}^{n} a_i^2} \tag{1}$$

The RMS data from the left and right pinion and gear calculated for the four tests the will be plotted and discussed in conjunction with the sideband index in the following sections of this paper.

Note that the accelerometers installed on the left side of the test rig were used to measure vibration for the pinion and gear installed on the left side of the gearbox. The accelerometers installed on the right side of the gearbox were used to measure vibration for the pinion and gear installed on the right side of the gearbox. The vibration data from the *left* accelerometer and the 1/rev signal on the pinion shaft were used to calculate *left* pinion CIs. The vibration data from the *left* accelerometer and the 1/rev signal on the gear shaft were used to calculate *left* gear CIs. The vibration data from the *right* accelerometer and the 1/rev signal on the pinion shaft were used to calculate *right* pinion CIs. The vibration data from the *right* accelerometer and the 1/rev signal on the gear shaft were used to calculate *right* gear CIs.

As mentioned in the previous section, sideband index methods were studied in this work for use in detecting surface fatigue damage to spiral bevel gear teeth. Sideband index methods were selected for use in this study due to success at detecting damage to spiral bevel gear teeth in several helicopters (Refs. 1 and 2) SI is a frequency domain based CI. The CI value is an average value of sideband amplitudes about the fundamental gear mesh frequency. The number of sidebands included in the calculation of the sideband CI can vary with different health monitoring systems.

All gears generate a dominant gear mesh (GM) frequency in the vibration signature due to each tooth impacts against the gear it is driving as the pinion and gear mesh. The gear (or pinion) mesh frequency is equal to the number of gear teeth multiplied by its speed. Gear sets also produce pairs of equally spaced n sidebands on either side of the gear mesh equal to (n#teeth ±n) multiplied by speed. Certain types of gear tooth damage, such as pitting on several teeth, can affect the amplitude of the sidebands. Increases in sideband amplitudes are often used to calculate a gear condition indicator.

Condition indicator (CI) SI was calculated for the left gear, left pinion, right gear and right pinion. For this CI, the time synchronous average data is converted to the frequency domain, then the amplitude of the average sidebands on either side of the gear mesh are trended. The MDSS system averages the amplitude of ±1 sideband on either side of the gear or pinion mesh to calculate its SI CI. The MSPU system averages the amplitude of ±3 sidebands on either side of the gear or pinion mesh to calculate its SI CI. For example, the pinion gear mesh is 19 time the rpm of the pinion. The MSPU system averages the amplitude of ±3 sidebands (16×rpm, 17×rpm, 18×rpm, 20×rpm, 21×rpm, and 22×rpm) to calculate SI.

Figure 5 illustrates the steps required to calculate RMS and SI for each reading. RMS uses the interpolated TSA data per Figure 3 to calculate the RMS of the TSA. SI uses the TSA to calculate an FFT. Then the amplitudes of the FFT on either side of the gear mesh (GM) are used to calculate SI indexes. Note that the x-axis of the plot showing the FFT of the right gear is in shaft orders or multiples of shaft speed. For example, since the gear has 41 teeth, the gear mesh frequency (teeth x rpm) shows up at 41 shaft orders.

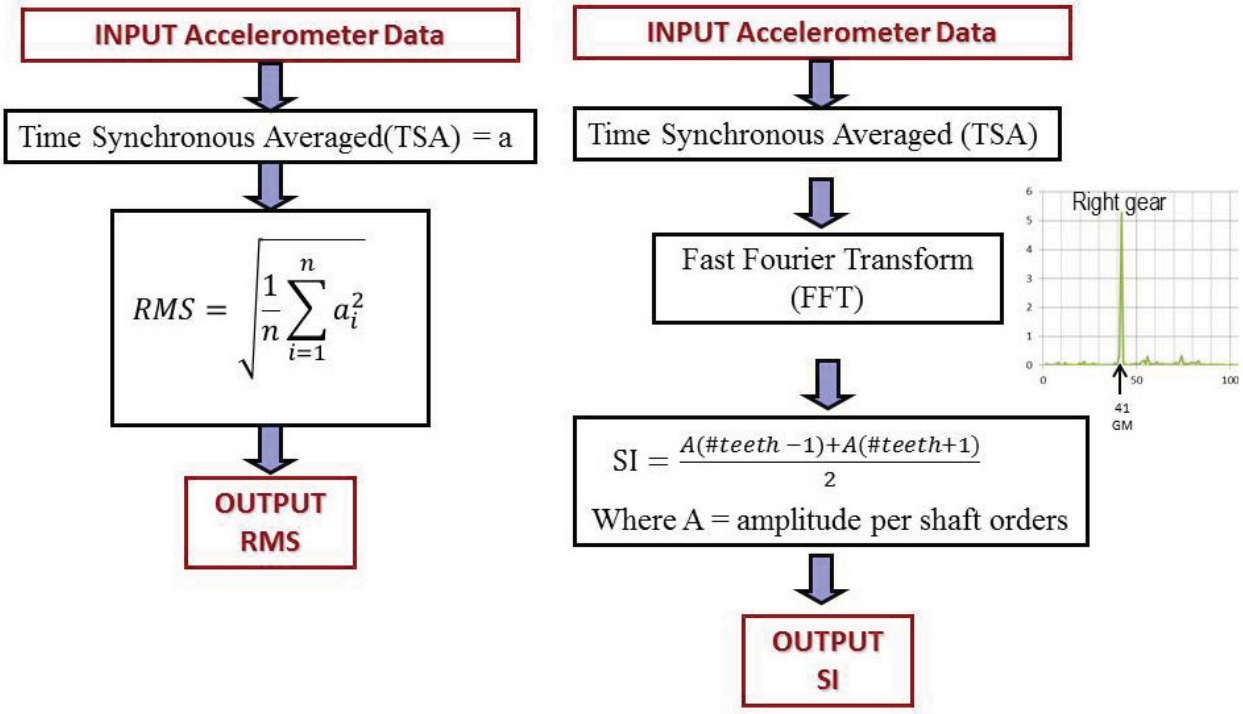

Figure 5.—RMS and SI calculations.

Experimental Data

Summaries of each test will be discussed in the following sections that include plots of debris generated and gear torque measured during each test. Reference 20 contains a detailed analysis of the oil debris generated and operational parameters measured during these tests. Torque was measured in inch-pounds and plotted in blue per the left y-axis. Debris generated was measured in milligrams and plotted in orange per the right y-axis. The x-axis was measured as the time of rig operation in minutes. The yellow triangles on the x-axis indicate the time when the gear and pinion teeth were inspected. During each test, RMS for the left and right pinion/gear set were plotted in volts. Multiplying the y-axis scale by 100 converts volts to g's.

Sidebands were calculated and plotted in several different variations to determine if trends were observed with varying levels and types of tooth damage. The ±3 individual sidebands for the left and right gear and pinion were calculated and plotted from vibration data collected on both the MDSS and MSPU systems. The average of ±3 sidebands for the left and right gear and pinion were calculated and plotted from vibration data collected on both the MDSS and MSPU systems. The average of ±1 sideband for the left and right gear and pinion were calculated and plotted from vibration data collected on both the MDSS and MSPU systems. The maximum ±3 sideband for the left and right gear and pinion were also calculated and plotted from vibration data collected on both the MDSS and MSPU systems.

Tables of mean and standard deviation values for individual sidebands for the left and right gear and pinion between inspection intervals and torque changes were also generated. Observations from the tabular and plotted data were included. Representative photos of gear and pinion teeth damage modes and their progression at the inspections intervals was provided in Appendix A. Plots of the MDSS and MSPU data of individual, average of ±1 sideband, ±3 sideband and maximum sideband will be included in Appendix B. Note that MSPU data will not be plotted for test 1 due to poor response of MSPU accelerometer for these tests. A summary of the operational data collected for each test averaged within each inspection period will be included in Appendix C. Only torque changes were plotted for this paper.

Future study is warranted of the effect the other operational parameters listed in Appendix C have on CI response, but outside the scope of this paper.

The purpose of plotting the data and generating the tables was to compare differences between sideband amplitudes for the gears, pinions, torque changes and failure modes. The hope going into this was that specific sidebands increased or decreased in values due to comparable operational and environmental conditions between tests.

Test 1

Figure 6 is a plot of debris generated and the torque during test 1. Figure 7 is a plot of RMS during test 1. Tooth damage photos for the gear and pinion during the inspection intervals can be found in Figures A.1.1 to A.1.5.

For test 1, Figures A.1.1 to A.1.5 illustrate the progression of damage on the gear and pinion teeth. For the left pinion, macropitting was observed on one pinion tooth at reading 1862 and on two teeth at reading 4814. For the left gear, macropitting was observed on three teeth at reading 4814 and five teeth at reading 6065. Macropitting was also observed on the right gear and pinion at reading 6065, the end of the test.

For test 1, per Figure 6, the rate of debris generation measured was 1.9 mg/hr at reading 1862, when spalling macropitting (4.3.4) was first observed on one left pinion tooth, although per Table 2, other types of damage occurred during this inspection interval on the right gear teeth. The rate decreased to 0.4 mg/hr when macropitting was observed on all of the teeth.

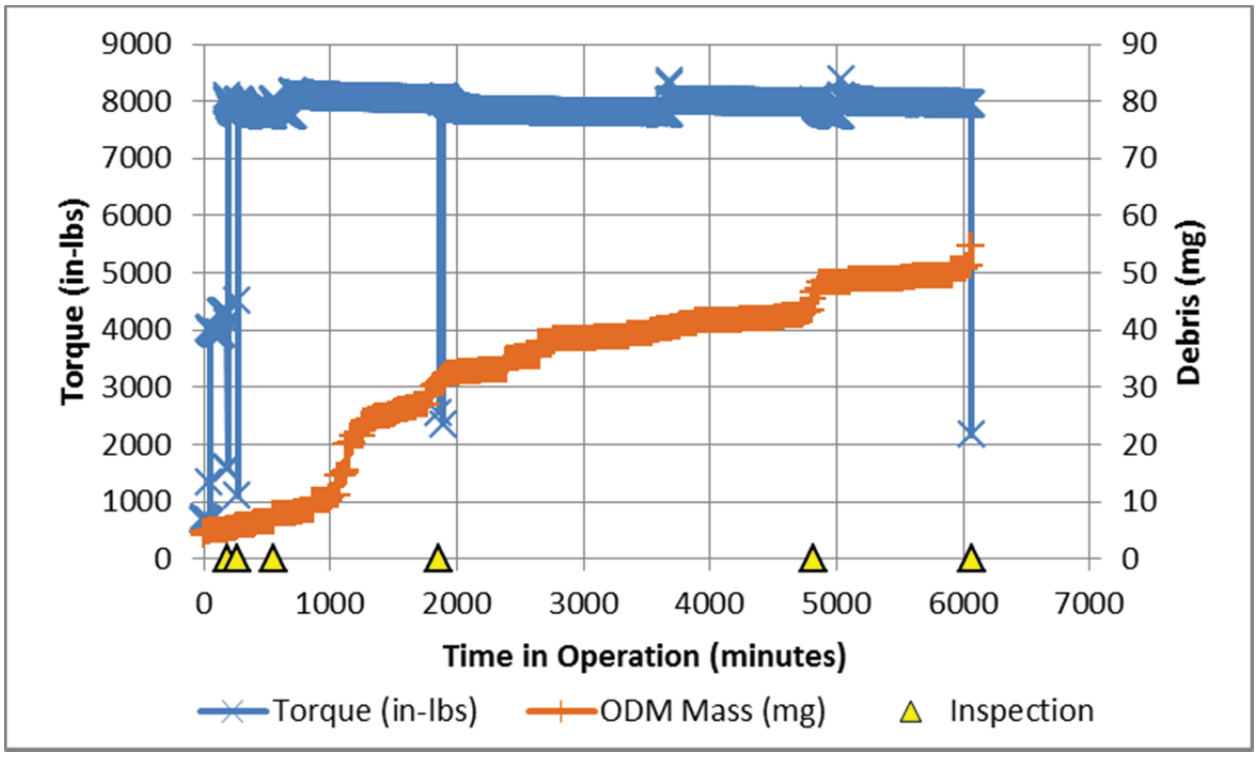

Figure 6.—Debris generated and torque during test 1.

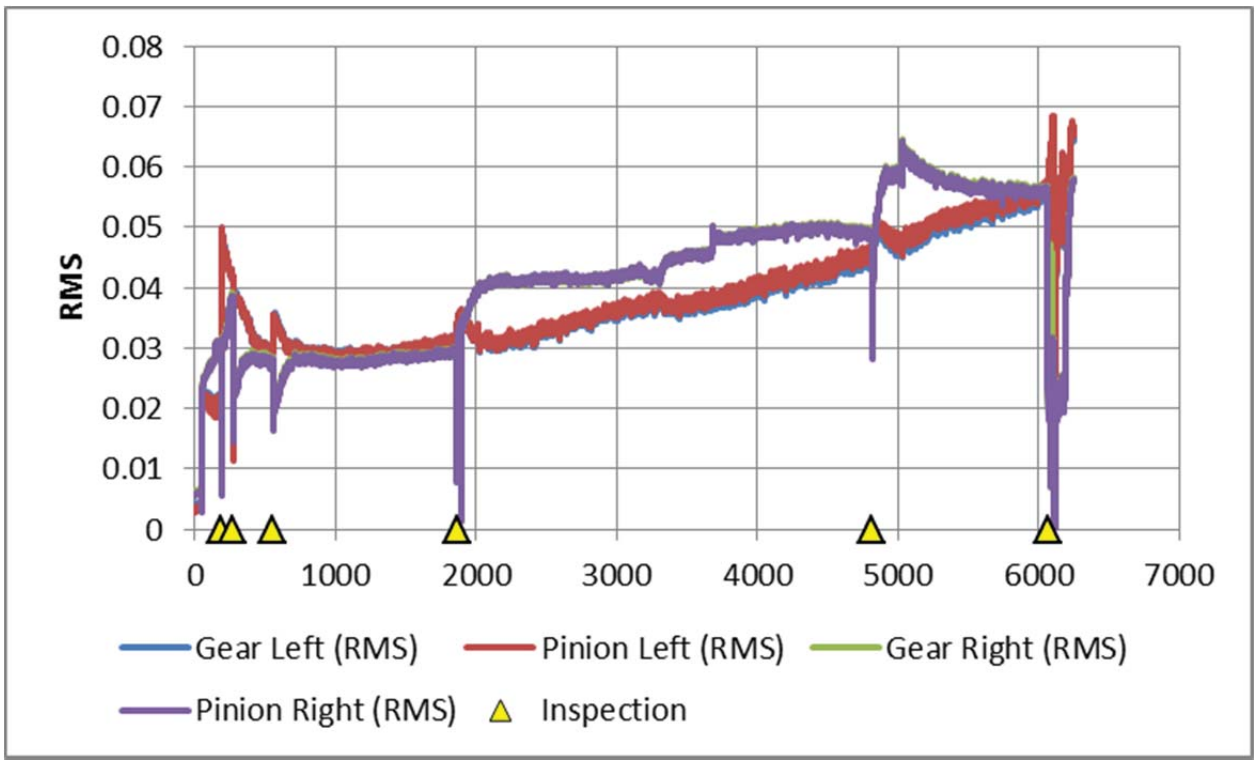

Figure 7.—RMS during test 1.

Per Figure 7, RMS could not be used to isolate the pinion from the gear on the left and right side of the test rig. The left gear and pinion RMS values tracked each other very closely as did the right gear and pinion. Both responded to the restarts after inspections, but the right side was significantly more sensitive than the left. The left RMS values trended well with damage progression.

Figures B.1.1, B.1.3, B.1.5, and B.1.7 are plots of the individual ±3 sideband and the gear mesh for the 41 tooth gears and the 19 tooth pinions for left gear, right gear, left pinion, right pinion during the test. The left y-axis is scaled for the ±3 sidebands. The right y-axis is scaled for the gear (Sig41) and pinion (SI19) meshes. The x-axis correlates to the time in operation of the test rig in minutes. The yellow triangles correlate to gear tooth inspections.

Figures B.1.2, B.1.4, B.1.6, and B.1.8 are plots of the average ±1 sidebands, average ±3 sidebands and the maximum of the ±3 sidebands for left gear, right gear, left pinion, right pinion during the test. The yellow triangles correlate to gear tooth inspections.

Table 11 is a summary of the mean and standard deviation values for the individual sidebands between each inspection interval. The columns highlighted in blue are the gear and pinion meshes. The cells highlighted in red have the maximum values within that inspection interval. The cells highlighted in yellow have the next maximum values. The cells highlighted in green have the minimum values.

TABLE 11.—SUMMARY OF SIDEBANDS FOR TEST 1

LWW9RXX10		Means							Standard Deviations						
		Left Gear							Left Gear						
Torque	Inspection	Slgl38	Slgl39	Slgl40	Slgl41	Slgl42	Slgl43	Slgl44	Slgl38	Slgl39	Slgl40	Slgl41	Slgl42	Slgl43	Slgl44
(in-lb)	Reading	SB-3	SB-2	SB-1	GM	SB+1	SB+2	SB+3	SB-3	SB-2	SB-1	GM	SB+1	SB+2	SB+3
4000	1-186	0.02	0.15	0.17	1.98	0.23	0.46	0.09	0.01	0.10	0.06	0.99	0.11	0.26	0.04
8000	187-269	0.03	0.07	0.30	5.87	0.31	0.13	0.14	0.01	0.02	0.06	1.06	0.05	0.06	0.05
8000	270-553	0.03	0.10	0.24	4.42	0.43	0.21	0.14	0.01	0.02	0.04	0.50	0.05	0.04	0.03
8000	554-1862	0.06	0.05	0.11	4.00	0.19	0.16	0.07	0.01	0.02	0.02	0.18	0.09	0.04	0.02
8000	1863-4814	0.06	0.03	0.15	4.88	0.14	0.37	0.13	0.02	0.01	0.04	0.51	0.04	0.10	0.06
8000	4815-6065	0.05	0.05	0.06	6.61	0.26	0.63	0.18	0.01	0.02	0.03	0.36	0.08	0.07	0.03
		Left Pinion							Left Pinion						
Torque	Inspection	Slpl16	Slpl17	Slpl18	Slpl19	Slpl20	Slpl21	Slpl22	Slpl16	Slpl17	Slpl18	Slpl19	Slpl20	Slpl21	Slpl22
(in-lb)	Reading	SB-3	SB-2	SB-1	GM	SB+1	SB+2	SB+3	SB-3	SB-2	SB-1	GM	SB+1	SB+2	SB+3
4000	1-186	0.03	0.07	0.15	1.98	0.58	0.08	0.09	0.01	0.03	0.10	0.99	0.33	0.05	0.06
8000	187-269	0.05	0.07	0.10	5.87	0.45	0.10	0.09	0.02	0.04	0.06	1.06	0.19	0.06	0.04
8000	270-553	0.05	0.07	0.07	4.42	0.57	0.10	0.10	0.03	0.03	0.04	0.50	0.16	0.06	0.05
8000	554-1862	0.08	0.07	0.08	4.00	0.42	0.12	0.09	0.04	0.03	0.04	0.18	0.12	0.05	0.04
8000	1863-4814	0.10	0.12	0.20	4.88	0.89	0.37	0.13	0.04	0.04	0.09	0.51	0.21	0.08	0.05
8000	4815-6065	0.15	0.22	0.32	6.61	1.30	0.44	0.12	0.04	0.04	0.05	0.36	0.14	0.08	0.05

LWW9RXX10		Means							Standard Deviations						
		Right Gear							Right Gear						
Torque	Inspection	Slgr38	Slgr39	Slgr40	Slgr41	Slgr42	Slgr43	Slgr44	Slgr38	Slgr39	Slgr40	Slgr41	Slgr42	Slgr43	Slgr44
(in-lb)	Reading	SB-3	SB-2	SB-1	GM	SB+1	SB+2	SB+3	SB-3	SB-2	SB-1	GM	SB+1	SB+2	SB+3
4000	1-186	0.06	0.24	0.10	3.03	0.23	0.17	0.10	0.02	0.14	0.03	1.37	0.06	0.11	0.04
8000	187-269	0.05	0.06	0.11	4.38	0.14	0.09	0.10	0.02	0.03	0.03	0.88	0.06	0.03	0.04
8000	270-553	0.04	0.08	0.08	3.59	0.11	0.11	0.13	0.01	0.03	0.03	0.32	0.04	0.03	0.03
8000	554-1862	0.02	0.08	0.06	3.73	0.09	0.26	0.03	0.01	0.02	0.01	0.28	0.04	0.04	0.01
8000	1863-4814	0.06	0.06	0.12	6.12	0.31	0.46	0.08	0.01	0.02	0.03	0.61	0.11	0.06	0.05
8000	4815-6065	0.07	0.09	0.08	7.86	0.52	0.40	0.14	0.01	0.01	0.03	0.46	0.05	0.05	0.02
		Right Pinion							Right Pinion						
Torque	Inspection	Slpr16	Slpr17	Slpr18	Slpr19	Slpr20	Slpr21	Slpr22	Slpr16	Slpr17	Slpr18	Slpr19	Slpr20	Slpr21	Slpr22
(in-lb)	Reading	SB-3	SB-2	SB-1	GM	SB+1	SB+2	SB+3	SB-3	SB-2	SB-1	GM	SB+1	SB+2	SB+3
4000	1-186	0.03	0.03	0.21	3.03	0.24	0.11	0.04	0.02	0.02	0.11	1.37	0.12	0.06	0.03
8000	187-269	0.03	0.08	0.15	4.38	0.22	0.12	0.05	0.01	0.03	0.04	0.88	0.09	0.07	0.02
8000	270-553	0.04	0.07	0.10	3.59	0.31	0.11	0.14	0.02	0.02	0.03	0.32	0.08	0.04	0.05
8000	554-1862	0.05	0.11	0.13	3.73	0.28	0.12	0.04	0.02	0.03	0.06	0.28	0.07	0.05	0.02
8000	1863-4814	0.07	0.15	0.39	6.12	0.64	0.29	0.09	0.03	0.02	0.07	0.61	0.06	0.10	0.03
8000	4815-6065	0.11	0.14	0.43	7.86	0.57	0.38	0.09	0.02	0.01	0.04	0.46	0.07	0.05	0.02

A summary of the response of the individual sidebands to damage between each inspection interval is listed below:

1. Left gear:
    a. The +2 sideband (SI43) had the largest value when damage was observed on the gear teeth.
    b. The +2 sideband (SI43) trended well after gear damage progressed.
    c. The +2 sideband (SI43) had the largest value at lower torque.
    d. The +1 sideband (SI42) had the largest value when no damage was observed on the gear teeth.
    e. The +1 sideband (SI42) trended after gear damage progressed.
2. Left pinion:
    a. The +1 sideband (SI20) had the largest value throughout the test.
    b. The +1 sideband (SI20) trended well after gear damage progressed to more than one tooth.
    c. The +1 sideband (SI20) had the largest value at lower torque.
3. Right gear:
    a. The +2 sideband (SI43) had the largest value when damage was observed on the gear teeth.
    b. The +2 sideband (SI43) trended well after gear damage progressed until reading 4814, then dropped below 1 sideband (SI42).
    c. The –2 sideband (SI39) and had the largest value at lower torque.
    d. The +1 sideband (SI42) trended after gear damage progressed.
4. Right pinion:
    a. The +1 sideband (SI20) had the largest value throughout the test.
    b. The +1 sideband (SI20) trended well after pinion damage progressed, but dropped slightly after reading 4814.
    c. The –1 sideband (SI18) trended well after pinion damage progressed, but dropped slightly after reading 4814.
    d. The +2 sideband (SI21) trended well after pinion damage progressed, but dropped slightly after reading 4814.
    e. The +1 sideband (SI20) had the largest value at lower torque.

A summary of the response of the average of ±3 sidebands, the average of ±1 sideband and the maximum of the ±3 sidebands is listed below:

1. Left gear:
    a. The maximum sideband trended well after gear damage began and progressed to several teeth.
    b. The average +1 sideband *did not* trend well to damage progression.
    c. The average +3 sideband trended after gear damage progressed.
2. Left pinion:
    a. The maximum sideband trended well after gear damage progressed to more than one tooth.
    b. The average +1 sideband trended after gear damage progressed to more than one tooth.
    c. The average +3 sideband trended after gear damage progressed to more than one tooth.
3. Right gear:
    a. The maximum sideband trended well when gear damage began and progressed to several teeth, but decreased slightly at the last inspection interval (4814–6065).
    b. The average ±1 sideband trended after gear damage progressed, but decreased slightly at last inspection interval (4814–6065).

c. The average ±3 sideband trended after gear damage progressed, but decreased slightly at last inspection interval (4814–6065).

4. Right pinion:
   a. The maximum sideband trended well when gear damage progressed to several teeth, but decreased slightly at the last inspection interval (4814–6065).
   b. The average ±1 sideband trended after gear damage progressed, but decreased slightly at last inspection interval (4814–6065).

Test 2

Figure 8 is a plot of debris generated and the torque during test 2. Figure 9 is a plot of RMS during test 2. Tooth damage photos for the gear and pinion during the inspection intervals can be found in Figure A.2.1.

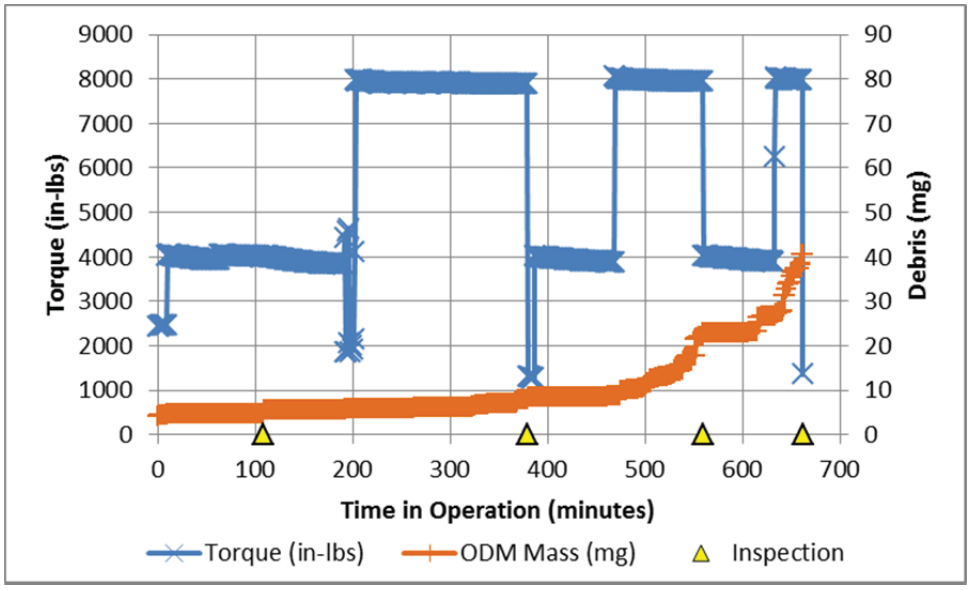

Figure 8.—Debris generated and torque during test 2.

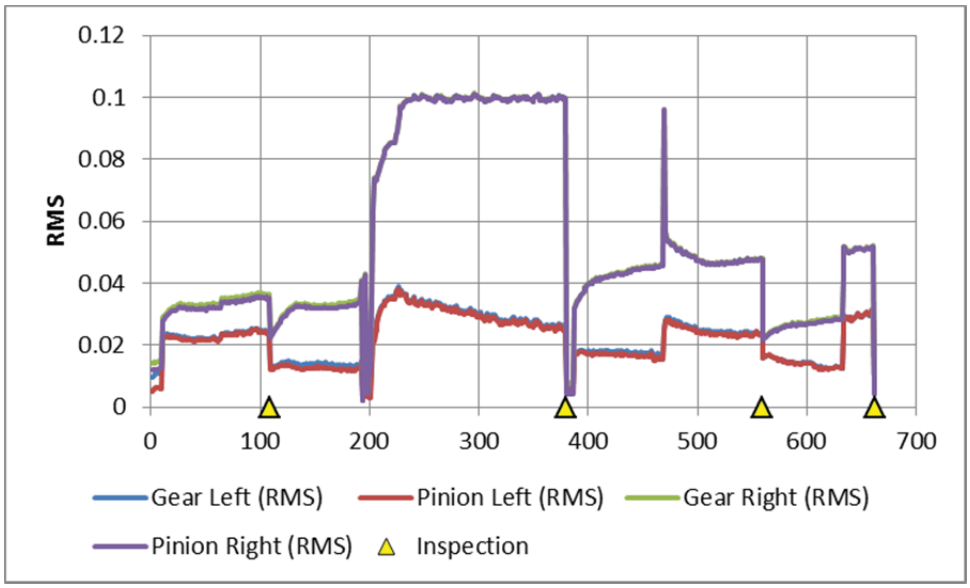

Figure 9.—RMS during test 2.

For test 2, Figure A.2.1 illustrates the progression of damage to five left pinion teeth. The other photos are representative pictures of one left gear tooth, on right gear tooth and one pinion tooth. The damage to these gears did not change after the inspection at reading 379. For the left pinion, no macropitting was observed on the pinion teeth at reading 379, 6.32 hours into the test. At reading 559, 9.32 hours into the test, 4.3.4 was observed on two pinion teeth. At reading 662, 11.03 hours into the test, 4.3.4 was observed on five teeth.

For test 2, per Figure 8, the rate of debris generation measured was at 8.96 mg/hr when progressive macropitting (4.3.2) was first observed on several teeth. The rate decreased to 3.75 mg/hr when the torque dropped to 4000 in.-lb. The debris generated then increased from 3.75 to 27.69 mg/hr when torque increased from 4000 to 8000 in.-lb, and spalling macropitting (4.3.4) was observed on five gear teeth.

Per Figure 9, RMS could not be used to isolate the pinion from the gear on the left and right side of the test rig. The left gear and pinion tracked each other very closely as did the right gear and pinion. Both responded to the restarts after inspections, but the right side was significantly more sensitive than the left. The left and right side RMS values did not trend well with damage progression due to the varying torque levels throughout the test. Both increased in value with increases in torque.

Figures B.2.1, B.2.5, B.2.9, and B.2.13 are plots of the individual ±3 sideband and the gear mesh for the 41 tooth gears and the 19 tooth pinions for left gear, right gear, left pinion, right pinion during the test from the MDSS. The left y-axis is scaled for the ±3 sidebands. The right y-axis is scaled for the gear (Sig41) and pinion (SI19) meshes. The x-axis correlates to the time in operation of the test rig in minutes. The yellow triangles correlate to gear tooth inspections.

Figures B.2.2, B.2.6, B.2.10, and B.2.14 are plots of the individual ±3 sideband and the gear mesh for the 41 tooth gears and the 19 tooth pinions for left gear, right gear, left pinion, right pinion during the test from the MSPU. The left y-axis is scaled for the ±3 sidebands. The right y-axis is scaled for the gear (Sig41) and pinion (SI19) meshes. The yellow triangles correlate to gear tooth inspections per Table 7.

Figures B.2.3, B.2.7, B.2.11, and B.2.15 are plots of the average ±1 sidebands, average ±3 sidebands and the maximum of the ±3 sidebands for left gear, right gear, left pinion, right pinion during the test from the MDSS. The yellow triangles correlate to gear tooth inspections.

Figures B.2.4, B.2.8, B.2.12, and B.2.16 are plots of the average ±1 sidebands, average ±3 sidebands and the maximum of the ±3 sidebands for left gear, right gear, left pinion, right pinion during the test from the MSPU. The yellow triangles correlate to gear tooth inspections per Table 7.

Table 12 is a summary of the mean and standard deviation values for the individual sidebands between each inspection interval. The columns highlighted in blue are the gear and pinion meshes. The cells highlighted in red have the maximum values within that inspection interval. The cells highlighted in yellow have the next maximum values. The cells highlighted in green have the minimum values.

For test 2, Figure A.2.1, in Appendix A, illustrates the progression of damage to five left pinion teeth. The other photos are representative pictures of one left gear tooth, on right gear tooth and one pinion tooth. The damage to these gears did not change after the initial inspection. For the left pinion, no macropitting was observed on the pinion teeth 6 hr into the test. Nine hours into the test, 4.3.4 was observed on two pinion teeth. Eleven hours into the test, 4.3.4 was observed on five teeth.

TABLE 12.—SUMMARY OF SIDEBANDS FOR TEST 2

L0505R0606		Means							Standard Deviations						
		Left Gear							Left Gear						
Torque	Inspection	SIgl38	SIgl39	SIgl40	SIgl41	SIgl42	SIgl43	SIgl44	SIgl38	SIgl39	SIgl40	SIgl41	SIgl42	SIgl43	SIgl44
(in-lb)	Reading	SB-3	SB-2	SB-1	GM	SB+1	SB+2	SB+3	SB-3	SB-2	SB-1	GM	SB+1	SB+2	SB+3
4000	1-108	0.08	0.14	0.25	2.91	0.20	0.31	0.34	0.03	0.07	0.05	0.67	0.04	0.17	0.04
4000	109-202	0.08	0.06	0.11	1.49	0.24	0.44	0.40	0.02	0.03	0.03	0.40	0.11	0.10	0.11
8000	203-379	0.03	0.04	0.28	3.99	0.13	0.48	0.12	0.01	0.01	0.02	0.52	0.04	0.03	0.05
4000	380-468	0.07	0.07	0.23	1.96	0.32	0.54	0.38	0.02	0.02	0.05	0.43	0.09	0.10	0.11
8000	469-559	0.01	0.04	0.30	3.30	0.31	0.41	0.09	0.01	0.01	0.01	0.22	0.02	0.03	0.02
4000	560-632	0.10	0.07	0.17	1.61	0.39	0.55	0.38	0.02	0.01	0.03	0.26	0.06	0.03	0.08
8000	633-662	0.01	0.04	0.31	3.80	0.34	0.34	0.07	0.01	0.01	0.06	0.56	0.06	0.06	0.02
		Left Pinion							Left Pinion						
Torque	Inspection	SIpl16	SIpl17	SIpl18	SIpl19	SIpl20	SIpl21	SIpl22	SIpl16	SIpl17	SIpl18	SIpl19	SIpl20	SIpl21	SIpl22
(in-lb)	Reading	SB-3	SB-2	SB-1	GM	SB+1	SB+2	SB+3	SB-3	SB-2	SB-1	GM	SB+1	SB+2	SB+3
4000	1-108	0.03	0.13	0.27	2.91	0.39	0.33	0.06	0.01	0.04	0.07	0.67	0.12	0.09	0.02
4000	109-202	0.02	0.14	0.25	1.49	0.29	0.27	0.04	0.01	0.06	0.08	0.40	0.08	0.06	0.01
8000	203-379	0.09	0.15	0.10	3.99	0.21	0.25	0.03	0.03	0.03	0.03	0.51	0.03	0.03	0.01
4000	380-468	0.07	0.08	0.21	1.96	0.44	0.28	0.03	0.01	0.03	0.06	0.43	0.09	0.07	0.01
8000	469-559	0.13	0.17	0.26	3.30	0.12	0.14	0.05	0.02	0.01	0.04	0.22	0.05	0.04	0.01
4000	560-632	0.10	0.11	0.27	1.61	0.35	0.29	0.03	0.01	0.02	0.06	0.26	0.06	0.02	0.01
8000	633-662	0.19	0.13	0.21	3.81	0.05	0.31	0.08	0.05	0.02	0.04	0.56	0.03	0.06	0.02

L0505R0606		Means							Standard Deviations						
		Right Gear							Right Gear						
Torque	Inspection	SIgr38	SIgr39	SIgr40	SIgr41	SIgr42	SIgr43	SIgr44	SIgr38	SIgr39	SIgr40	SIgr41	SIgr42	SIgr43	SIgr44
(in-lb)	Reading	SB-3	SB-2	SB-1	GM	SB+1	SB+2	SB+3	SB-3	SB-2	SB-1	GM	SB+1	SB+2	SB+3
4000	1-108	0.09	0.11	0.16	4.36	0.06	0.46	0.27	0.02	0.03	0.04	0.85	0.04	0.04	0.08
4000	109-202	0.14	0.05	0.12	4.18	0.11	0.28	0.21	0.04	0.03	0.04	0.99	0.07	0.09	0.07
8000	203-379	0.05	0.07	0.33	13.65	0.44	0.15	0.14	0.01	0.02	0.04	0.96	0.05	0.05	0.02
4000	380-468	0.09	0.13	0.13	5.45	0.22	0.35	0.24	0.02	0.03	0.04	1.57	0.08	0.11	0.09
8000	469-559	0.02	0.09	0.21	6.80	0.30	0.12	0.08	0.01	0.01	0.02	0.79	0.05	0.03	0.01
4000	560-632	0.15	0.17	0.07	3.64	0.14	0.37	0.19	0.02	0.02	0.02	0.24	0.02	0.05	0.05
8000	633-662	0.02	0.08	0.23	6.85	0.24	0.12	0.07	0.01	0.01	0.04	1.25	0.05	0.03	0.02
		Right Pinion							Right Pinion						
Torque	Inspection	SIpl16	SIpl17	SIpl18	SIpl19	SIpl20	SIpl21	SIpl22	SIpl16	SIpl17	SIpl18	SIpl19	SIpl20	SIpl21	SIpl22
(in-lb)	Reading	SB-3	SB-2	SB-1	GM	SB+1	SB+2	SB+3	SB-3	SB-2	SB-1	GM	SB+1	SB+2	SB+3
4000	1-108	0.04	0.16	0.22	4.36	0.19	0.20	0.03	0.01	0.03	0.05	0.85	0.04	0.06	0.01
4000	109-202	0.03	0.15	0.18	4.18	0.20	0.18	0.02	0.01	0.03	0.04	0.99	0.10	0.04	0.01
8000	203-379	0.05	0.08	0.19	13.65	0.20	0.27	0.03	0.02	0.01	0.03	0.96	0.05	0.02	0.01
4000	380-468	0.02	0.17	0.23	5.45	0.20	0.20	0.10	0.01	0.03	0.05	1.57	0.06	0.04	0.02
8000	469-559	0.04	0.12	0.16	6.80	0.29	0.16	0.21	0.01	0.01	0.04	0.79	0.05	0.03	0.05
4000	560-632	0.02	0.10	0.24	3.64	0.07	0.19	0.22	0.01	0.02	0.02	0.24	0.03	0.03	0.02
8000	633-662	0.05	0.09	0.17	6.85	0.31	0.18	0.21	0.02	0.02	0.03	1.25	0.06	0.04	0.03

A summary of the response of the individual sidebands to damage between each inspection interval is listed below:

1. Left gear:
    a. The +2 sideband (SI43) had the largest value when damage was observed on the gear teeth.
    b. After damage was observed, the +2 sideband (SI43) increased with lower torque and decreased with higher torques.
    c. The +3 sideband (SI44) had the largest value when no damage was observed on the gear teeth during run-in.
    d. After damage was observed, the following increased with lower torque and decreased with higher torques: –3 (SI38), –2 (SI39), +1(SI42), +2(SI43) and +3(SI44).
    e. After damage was observed, the following increased with higher torque and decreased with lower torques: –1 (SI40), and gear mesh (SI41).
2. Left pinion:
    a. The +1 sideband (SI20) and +2 sidebands (SI21) had the largest values during the test, but both *did not* trend well with damage.
    b. After damage was observed, the following increased with lower torque and decreased with higher torques: + (SI20) and +2 (SI21)
    c. The following did not indicate trends with torque changes: –1 (SI18) and +2 (SI22)
    d. After damage was observed, the following increased with higher torque and decreased with lower torques: –3 (SI16), –2 (SI17) and gear mesh (SI19).
    e. If you separate the trends into torque bands, the only sideband that trended with damage at 8000 in.-lbs torque was –3 (SI16).
3. Right gear:
    a. The +1 sideband (SI42) and +2 sidebands (SI43) had the largest values during the test, but both *did not* trend well with damage.
    b. After damage was observed, the following increased with lower torque and decreased with higher torques: –3 (SI38) and +2 (SI43) and +3 SI44.
    c. The following did not indicate trends torque changes: –2(SI39)
    d. After damage was observed, the following increased with higher torque and decreased with lower torques: –1(SI40), +1(SI42) and gear mesh (SI41).
    e. If you separate the trends into torque bands, no sideband trended with damage at 8000 in.-lbs torque.
4. Right pinion:
    a. The –1 sideband (SI18), +1 sideband (SI20) and +2 sideband (SI21) had the largest values during the test, but *did not* trend well with damage.
    b. After damage was observed, the following increased with lower torque and decreased with higher torques: –1 (SI18).
    c. The following did not indicate trends with torque changes: –2(SI17), +2 (SI21) and +3(SI22)
    d. After damage was observed, the following increased with higher torque and decreased with lower torques: –3 (SI16), +1 (SI20) and gear mesh (SI19).
    e. If you separate the trends into torque bands, the only sideband that trended with damage at 8000 in.-lbs torque was +1 (SI20).

A summary of the response of the average of +3 sidebands, the average of +1 sideband and the maximum of the +3 sidebands is listed below:

1. Left gear:
    a. The maximum sideband, average ±1 sideband and ±3 sideband *did not* trend well with damage.
    b. The maximum sideband and ±3 sideband increased with lower torque and decreased with higher torques.
    c. The +1 sideband did not trend with torque changes
2. Left pinion:
    a. The maximum sideband, average ±1 sideband and ±3 sideband did not trend well with damage.
    b. The maximum sideband, ±1 sideband and ±3 sideband increased with lower torque and decreased with higher torques.
3. Right gear:
    a. The maximum sideband, average + sideband and ±3 sideband *did not* trend well with damage.
    b. The ±1 sideband and ±3 sideband increased with lower torque and decreased with higher torques.
    c. The maximum sideband did not trend with torque changes
4. Right pinion:
    a. The maximum sideband, average ±1 sideband and ±3 sideband *did not* trend well with damage.
    b. The maximum sideband, ±1 sideband and ±3 sideband increased with higher torques and decreased with lower torques.

Test 3

Figure 10 is a plot of debris generated and the torque during test 3. Figure 11 is a plot of RMS during test 3. Tooth damage photos for the gear and pinion during the inspection intervals can be found in Figure A.3.1 to A.3.2.

For test 3, Figures A.3.1 and A.3.2 illustrate the progression of damage to five right and left pinion teeth. No macropitting was observed on the pinion teeth at reading 184, 3.07 hr into the test. At reading 482, 8.67 hr into the test, a pit was observed on a right pinion tooth. Several more pits were observed at reading 686, 11.43 hr into the test on the right pinion teeth and one pit on a left pinion tooth.

For test 3, per Figure 10, the rate of debris generation measured increased when torque increased from 6,000 to 8,000 in.-lb. For this test, the torque was not decreased when the macropitting was observed on the teeth. The 6.37 mg/hr rate of debris generation when spalling macropitting (4.3.4) was observed at 8,000 in.-lb was higher than the 3.75 mg/hr rate of debris generation when spalling macropitting (4.3.4) was observed at 4,000 in.-lb for test 2.

Per Figure 11, RMS could not be used to isolate the pinion from the gear on the left and right side of the test rig. The left gear and pinion tracked each other very closely as did the right gear and pinion. Both responded to the restarts after inspections, but the right side was significantly more sensitive than the left. The left and right side RMS values did not trend well with damage progression due to the varying torque levels throughout the test. The right side RMS values decreased when the torque increased from 6000 to 8000 in.-lbs. At 8000 in.-lbs, the right side showed a slight increasing trend with damage.

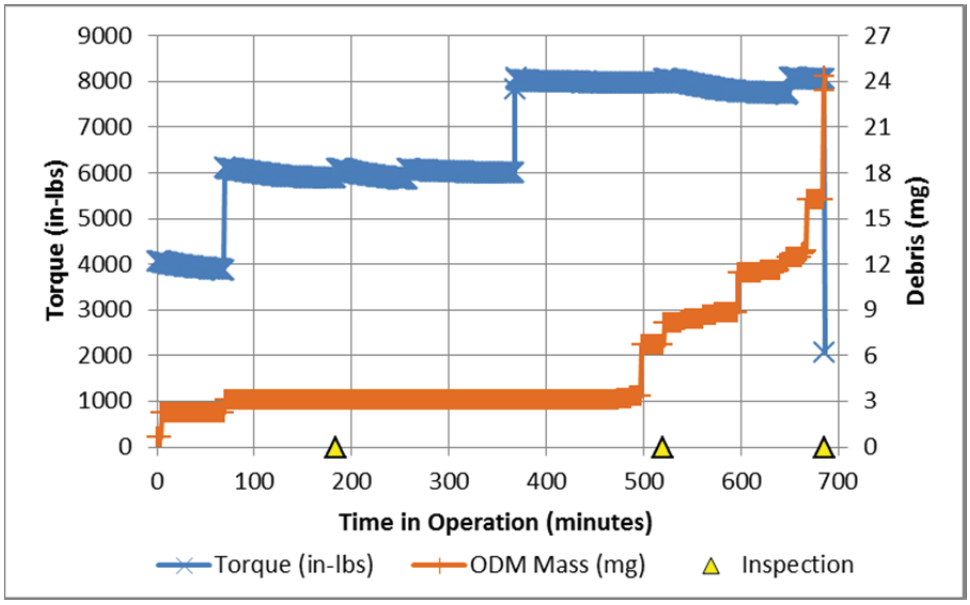

Figure 10.—Debris generated and torque during test 3.

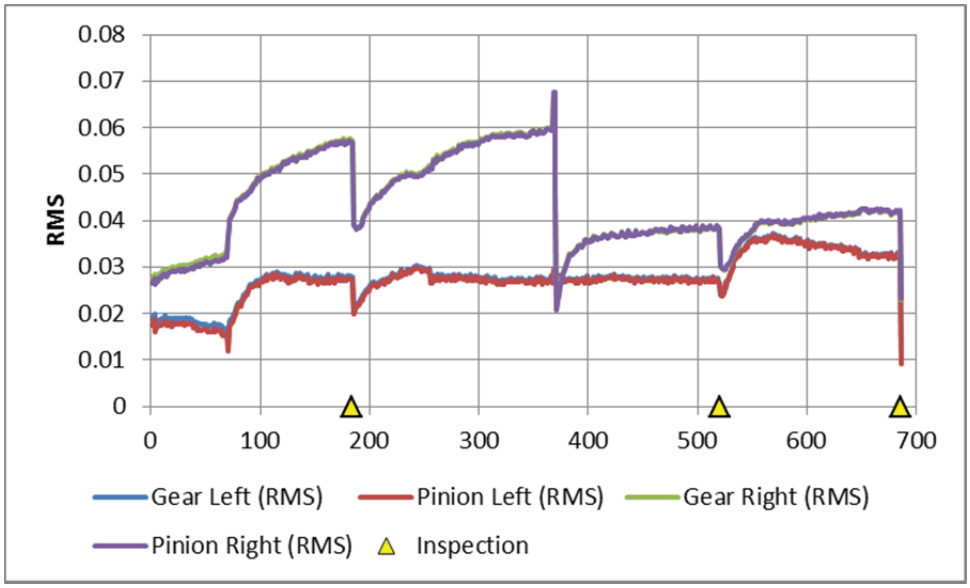

Figure 11.—RMS during test 3.

Figures B.3.1, B.3.5, B.3.9, and B.3.13 are plots of the individual ±3 sideband and the gear mesh for the 41 tooth gears and the 19 tooth pinions for left gear, right gear, left pinion, right pinion during the test from the MDSS. The left y-axis is scaled for the ±3 sidebands. The right y-axis is scaled for the gear (Sig41) and pinion (SI19) meshes. The x-axis correlates to the time in operation of the test rig in minutes. The yellow triangles correlate to gear tooth inspections.

Figures B.3.2, B.3.6, B.3.10, and B.3.14 are plots of the individual ±3 sideband and the gear mesh for the 41 tooth gears and the 19 tooth pinions for left gear, right gear, left pinion, right pinion during the test from the MSPU. The left y-axis is scaled for the ±3 sidebands. The right y-axis is scaled for the gear (Sig41) and pinion (SI19) meshes. The yellow triangles correlate to gear tooth inspections per Table 8.

Figures B.3.3, B.3.7, B.3.11, and B.3.15 are plots of the average ±1 sidebands, average ±3 sidebands and the maximum of the ±3 sidebands for left gear, right gear, left pinion, right pinion during the test from the MDSS. The yellow triangles correlate to gear tooth inspections.

Figures B.3.4, B.3.8, B.3.12, and B.3.16 are plots of the average ±1 sidebands, average ±3 sidebands and the maximum of the ±3 sidebands for left gear, right gear, left pinion, right pinion during the test from the MSPU. The yellow triangles correlate to gear tooth inspections per Table 8.

Table 13 is a summary of the mean and standard deviation values for the individual sidebands between each inspection interval. The columns highlighted in blue are the gear and pinion meshes. The cells highlighted in red have the maximum values within that inspection interval. The cells highlighted in yellow have the next maximum values. The cells highlighted in green have the minimum values.

For test 3, Figures A.3.1 and A.3.2 in Appendix A, illustrate the progression of damage to six right and left pinion teeth. No macro-pitting was observed on the pinion teeth 3 hr into the test. Eight hours into the test, a pit was observed on a right pinion tooth. Several more pits were observed 11 hr into the test on the right pinion teeth and one pit on a left pinion tooth.

TABLE 13.—SUMMARY OF SIDEBANDS FOR TEST 3

L0701R0802		Means							Standard Deviations						
		Left Gear							Left Gear						
Torque	Inspection	SIgl38	SIgl39	SIgl40	SIgl41	SIgl42	SIgl43	SIgl44	SIgl38	SIgl39	SIgl40	SIgl41	SIgl42	SIgl43	SIgl44
(in-lb)	Reading	SB-3	SB-2	SB-1	GM	SB+1	SB+2	SB+3	SB-3	SB-2	SB-1	GM	SB+1	SB+2	SB+3
4000	1-69	0.12	0.11	0.05	2.20	0.29	0.30	0.42	0.02	0.01	0.02	0.11	0.09	0.03	0.05
6000	70-184	0.06	0.12	0.15	3.50	0.33	0.17	0.13	0.01	0.03	0.01	0.45	0.03	0.08	0.03
6000	185-367	0.06	0.08	0.15	3.66	0.35	0.12	0.09	0.01	0.02	0.02	0.23	0.04	0.08	0.02
8000	368-520	0.03	0.06	0.19	3.74	0.26	0.14	0.06	0.01	0.01	0.02	0.06	0.02	0.01	0.01
8000	521-686	0.03	0.12	0.14	4.61	0.39	0.26	0.11	0.01	0.04	0.05	0.48	0.07	0.03	0.03
		Left Pinion							Left Pinion						
Torque	Inspection	SIpl16	SIpl17	SIpl18	SIpl19	SIpl20	SIpl21	SIpl22	SIpl16	SIpl17	SIpl18	SIpl19	SIpl20	SIpl21	SIpl22
(in-lb)	Reading	SB-3	SB-2	SB-1	GM	SB+1	SB+2	SB+3	SB-3	SB-2	SB-1	GM	SB+1	SB+2	SB+3
4000	1-69	0.01	0.10	0.15	2.20	0.22	0.28	0.04	0.01	0.01	0.06	0.11	0.05	0.03	0.01
6000	70-184	0.06	0.12	0.16	3.50	0.08	0.33	0.05	0.02	0.02	0.02	0.45	0.03	0.06	0.01
6000	185-367	0.06	0.15	0.23	3.66	0.08	0.34	0.06	0.01	0.02	0.02	0.23	0.01	0.04	0.01
8000	368-520	0.07	0.05	0.26	3.74	0.28	0.29	0.03	0.02	0.02	0.02	0.06	0.05	0.04	0.01
8000	521-686	0.09	0.07	0.22	4.61	0.49	0.30	0.05	0.02	0.02	0.03	0.48	0.06	0.04	0.02
L0701R0802		Means							Standard Deviations						
		Right Gear							Right Gear						
Torque	Inspection	SIgr38	SIgr39	SIgr40	SIgr41	SIgr42	SIgr43	SIgr44	SIgr38	SIgr39	SIgr40	SIgr41	SIgr42	SIgr43	SIgr44
(in-lb)	Reading	SB-3	SB-2	SB-1	GM	SB+1	SB+2	SB+3	SB-3	SB-2	SB-1	GM	SB+1	SB+2	SB+3
4000	1-69	0.16	0.05	0.10	4.10	0.13	0.28	0.22	0.02	0.02	0.02	0.21	0.03	0.04	0.04
6000	70-184	0.04	0.31	0.09	7.20	0.12	0.53	0.05	0.01	0.07	0.03	0.68	0.03	0.20	0.03
6000	185-367	0.05	0.34	0.10	7.40	0.15	0.55	0.04	0.02	0.08	0.03	0.83	0.04	0.18	0.02
8000	368-520	0.01	0.15	0.18	5.05	0.29	0.22	0.05	0.01	0.01	0.02	0.68	0.03	0.02	0.01
8000	521-686	0.02	0.16	0.20	5.40	0.26	0.22	0.04	0.01	0.03	0.04	0.51	0.06	0.05	0.01
		Right Pinion							Right Pinion						
Torque	Inspection	SIpl16	SIpl17	SIpl18	SIpl19	SIpl20	SIpl21	SIpl22	SIpl16	SIpl17	SIpl18	SIpl19	SIpl20	SIpl21	SIpl22
(in-lb)	Reading	SB-3	SB-2	SB-1	GM	SB+1	SB+2	SB+3	SB-3	SB-2	SB-1	GM	SB+1	SB+2	SB+3
4000	1-69	0.02	0.05	0.15	4.10	0.47	0.09	0.08	0.01	0.01	0.03	0.21	0.02	0.02	0.03
6000	70-184	0.04	0.13	0.13	7.20	0.55	0.09	0.09	0.01	0.03	0.02	0.67	0.06	0.04	0.03
6000	185-367	0.04	0.15	0.13	7.40	0.56	0.08	0.05	0.01	0.02	0.03	0.83	0.04	0.02	0.02
8000	368-520	0.03	0.06	0.10	5.05	0.87	0.13	0.10	0.01	0.01	0.02	0.68	0.13	0.03	0.02
8000	521-686	0.07	0.06	0.14	5.40	0.99	0.19	0.07	0.02	0.02	0.03	0.51	0.14	0.06	0.03

A summary of the response of the individual sidebands to damage between each inspection interval is listed below:

1. Left gear:
    a. The +1 sideband (SI42) had the largest value when damage was observed on the gear teeth, but did not trend upward between inspection interval 368-520.
    b. The +3 sideband (SI44) had the largest value when no damage was observed on the gear teeth during run-in.
    c. After damage was observed, the following increased with lower torque and decreased with higher torques: –3 (SI38) and +3(SI44).
    d. After damage was observed, the following increased with higher torque and decreased with lower torques: –1 (SI40), and gear mesh (SI41).
    e. The following did not indicate trends with torque changes: –2 (SI39), +1 (SI42) and +2 (SI43).
2. Left pinion:
    a. The +1 sideband (SI20) and +2 sidebands (SI21) had the largest values during the test and +1 sideband (SI20) trended well with damage.
    b. The following did not indicate trends with torque changes: –2 (SI17), +1(SI20), +2(SI21) and +2 (SI22).
    c. After damage was observed, the following increased with higher torque and decreased with lower torques: –3 (SI16), –1 (SI18) and gear mesh (SI19).
    d. If you separate the trends into torque bands, *none* trended with damage at 8000 in.-lbs torque.
3. Right gear:
    a. The +1 sideband (SI42) and +2 sidebands (SI43) had the largest values during the test, but both *did not* trend well with damage.
    b. After damage was observed, the following increased with lower torque and decreased with higher torques: –3 (SI38).
    c. The following did not indicate trends with torque changes: –1(SI40), +1(SI42) and +3(SI44).
    d. The following were sensitive to torque changes but increased and decreased: –2(SI39), +2(SI43) and gear mesh (SI41).
    e. If you separate the trends into torque bands, no sideband trended with damage at 8000 in.-lbs torque.
4. Right pinion:
    a. The +1 sideband (SI20) had the largest values during the test and trended well with damage.
    b. None of the sidebands indicated significant trends with torque changes.
    c. If you separate the trends into torque bands, the following sideband trended with damage at 8000 in-lbs torque: –3 (SI16), +1 (SI20), +2(SI21).

A summary of the response of the average of +3 sidebands, the average of +1 sideband and the maximum of the +3 sidebands is listed below:

1. Left gear:
    a. The maximum sideband, average ±1 sideband and ±3 sideband *did not* trend well with damage.
    b. The maximum sideband increased with lower torque and decreased with higher torques.
    c. The ±1 and ±3 sideband did not trend with torque changes.

2. Left pinion:
    a. The maximum sideband, average ±1 sideband and ±3 sideband *did not* trend well with damage from inspection interval 368–520.
    b. The maximum sideband, and ±3 sideband trend well with damage from inspection interval 521-686.
    c. The ±1 sideband increased with lower torque and decreased with higher torques.
3. Right gear:
    a. The maximum sideband, and ±3 sideband *did not* trend well with damage.
    b. The maximum sideband and ±3 sideband increased and decreased with torque changes.
    c. The ±1 sideband had the highest value when damage occurred.
4. Right pinion:
    a. The maximum sideband, average ±1 sideband and ±3 sideband all trended with damage at 8000 in.-lbs.
    b. The maximum sideband slightly increased with higher torques and decreased with lower torques.

Test 4

Figure 12 is a plot of debris generated and the torque during test 4. Figure 13 is a plot of RMS during test 4. Tooth damage photos for the gear and pinion during the inspection intervals can be found in Figures A.4.1 to A.4.3.

For test 4, Figures A.4.1 to A.4.3 illustrate no macropitting was observed on the pinion teeth at reading 1829, 30.48 hr into the test. At reading 4034, 67.23 hr into the test, several pits were observed on the left gear teeth and micropitting on both the left and right pinion teeth. The torque remained at 6000 in.-lb during the test.

For test 4, per Figure 12, the rate of debris generation measured was at 0.51 mg/hr rate of debris generation when spalling macropitting (4.3.4) was observed at 6000 in.-lb This rate was lower than the 3.75 mg/hr rate of debris generation when spalling macropitting (4.3.4) was observed at 4000 in.-lb for test 2, and lower than the 6.37 mg/hr rate of debris generation when spalling macropitting (4.3.4) was observed at 8000 in.-lb for test 3.

Per Figure 13, RMS could not be used to isolate the pinion from the gear on the left and right side of the test rig. The left gear and pinion tracked each other very closely as did the right gear and pinion. Both responded to the restarts after inspections, but the right side was significantly more sensitive than the left. The left and right side RMS values did not trend well with damage progression until after reading 1829, then showed and increasing trend with damage. Torque was held at 6000 in.-lbs during this time period.

Figures B.4.1, B.4.5, B.4.9, and B.4.13 are plots of the individual ±3 sideband and the gear mesh for the 41 tooth gears and the 19 tooth pinions for left gear, right gear, left pinion, right pinion during the test from the MDSS. The left y-axis is scaled for the ±3 sidebands. The right y-axis is scaled for the gear (Sig41) and pinion (SI19) meshes. The x-axis correlates to the time in operation of the test rig in minutes. The yellow triangles correlate to gear tooth inspections.

Figures B.4.2, B.4.6, B.4.10, and B.4.14 are plots of the individual ±3 sideband and the gear mesh for the 41 tooth gears and the 19 tooth pinions for left gear, right gear, left pinion, right pinion during the test from the MSPU. The left y-axis is scaled for the ±3 sidebands. The right y-axis is scaled for the gear (Sig41) and pinion (SI19) meshes. The yellow triangles correlate to gear tooth inspections per Table 9.

Figures B.4.3, B.4.7, B.4.11, and B.4.15 are plots of the average ±1 sidebands, average ±3 sidebands and the maximum of the ±3 sidebands for left gear, right gear, left pinion, right pinion during the test from the MDSS. The yellow triangles correlate to gear tooth inspections.

Figures B.4.4, B.4.8, B.4.12, and B.4.16 are plots of the average ±1 sidebands, average ±3 sidebands and the maximum of the ±3 sidebands for left gear, right gear, left pinion, right pinion during the test from the MSPU. The yellow triangles correlate to gear tooth inspections per Table 9.

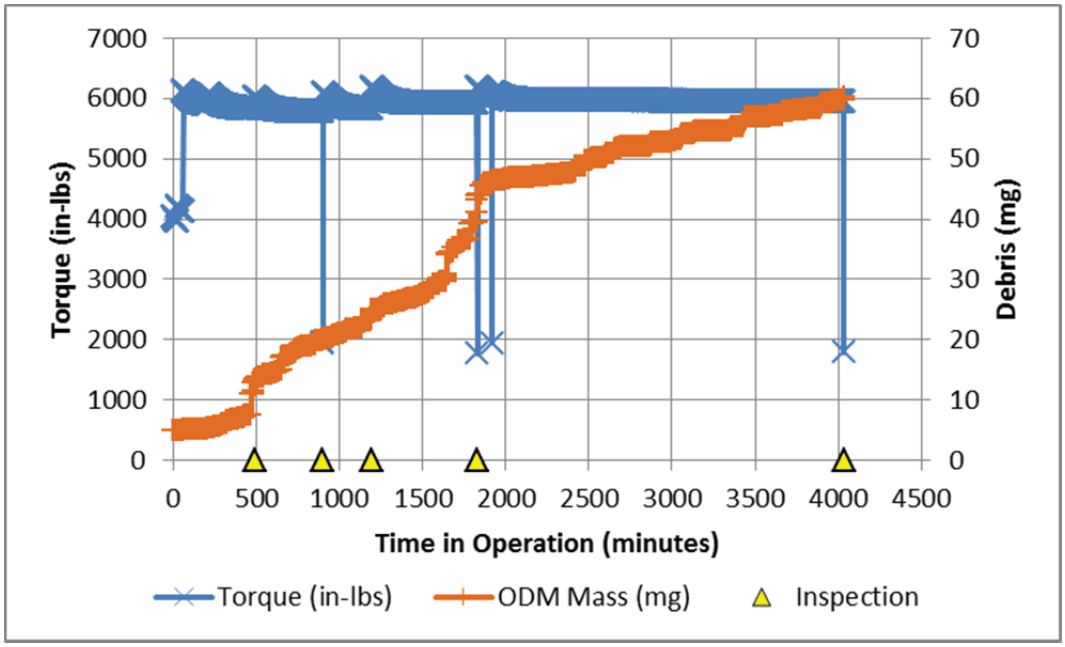

Figure 12.—Debris generated and torque during test 4.

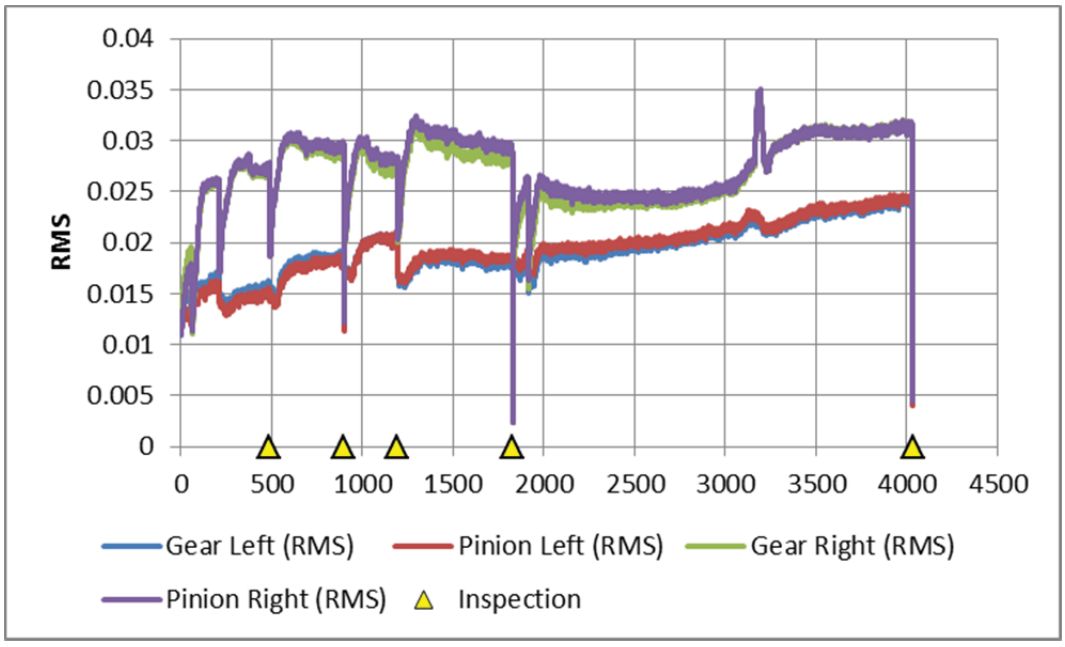

Figure 13.—RMS during test 4.

Table 14 is a summary of the mean and standard deviation values for the individual sidebands between each inspection interval. The columns highlighted in blue are the gear and pinion meshes. The cells highlighted in red have the maximum values within that inspection interval. The cells highlighted in yellow have the next maximum values. The cells highlighted in green have the minimum values.

For test 4, Figures A.4.1 to A.4.3, in Appendix A, illustrate no macropitting was observed on the pinion teeth 30 hr into the test. Sixty-seven hours into the test, several pits were observed on the left gear teeth and micropitting on both the left and right pinion teeth. The torque remained at 6000 in.-lb during the test.

TABLE 14.—SUMMARY OF SIDEBAND FOR TEST 4

L1103R1204		Means							Standard Deviations						
		Left Gear							Left Gear						
Torque	Inspection	Slgl38	Slgl39	Slgl40	Slgl41	Slgl42	Slgl43	Slgl44	Slgl38	Slgl39	Slgl40	Slgl41	Slgl42	Slgl43	Slgl44
(in-lb)	Reading	SB-3	SB-2	SB-1	GM	SB+1	SB+2	SB+3	SB-3	SB-2	SB-1	GM	SB+1	SB+2	SB+3
4000	1-60	0.13	0.14	0.18	1.61	0.16	0.33	0.44	0.02	0.04	0.02	0.07	0.08	0.05	0.07
6000	61-489	0.04	0.11	0.16	1.86	0.23	0.20	0.24	0.01	0.02	0.03	0.11	0.03	0.05	0.05
6000	490-901	0.04	0.10	0.17	2.25	0.22	0.17	0.28	0.01	0.01	0.02	0.19	0.02	0.04	0.03
6000	902-1196	0.04	0.09	0.14	2.53	0.23	0.16	0.26	0.01	0.03	0.03	0.21	0.02	0.06	0.04
6000	1197-1829	0.03	0.08	0.14	2.28	0.21	0.12	0.23	0.01	0.02	0.03	0.12	0.03	0.04	0.03
6000	1830-4034	0.04	0.07	0.09	2.65	0.16	0.11	0.20	0.01	0.01	0.02	0.28	0.04	0.04	0.03
		Left Pinion							Left Pinion						
Torque	Inspection	Slpl16	Slpl17	Slpl18	Slpl19	Slpl20	Slpl21	Slpl22	Slpl16	Slpl17	Slpl18	Slpl19	Slpl20	Slpl21	Slpl22
(in-lb)	Reading	SB-3	SB-2	SB-1	GM	SB+1	SB+2	SB+3	SB-3	SB-2	SB-1	GM	SB+1	SB+2	SB+3
4000	1-60	0.03	0.09	0.08	1.61	0.19	0.24	0.08	0.02	0.01	0.02	0.07	0.02	0.02	0.03
6000	61-489	0.04	0.08	0.12	1.86	0.11	0.32	0.06	0.02	0.02	0.02	0.11	0.03	0.04	0.02
6000	490-901	0.06	0.07	0.11	2.26	0.05	0.31	0.10	0.02	0.01	0.02	0.19	0.02	0.03	0.02
6000	902-1196	0.04	0.11	0.10	2.53	0.05	0.32	0.18	0.03	0.01	0.01	0.21	0.04	0.03	0.04
6000	1197-1829	0.11	0.12	0.09	2.28	0.05	0.34	0.31	0.03	0.01	0.02	0.12	0.03	0.04	0.04
6000	1830-4034	0.13	0.12	0.23	2.65	0.15	0.33	0.25	0.03	0.02	0.04	0.28	0.02	0.05	0.06
L1103R1204		Means							Standard Deviations						
		Right Gear							Right Gear						
Torque	Inspection	Slgr38	Slgr39	Slgr40	Slgr41	Slgr42	Slgr43	Slgr44	Slgr38	Slgr39	Slgr40	Slgr41	Slgr42	Slgr43	Slgr44
(in-lb)	Reading	SB-3	SB-2	SB-1	GM	SB+1	SB+2	SB+3	SB-3	SB-2	SB-1	GM	SB+1	SB+2	SB+3
4000	1-60	0.21	0.08	0.03	2.05	0.16	0.27	0.07	0.03	0.02	0.02	0.33	0.06	0.02	0.04
6000	61-489	0.05	0.12	0.12	3.36	0.27	0.15	0.05	0.01	0.04	0.02	0.54	0.04	0.03	0.03
6000	490-901	0.06	0.13	0.13	3.88	0.33	0.15	0.03	0.01	0.03	0.02	0.33	0.04	0.02	0.03
6000	902-1196	0.06	0.11	0.12	3.69	0.37	0.12	0.05	0.01	0.03	0.03	0.33	0.04	0.02	0.03
6000	1197-1829	0.05	0.09	0.13	3.88	0.40	0.14	0.06	0.01	0.02	0.03	0.28	0.03	0.02	0.02
6000	1830-4034	0.07	0.08	0.12	3.54	0.47	0.17	0.08	0.01	0.01	0.02	0.50	0.03	0.03	0.02
		Right Pinion							Right Pinion						
Torque	Inspection	Slpl16	Slpl17	Slpl18	Slpl19	Slpl20	Slpl21	Slpl22	Slpl16	Slpl17	Slpl18	Slpl19	Slpl20	Slpl21	Slpl22
(in-lb)	Reading	SB-3	SB-2	SB-1	GM	SB+1	SB+2	SB+3	SB-3	SB-2	SB-1	GM	SB+1	SB+2	SB+3
4000	1-60	0.03	0.05	0.20	2.05	0.40	0.07	0.14	0.01	0.01	0.02	0.33	0.04	0.03	0.05
6000	61-489	0.04	0.05	0.41	3.36	0.70	0.13	0.15	0.01	0.02	0.04	0.54	0.08	0.05	0.03
6000	490-901	0.04	0.05	0.44	3.88	0.78	0.21	0.21	0.01	0.02	0.04	0.32	0.11	0.04	0.03
6000	902-1196	0.02	0.06	0.41	3.69	0.94	0.26	0.15	0.01	0.02	0.05	0.33	0.12	0.03	0.05
6000	1197-1829	0.05	0.06	0.45	3.88	0.98	0.27	0.10	0.02	0.01	0.03	0.28	0.09	0.03	0.06
6000	1830-4034	0.11	0.04	0.54	3.54	0.78	0.25	0.21	0.02	0.02	0.04	0.50	0.12	0.08	0.10

A summary of the response of the individual sidebands to damage between each inspection interval is listed below:

1. Left gear:
    a. The +3 sideband (SI44) had the largest value when damage was observed on the gear teeth.
    b. Since torque remained at 6000 in.-lbs after run-in, no effects due to torque changes could be evaluated for this test.
    c. None of the sidebands trended with damage at 6000 in.-lbs. Although the values increased as damage progressed at the end of the test for +1(SI42) and +2(SI43), these values were higher at the beginning of the test.
2. Left pinion:
    a. The +2 sidebands (SI21) had the largest values during the test, but both *did not* trend well with damage.
    b. None of the sidebands trended with damage at 6000 in.-lbs. Although +3(SI22) increased when damage was first observed on the gear teeth, it dropped in value later in the test.
3. Right gear:
    a. The +1 sideband (SI42) and +2 sidebands (SI43) had the largest values during the test.
    b. The +1 sideband (SI42) increased with damage.
4. Right pinion:
    a. The +1 sideband (SI20) had the largest values during the test, increased with damage, decreased as the test progressed along with +2 (SI21).

A summary of the response of the average of +3 sidebands, the average of +1 sideband and the maximum of the +3 sidebands is listed below:

1. Left gear:
    a. The maximum sideband, average ±1 sideband and ±3 sideband *did not* trend well with damage.
    b. Although the values seem to increase at reading 3500 as damage these values were higher at the beginning of the test.
2. Left pinion:
    a. The ±3 sideband *did* trend with damage.
3. Right gear:
    a. The maximum sideband, average +1 sideband and +3 sideband increased with damage until reading 3200, then decreased.
4. Right pinion:
    a. The maximum sideband, average ±1 sideband and ±3 sideband increased with damage until inspection 1196, then decreased.

Discussion of Results

Many factors affect the gear CI's ability to respond to tooth damage through vibration response. The response of the accelerometer to a specific fault can depend on the sensor specifications, the signal processing of the raw signal, mounting and its location. The CI method of calculation, operational conditions and type of failure mode can also affect its response.

For these tests, accelerometer specifications, signal processing, mounting, location and structure remained the same for all four tests. Per table 10, the physical inputs {I} such as speed, temperatures and oil pressures remained within a small range for all tests once they reached steady-state conditions after restarting. Torque varied for several tests. The internal response {R} can change due to damage, but also type of failure mode and level of damage. Due to the design of our test rig, the internal response of the

gear set on the left side may affect the right side. It was also found that the right and left side of our test rig responded differently to the varying levels of torque. The measured output {O}, vibration response from the left and right accelerometers then feeds into a CI calculation for the left gear, left pinion, right gear and right pinion. Each CI can respond differently to varying torque levels and varying levels of damage.

Reviewing the RMS values for the four tests, several observations could be made. During test one, RMS values for all four components trended with damage when torque was maintained. RMS values for the right gear and pinion were significantly more sensitive to torque changes and shutdowns than the left for all four tests. During tests two and three, no RMS values trended with component damage, most likely due to varying torque levels throughout the test. During test four, RMS values for the left gear and pinion trended with component damage when torque was maintained.

Individual sidebands, average and maximum sidebands responded differently for each test, torques, damage modes and components. In regards to torque changes, one interesting observation is that the amplitude changes with load, but not necessarily in a positive direction—lower torques produce higher amplitudes for some sidebands.

Assessing whether a change in any particular condition indicator or sideband feature was due to only a change in damage level, a change in operating condition or some combination of both was a challenge since there are gaps in the data across all tests in regards to the different operating conditions. From what has been learned during this preliminary investigation, future tests are planned to determine the magnitude of these effects on the CI data collected. However, an initial investigation of the response of the different sideband indexes to damage modes will be presented.

To perform the assessment required assigning a continuous monotonic increasing value to the different damage modes observed during each inspection interval. The values chosen for each test are listed in Table 15. The values were chosen based on the level of damage and the damage of the most interest for this study. A value of 0.1 was assigned to gear teeth broken in with no damage while a value of 5 indicates progressive macro-pitting on two or more gear teeth. Optimization of defining and assigning values to the damage modes for future tests is also planned.

Damage values based on component tooth damage were generated for each reading for each test. Figure 14 is a plot of the damage values from Table 15 for test 1. An average damage value was also calculated for all 4 components for each reading. A fifth parameter, referred to as 4.3.2 Progressive, is a damage value when progressive pitting was observed on two or more teeth on any of the four components. For example, during test 1, this value was 0.1 until reading 1862. After this reading, the damage value remained at 5 for the rest of the test. Values were assigned and used to determine the sensitivity of the CI to this specific failure mode. Also note for tests 2 and 3, the torque changed within an inspection interval. Further work is required to optimize the values or classify and cluster them with additional information.

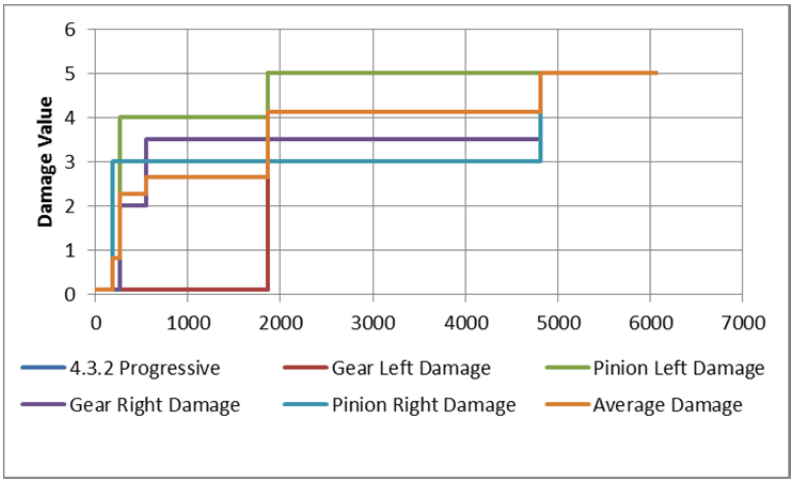

Figure 14.—Damage values for test 1.

TABLE 15.—ASSIGNED DAMAGE VALUES FOR DAMAGE MODES

Test 1	Rdg(Min)	Torque	Gear Left	Pinion Left	Gear Right	Pinion Right
Start	0	0	0.1	0.1	0.1	0.1
Run-in	60	4000	0.1	0.1	0.1	0.1
Inspection	1-186	4000	0.1	0.1	0.1	0.1
Inspection	187-269	8000	0.1	0.1	0.1	3
Inspection	270-553	8000	0.1	4	2	3
Inspection	554-1862	8000	0.1	4	3.5	3
Inspection	1863-4814	8000	5	5	3.5	3
Inspection	4815-6065	8000	5	5	5	5
Test 2	Rdg(Min)	Torque	Gear Left	Pinion Left	Gear Right	Pinion Right
Start	0	0	0.1	0.1	0.1	0.1
Run-in	60	4000	0.1	0.1	0.1	0.1
Inspection	1-108	4000	0.1	0.1	0.1	0.1
	202	4000	1	2	2	3
Inspection	109-379	8000	1	2	2	3
	468	4000	1	5	2	3
Inspection	380-559	8000	1	5	2	3
	632	4000	1	5	2	3
Inspection	560-662	8000	1	5	2	3
Test 3	Rdg(Min)	Torque	Gear Left	Pinion Left	Gear Right	Pinion Right
Start	0	4000	0.1	0.1	0.1	0.1
Run-in	69	4000	0.1	0.1	0.1	0.1
Inspection	69-184	6000	1	0.1	0.1	0.1
	367	6000	1	4	2	4
Inspection	185-520	8000	1	4	2	4
Inspection	521-686	8000	1	4	2	5
Test 4	Rdg(Min)	Torque	Gear Left	Pinion Left	Gear Right	Pinion Right
Start	0	4000	0.1	0.1	0.1	0.1
Run-in	60	4000	0.1	0.1	0.1	0.1
Inspection	61-489	6000	1	0.1	2	4
Inspection	490-901	6000	1	4	2	4
Inspection	902-1196	6000	1	4	2	4
Inspection	1197-1829	6000	1	4	2	4
Inspection	1830-4034	6000	5	4	2	4

To assess the relationship between the different parameters, Pearson Correlation Coefficients (r) were calculated for the parameters. Correlations coefficients measure the strength and direction of the linear relationship between two parameters (Ref. 21). Correlation coefficients are calculated by dividing the covariance of the two variables by the product of their standard deviations. Its value ranges between –1 and +1. A perfect linear relationship between two parameters will have a correlation coefficient of 1 or –1. The focus for this analysis will be on r values greater than or equal to 0.8, indicating a CI response with a strong correlation to damage modes. A correlation matrix is generated for each test showing the linear relationship between CIs for the four components, torque, oil debris mass, and the six damage values calculated for the damage modes. Note that this method will only indicate linear relationships between parameters.

One example of this analyses applied to test 1 will be presented. The left and right, gear and pinion, maximum and average ±1 sideband indexes were calculated for comparison. Per review of the data in Table 11 the –3 sideband and the +3 sideband had the least response due to damage as compared to the ±1 and ±2 sidebands. For this reason, the average ±2 sidebands were calculated instead of the ±3 for all four components for comparison using the correlation coefficients. The correlation tables for test 1 is shown in Table 16.

TABLE 16.—TEST 1 CORRELATION TABLE

Test 1 Correlation Coefficient Matrix																
Test List Names:	Gear left max SI	Gear Left mean 2SI	Gear Left mean 1SI	Pinion Left max SI	Pinion Left mean 2SI	Pinion Left mean 1SI	Gear Right max SI	Gear Right mean 2SI	Gear Right mean 1SI	Pinion Right max SI	Pinion Right mean 2SI	Pinion Right mean 1SI	ODM Mass (mg)
Gear left max SI	1.00												
Gear Left mean 2SI	0.93	1.00											
Gear Left mean 1SI	0.15	0.44	1.00										
Pinion Left max SI	0.82	0.69	-0.18	1.00									
Pinion Left mean 2SI	0.81	0.67	-0.24	0.97	1.00								
Pinion Left mean 1SI	0.83	0.69	-0.21	0.99	0.98	1.00							
Gear Right max SI	0.58	0.44	-0.43	0.81	0.87	0.82	1.00						
Gear Right mean 2SI	0.77	0.64	-0.27	0.89	0.93	0.91	0.92	1.00					
Gear Right mean 1SI	0.79	0.64	-0.23	0.89	0.92	0.90	0.87	0.96	1.00				
Pinion Right max SI	0.82	0.69	-0.18	1.00	0.97	0.99	0.81	0.89	0.89	1.00			
Pinion Right mean 2SI	0.59	0.46	-0.35	0.85	0.90	0.86	0.90	0.90	0.85	0.85	1.00		
Pinion Right mean 1SI	0.50	0.38	-0.36	0.79	0.83	0.80	0.89	0.85	0.79	0.79	0.98	1.00	
ODM Mass (mg)	0.53	0.36	-0.50	0.80	0.88	0.82	0.91	0.83	0.80	0.80	0.90	0.87	1.00
4.3.2 Progressive	0.48	0.36	-0.39	0.72	0.80	0.72	0.88	0.82	0.79	0.72	0.91	0.92	0.88
Gear Left Damage	0.48	0.36	-0.33	0.72	0.80	0.72	0.88	0.82	0.79	0.72	0.91	0.92	0.88
Pinion Left Damage	0.18	0.05	-0.34	0.46	0.53	0.45	0.60	0.45	0.42	0.46	0.65	0.63	0.72
Gear Right Damage	0.38	0.21	-0.38	0.57	0.63	0.57	0.60	0.47	0.50	0.57	0.53	0.46	0.75
Pinion Right Damage	0.56	0.44	-0.08	0.61	0.64	0.61	0.47	0.44	0.53	0.61	0.45	0.35	0.64
Average Damage	0.49	0.34	-0.35	0.73	0.80	0.73	0.82	0.72	0.72	0.73	0.82	0.79	0.92

Test 1 Correlation Coefficient Matrix					
Test List Names:	4.3.2 Progressive	Gear Left Damage	Pinion Left Damage	Gear Right Damage	Pinion Right Damage
4.3.2 Progressive	1.00				
Gear Left Damage	1.00	1.00			
Pinion Left Damage	0.69	0.69	1.00		
Gear Right Damage	0.52	0.52	0.78	1.00	
Pinion Right Damage	0.41	0.41	0.57	0.87	1.00
Average Damage	0.87	0.87	0.88	0.86	0.76

For test 1, ±2 average sidebands for the left pinion, right gear and right pinion, ±1 average sidebands for the right pinion and maximum sidebands for the right gear had a strong correlation to damage mode 4.3.2. Average damage had a strong correlation to ±2 average sidebands for the left and right pinion and the maximum sidebands for the right gear. Oil debris mass sensor also correlated to damage mode 4.3.2 and average damage values. *All* 4 components had 4.3.2 damage at the end of the test. Note that no left gear sideband index values responded well to damage. One interesting observation was that a correlation coefficient value of 1 existed between the left pinion and right pinion maximum sideband values for all four tests. This indicates the coupling of the right and left pinion through their shafts in our test rig. Use of this CI to differentiate between the two components if only one had damage may be challenging. Results of the correlation coefficient analysis indicated strong linear correlations did not exist between several of the CIs measured during varying test conditions. However, non-linear correlations may exist between the CIs, damage modes and operating conditions that will require further analysis with different methods. Future test data will need to be generated that enables grouping the data into comparable torques and damage levels for comparison.

Summary

The purpose of this analysis was to evaluate the ability of gear CI to detect contact fatigue damage on spiral bevel gear teeth. Tests were performed in the NASA Glenn Spiral Bevel Gear Fatigue Rig on eight prototype gear sets during four damage progression tests. Vibration data was measured at varying torque, while varying modes and levels of tooth damage were observed. Due to the prototype gear design, failures modes in addition to contact fatigue occurred during testing.

Gear condition indicator (CI) sideband index and individual sideband amplitudes were assessed to determine if they could detect contact fatigue damage on spiral bevel gear teeth. For these tests, individual, average and maximum sideband indexes (SI) responded differently for each test, torques, damage levels, damage modes and component.

The performance of CI, RMS, was also evaluated for its ability to detect spiral bevel gear tooth damage. RMS values trended with damage progression when torque was maintained but did not trend well with damage progression at varying torque levels. It was also found that the RMS values for the right side of our test rig were significantly more sensitive to torque changes than the left side.

Lessons learned during this preliminary investigation will be used to define the testing and analysis methods for future testing of forty-two final design gear sets.

Appendix A.—Representative Photos of Gear and Pinion Teeth Damage

Figure A.1.1.—Test 1 gear and pinion damage modes.

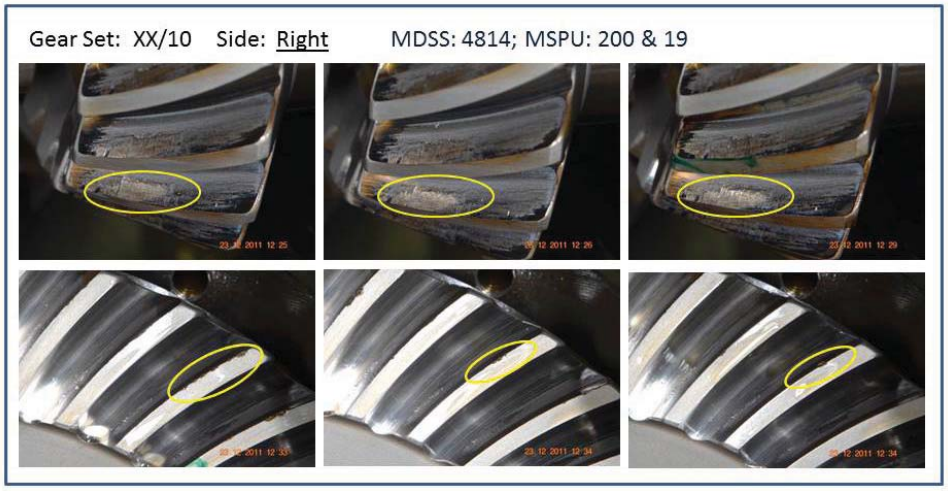

Figure A.1.2.—Test 1 gear and pinion damage modes.

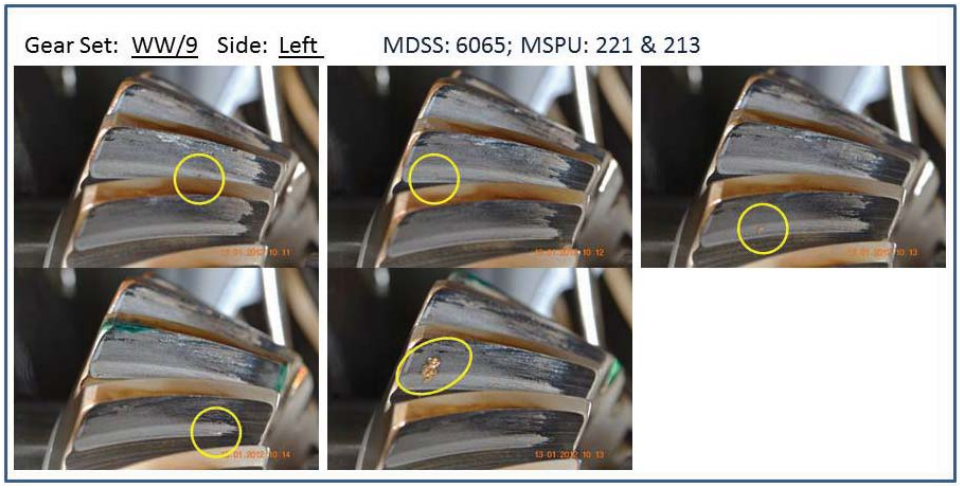

Figure A.1.3.—Test 1 gear and pinion damage modes.

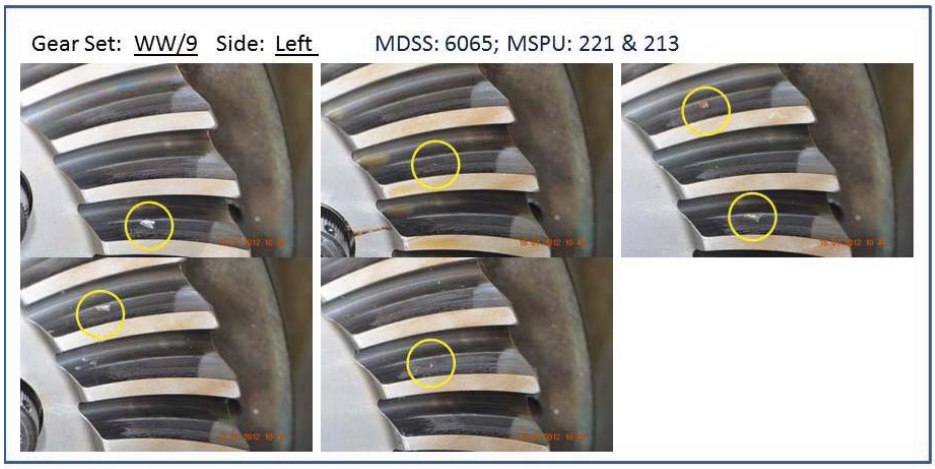

Figure A.1.4.—Test 1 gear and pinion damage modes.

Figure A.1.5.—Test 1 gear and pinion damage modes.

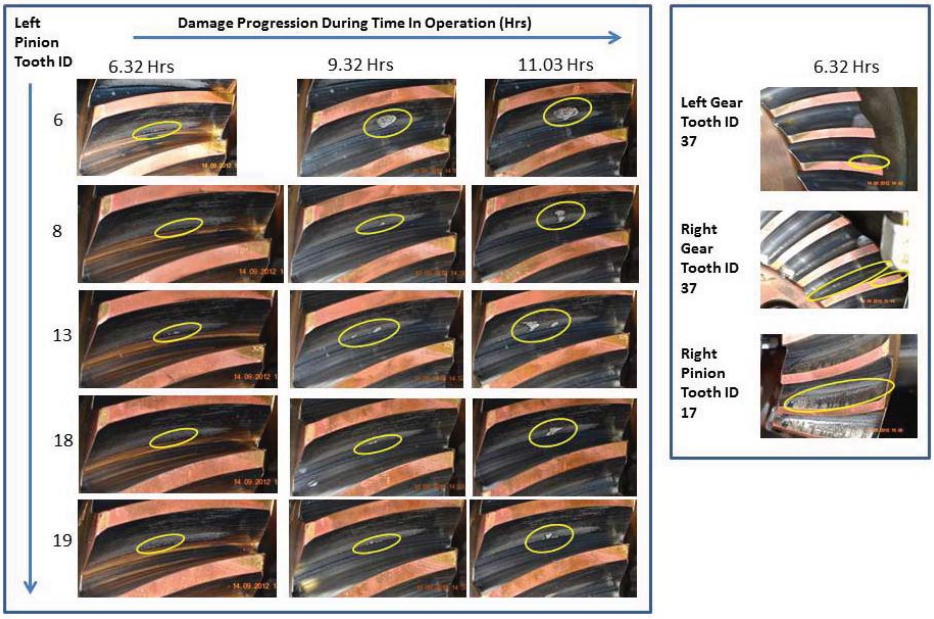

Figure A.2.1.—Test 2 gear and pinion damage modes.

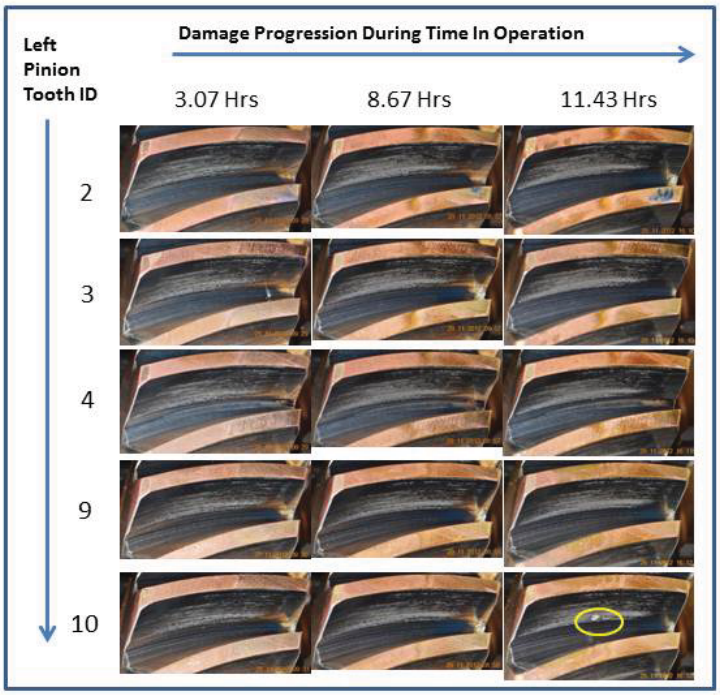

Figure A.3.1.—Test 3 gear and pinion damage modes.

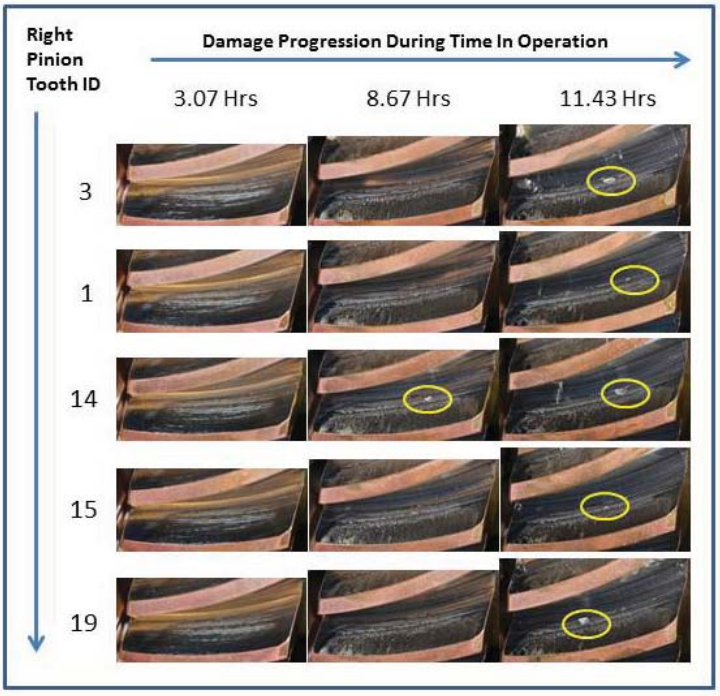

Figure A.3.2.—Test 3 gear and pinion damage modes.

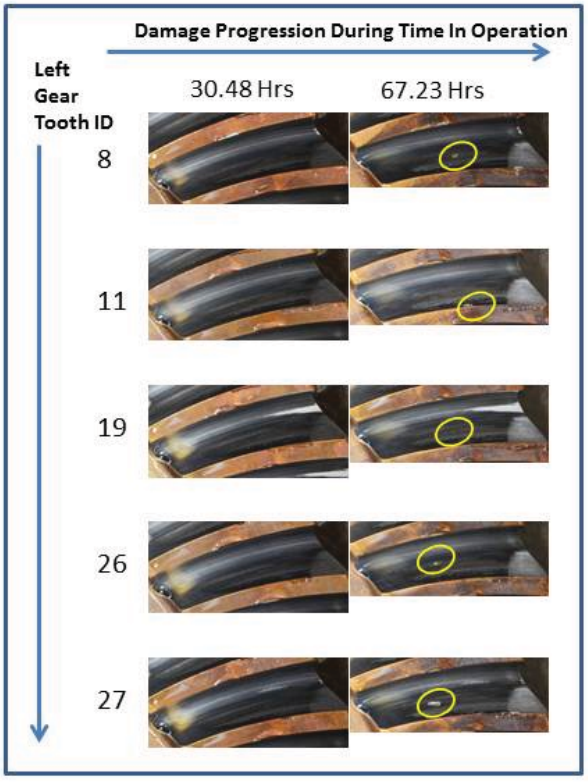

Figure A.4.1.—Test 4 gear and pinion damage modes.

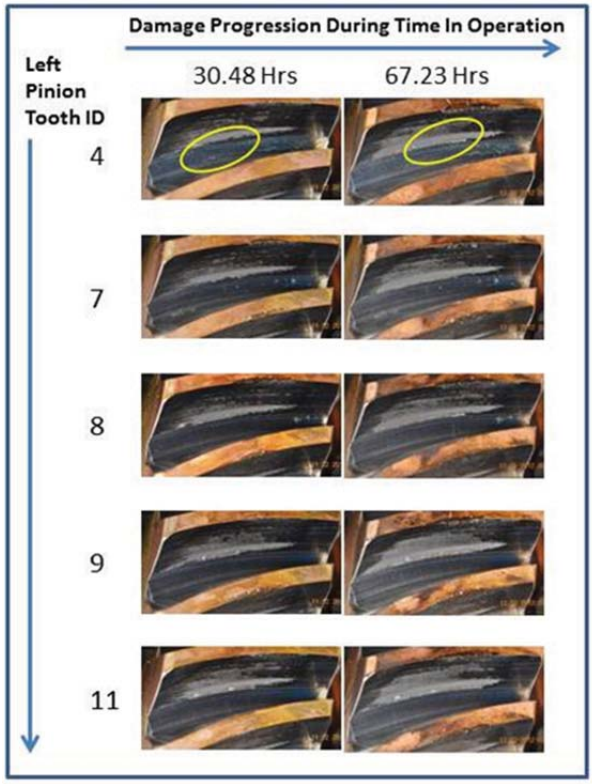

Figure A.4.2.—Test 4 gear and pinion damage modes.

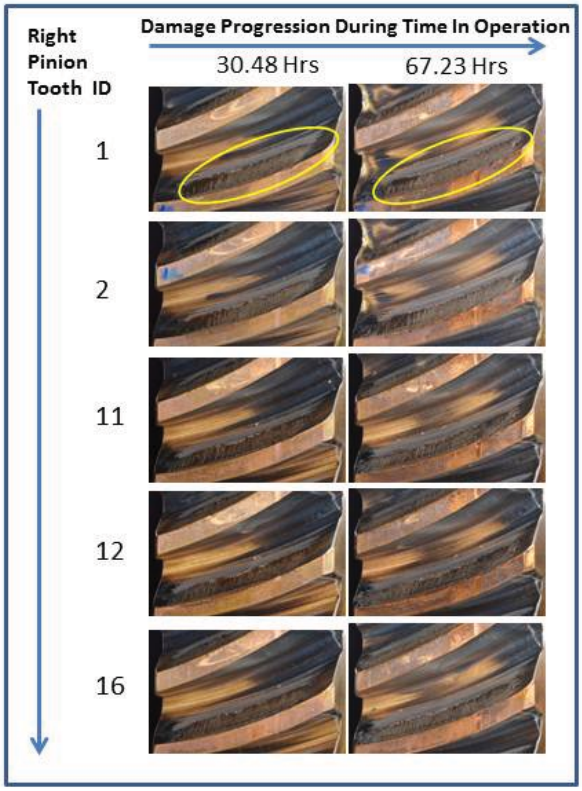

Figure A.4.3.—Test 4 gear and pinion damage modes.

Appendix B.—Plots of MDSS and MSPU Individual, Average of ±1 Sideband, ±3 Sideband and Maximum Sideband

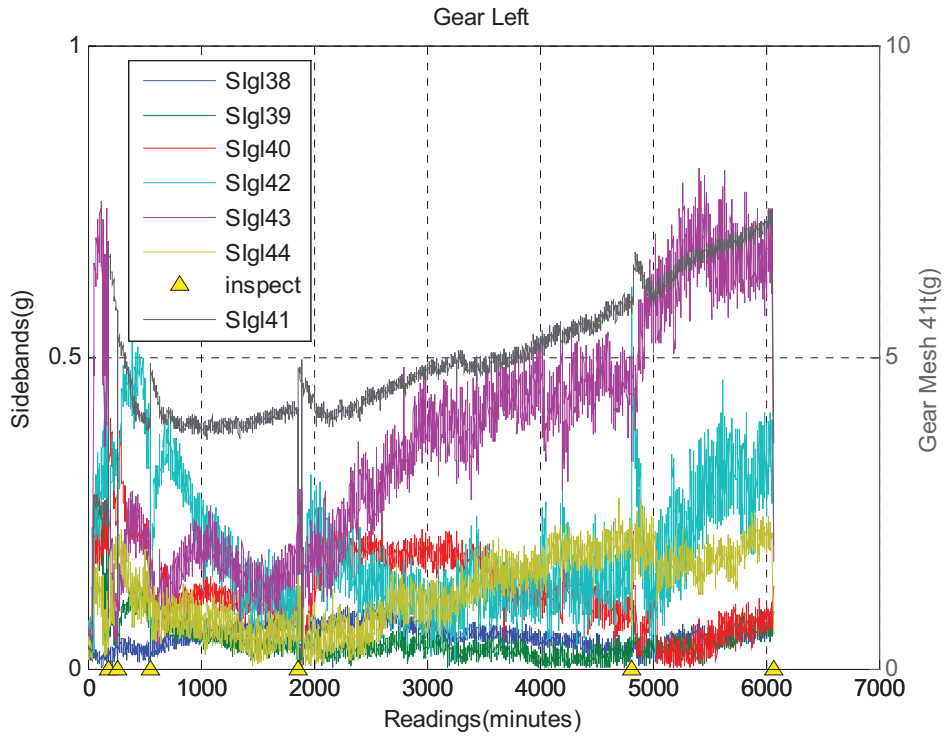

Figure B.1.1.—Test 1 plot of left gear individual sidebands for MDSS.

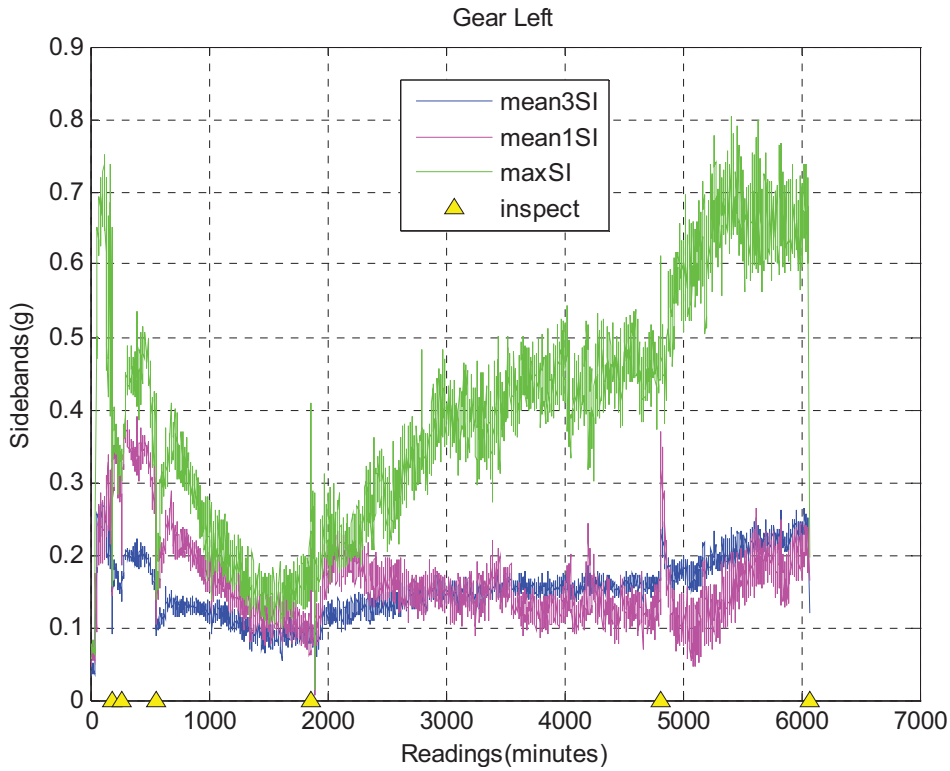

Figure B.1.2.—Test 1 plot of left gear average and maximum sidebands for MDSS.

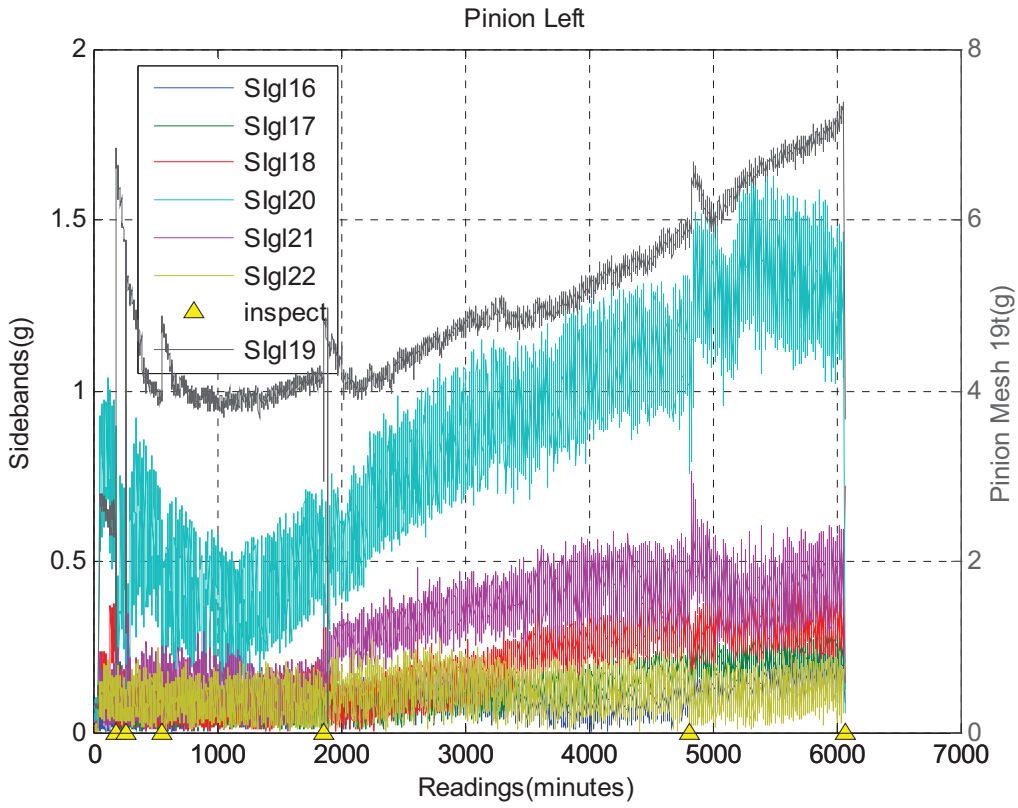

Figure B.1.3.—Test 1 plot of left pinion individual sidebands for MDSS.

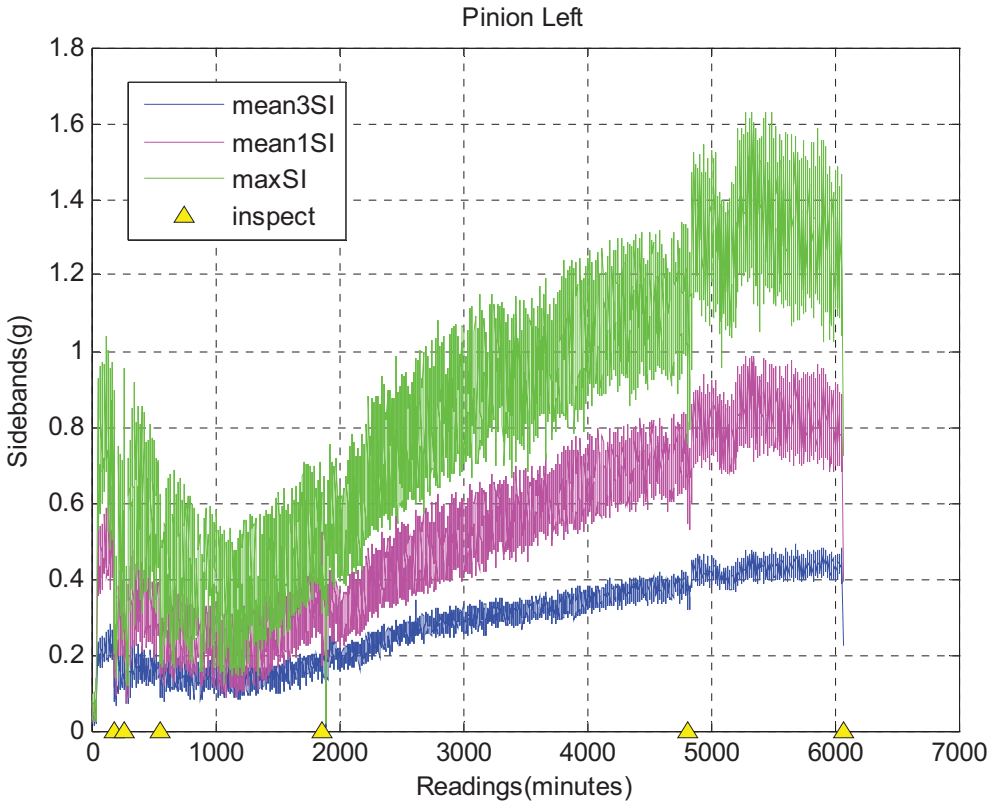

Figure B.1.4.—Test 1 plot of left pinion average and maximum sidebands for MDSS.

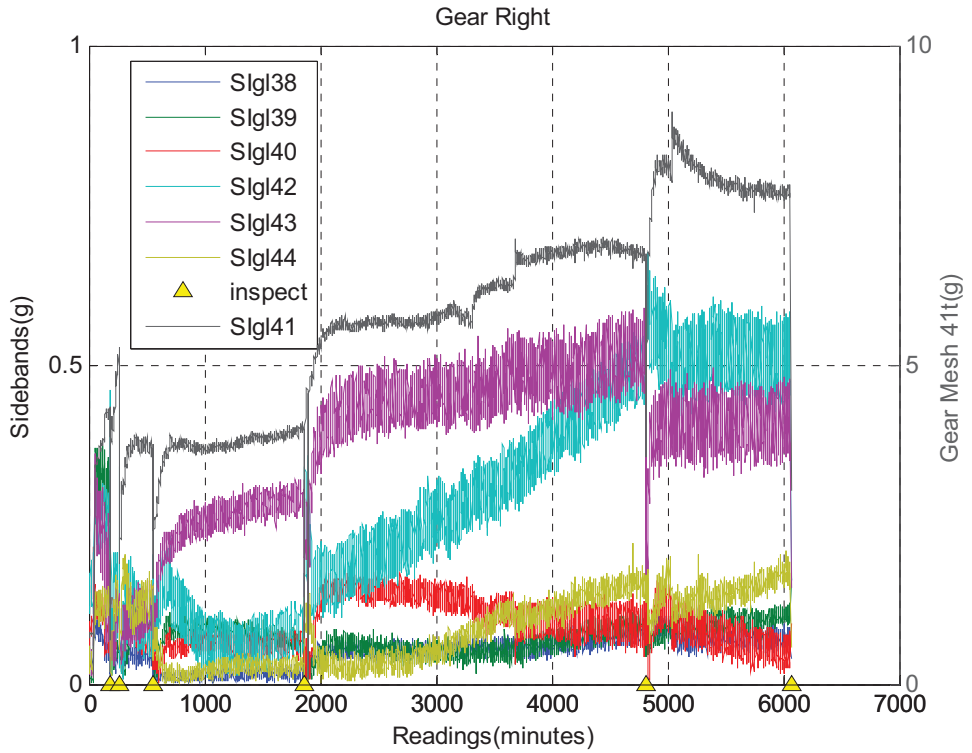

Figure B.1.5.—Test 1 plot of right gear individual sidebands for MDSS.

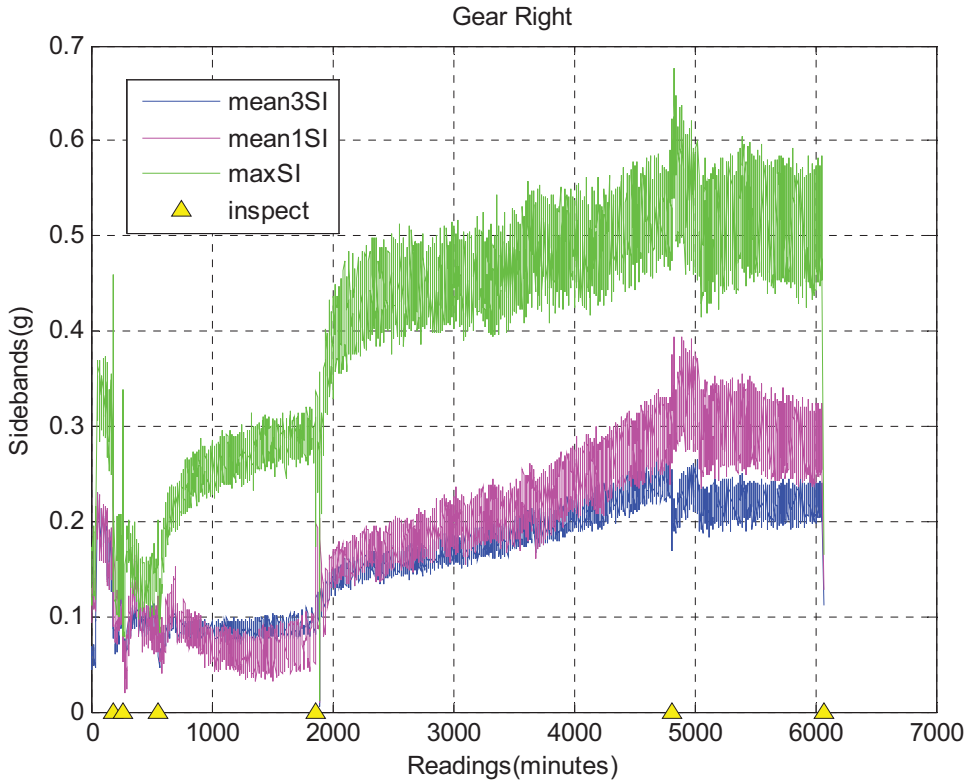

Figure B.1.6.—Test 1 plot of right gear average and maximum sidebands for MDSS.

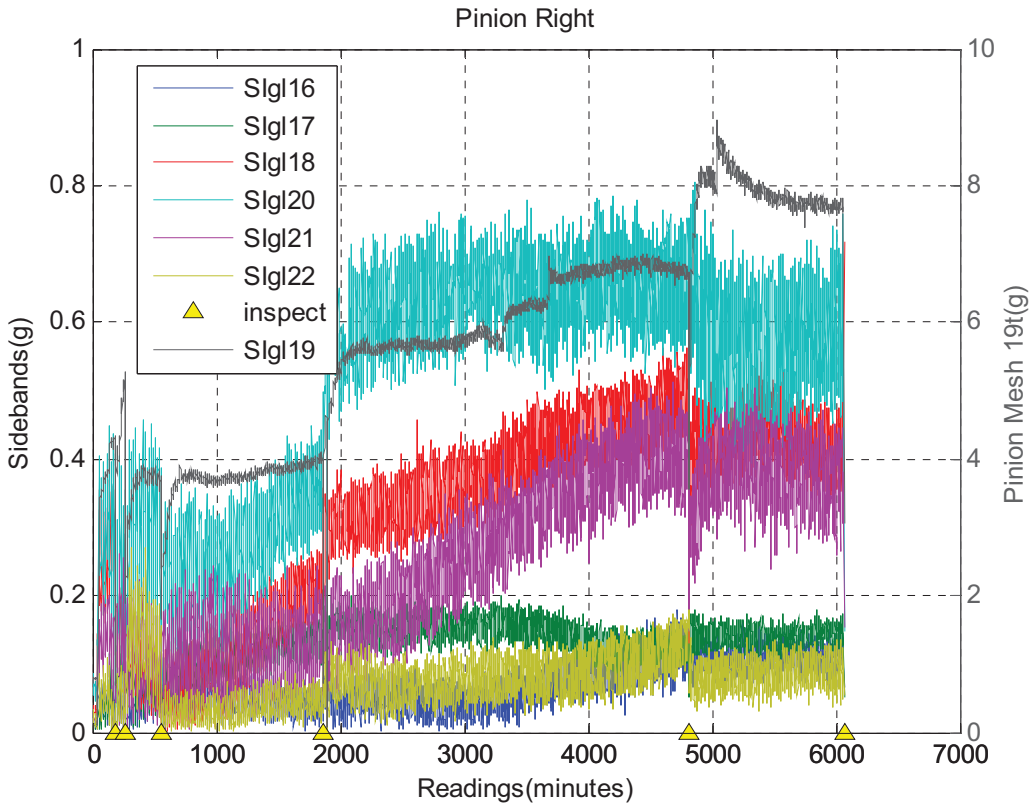

Figure B.1.7.—Test 1 plot of right pinion individual sidebands for MDSS.

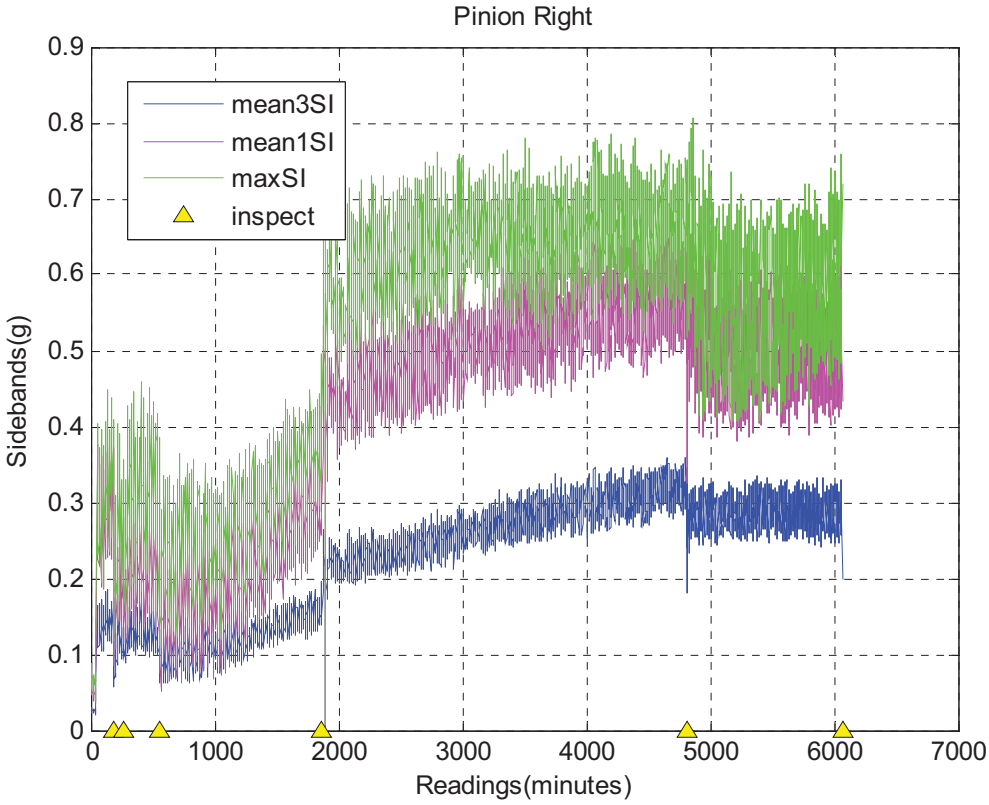

Figure B.1.8.—Test 1 plot of right pinion average and maximum sidebands for MDSS.

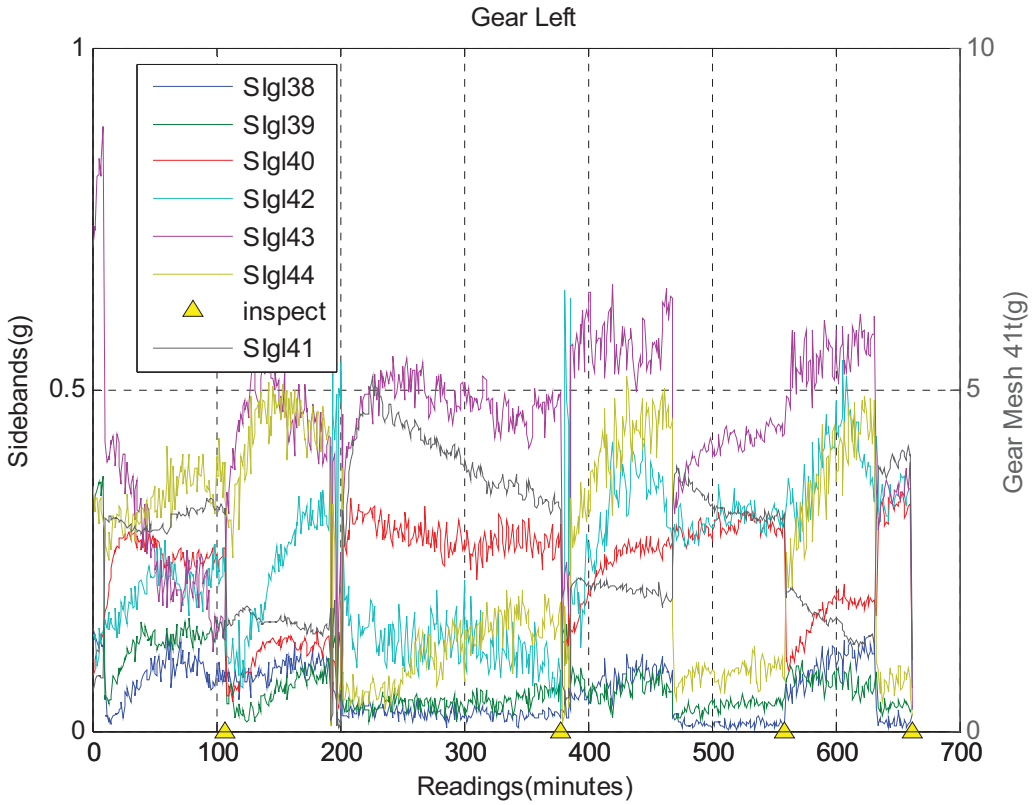

Figure B.2.1.—Test 2 plot of left gear individual sidebands for MDSS.

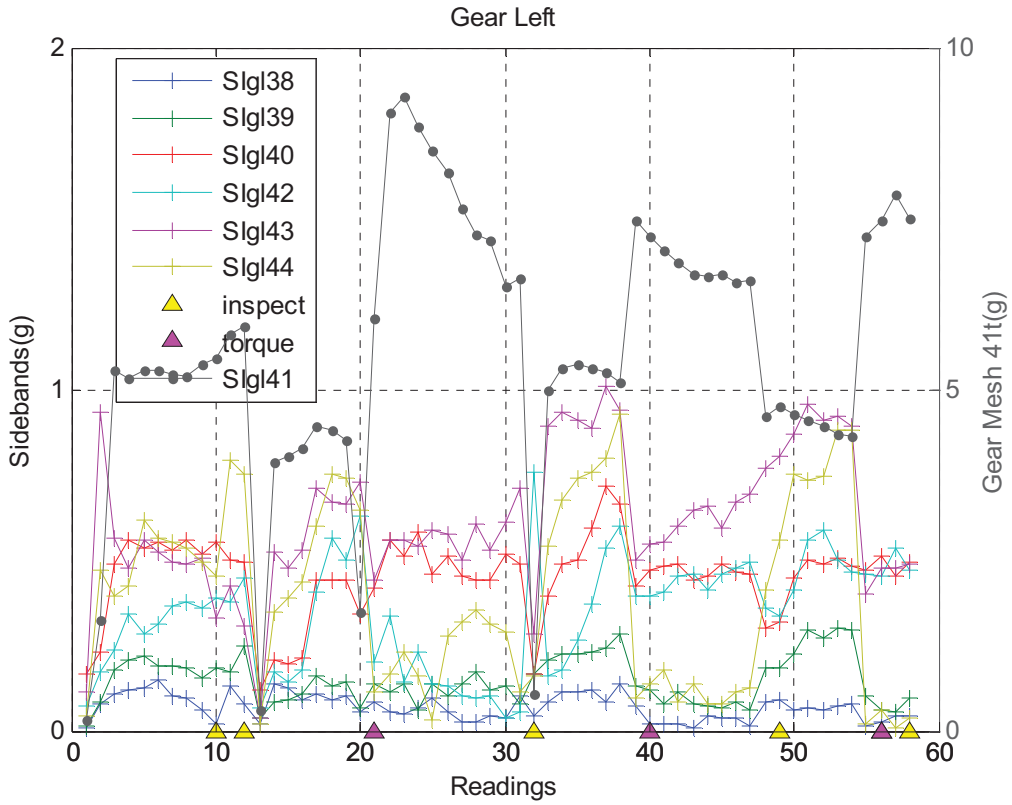

Figure B.2.2.—Test 2 plot of left gear individual sidebands for MSPU.

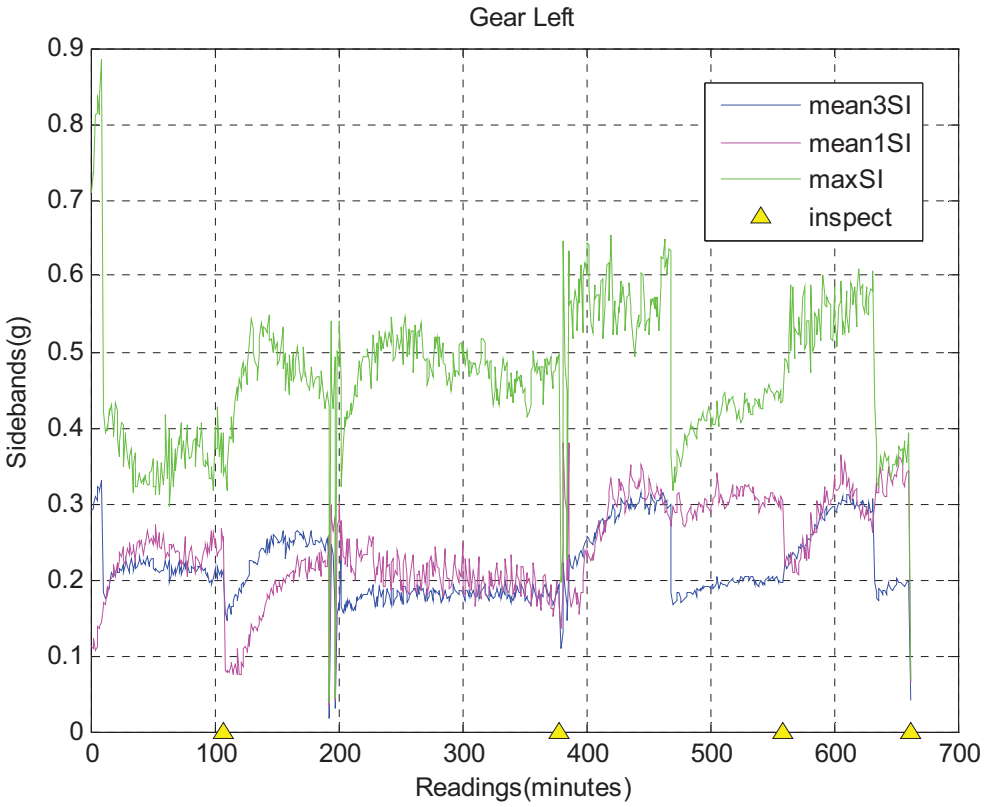

Figure B.2.3.—Test 2 plot of left gear average and maximum sidebands for MDSS.

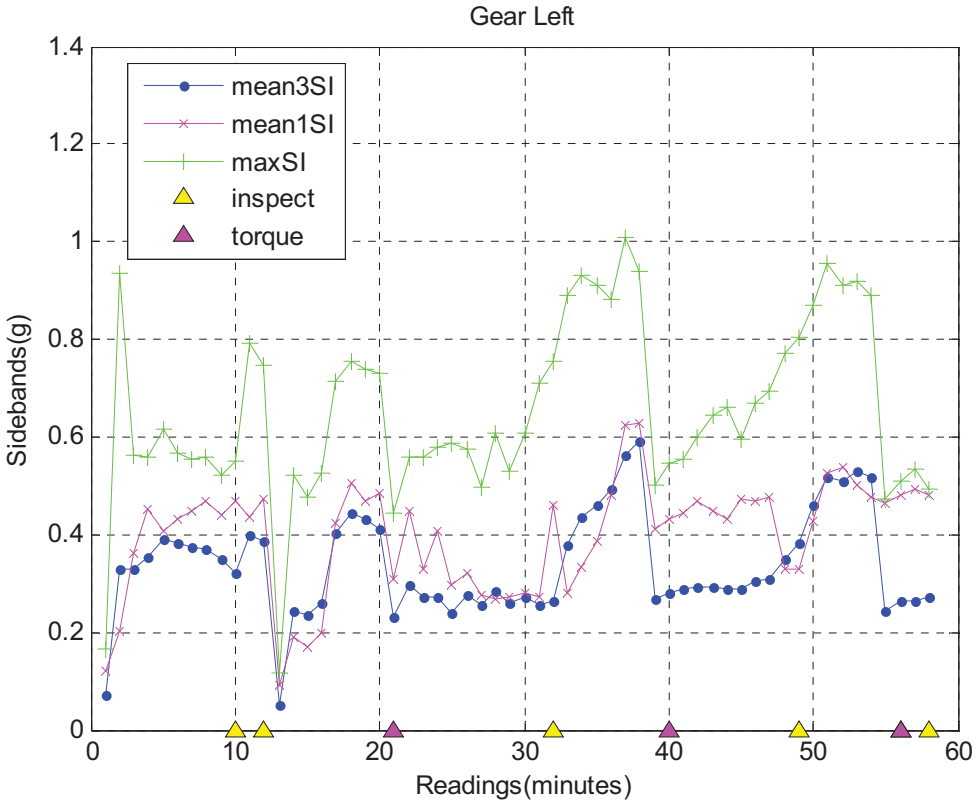

Figure B.2.4.—Test 2 plot of left gear average and maximum sidebands for MSPU.

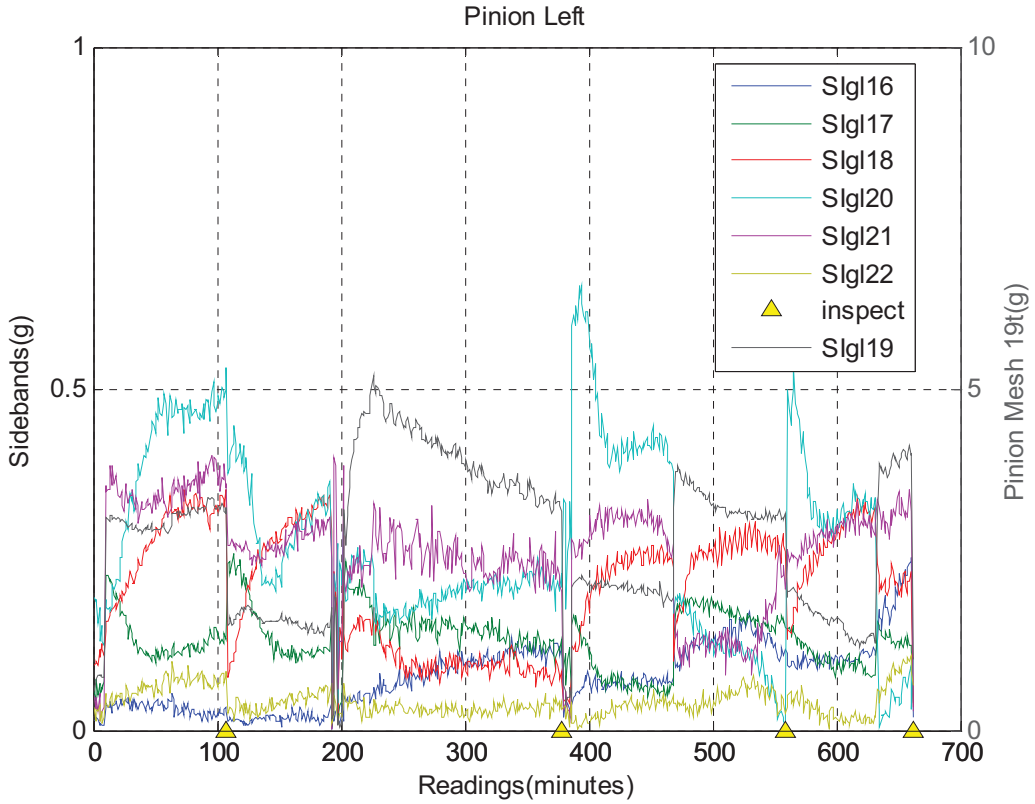

Figure B.2.5.—Test 2 plot of left pinion individual sidebands for MDSS.

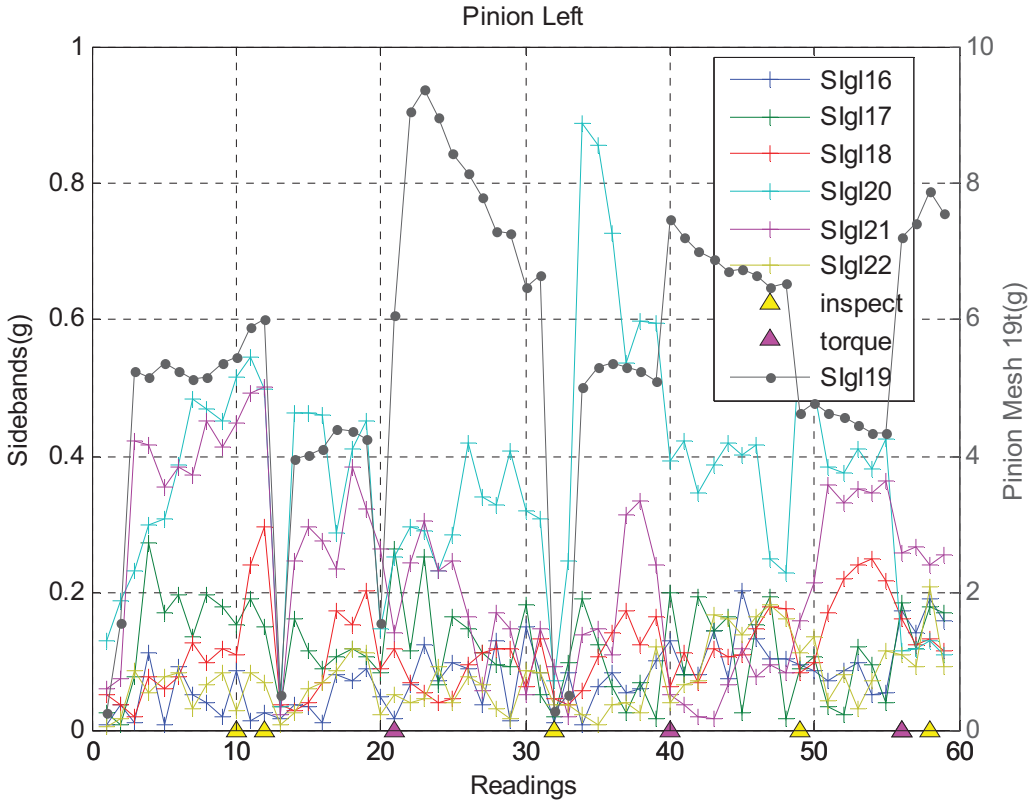

Figure B.2.6.—Test 2 plot of left pinion individual sidebands for MSPU.

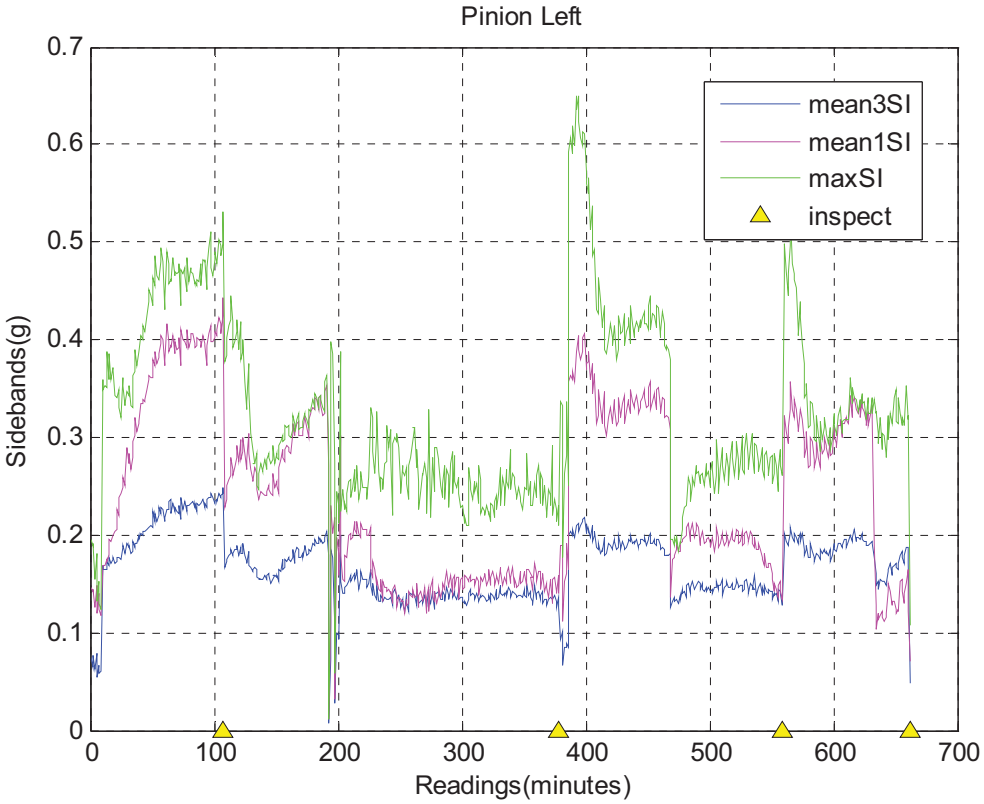

Figure B.2.7.—Test 2 plot of left pinion average and maximum sidebands for MDSS.

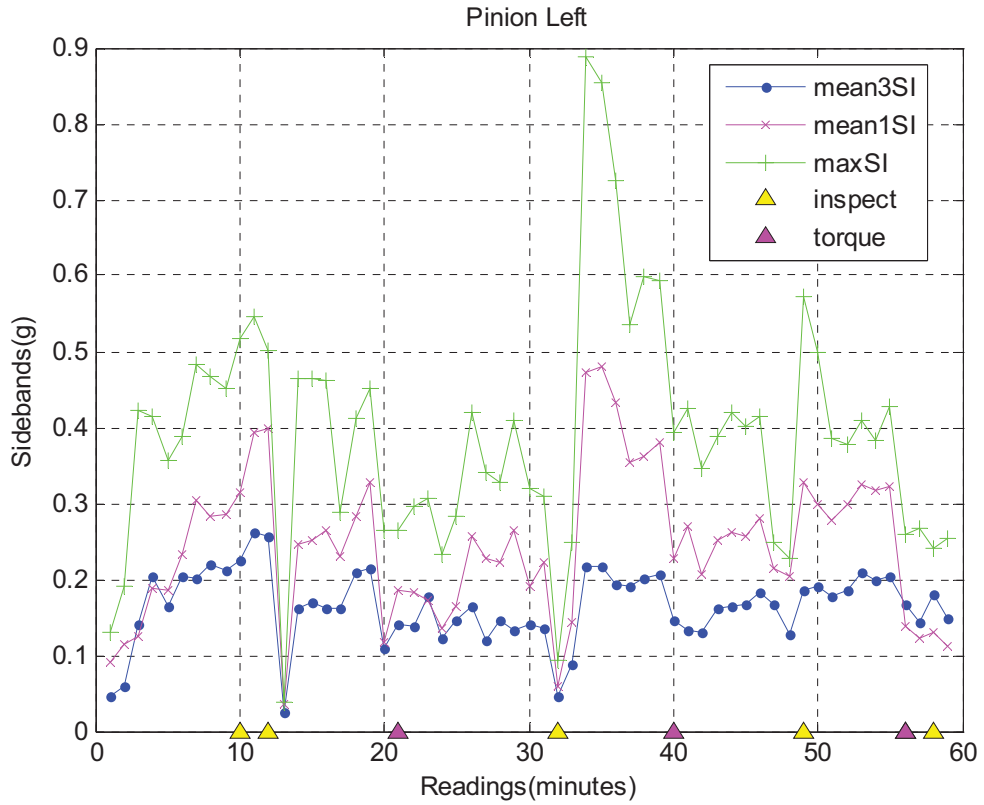

Figure B.2.8.—Test 2 plot of left pinion average and maximum sidebands for MSPU.

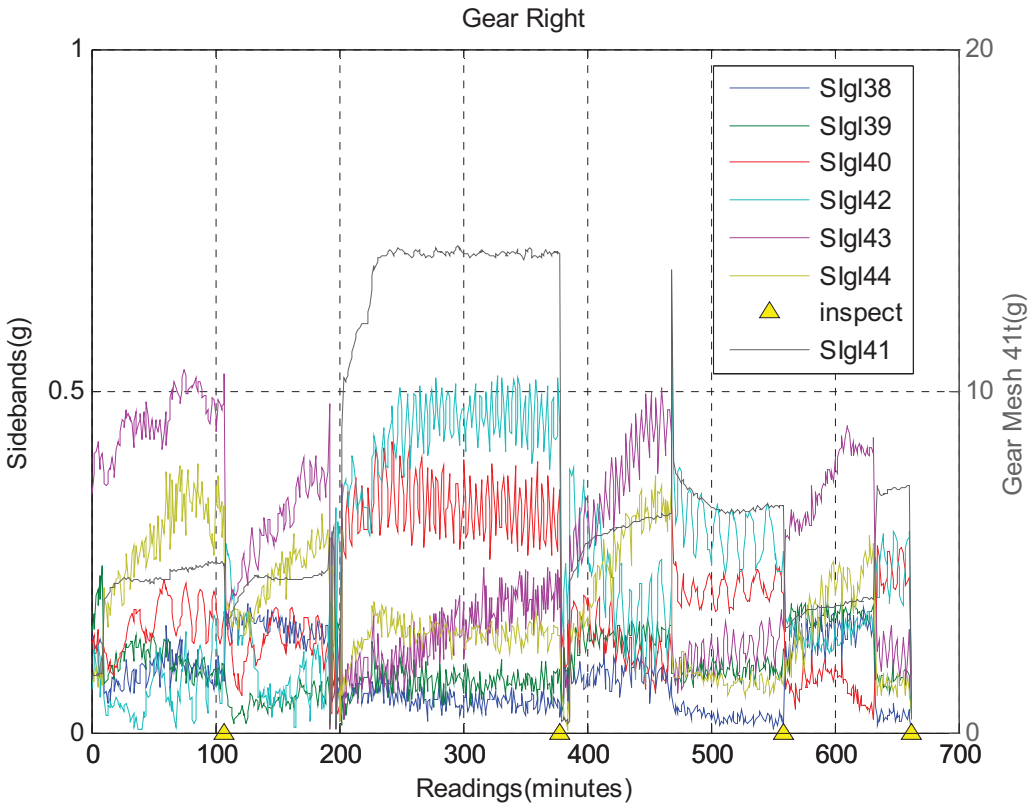

Figure B.2.9.—Test 2 plot of right gear individual sidebands for MDSS.

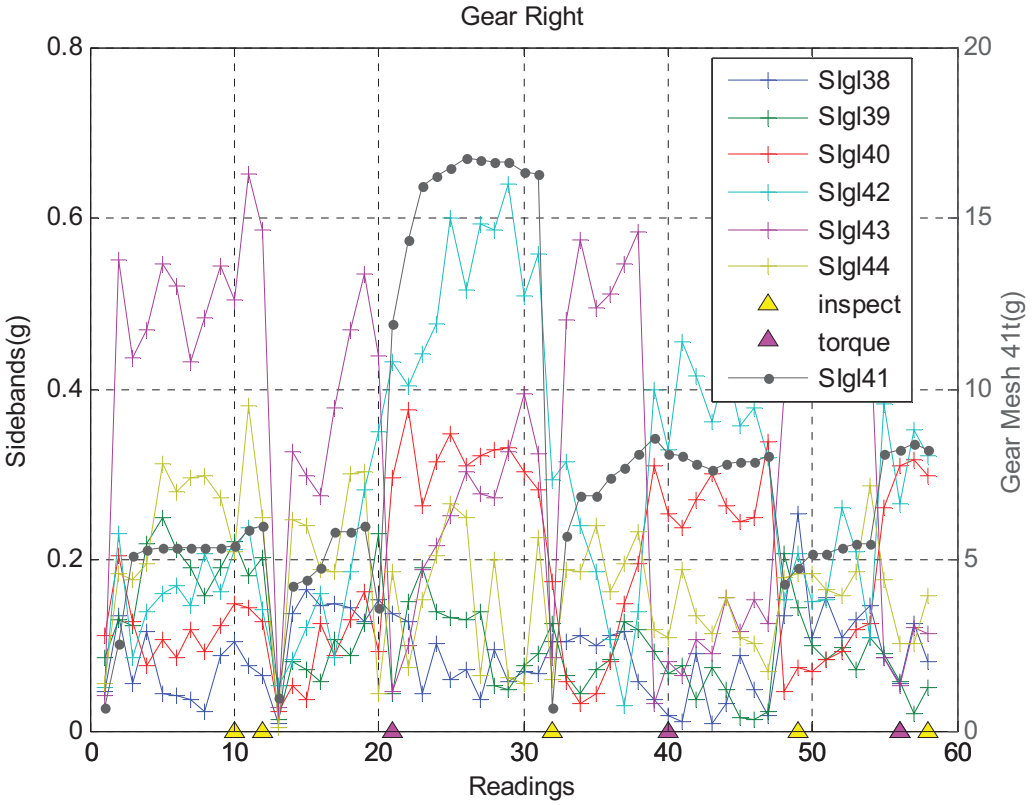

Figure B.2.10.—Test 2 plot of right gear individual sidebands for MSPU.

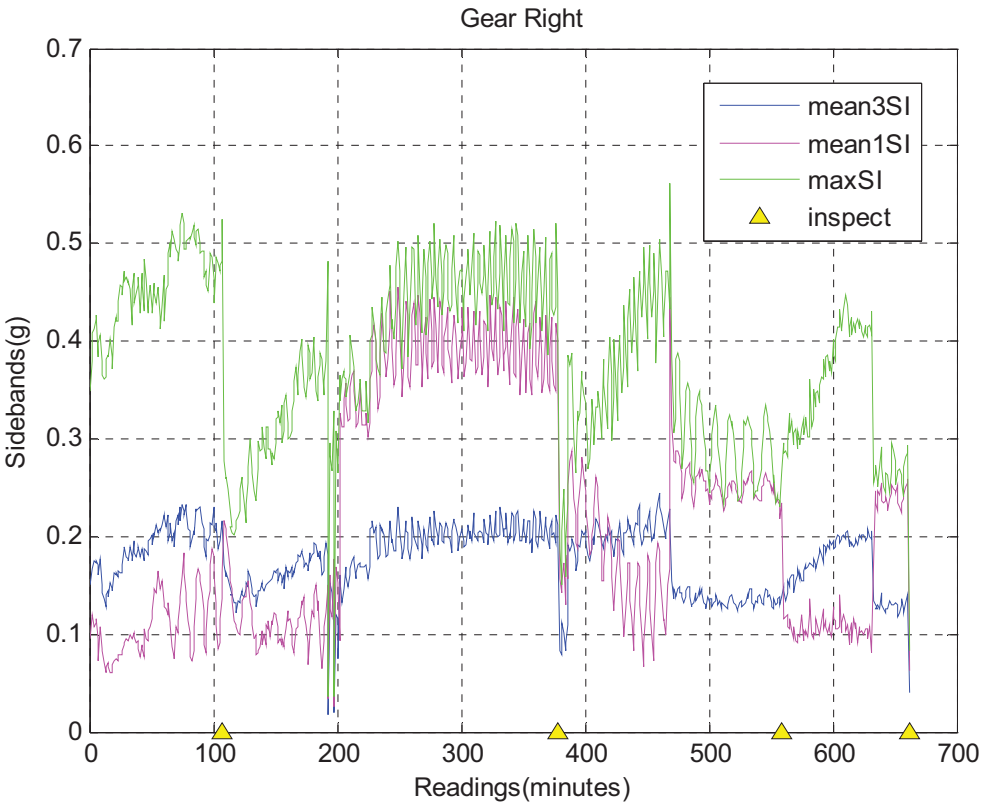

Figure B.2.11.—Test 2 plot of right gear average and maximum sidebands for MDSS.

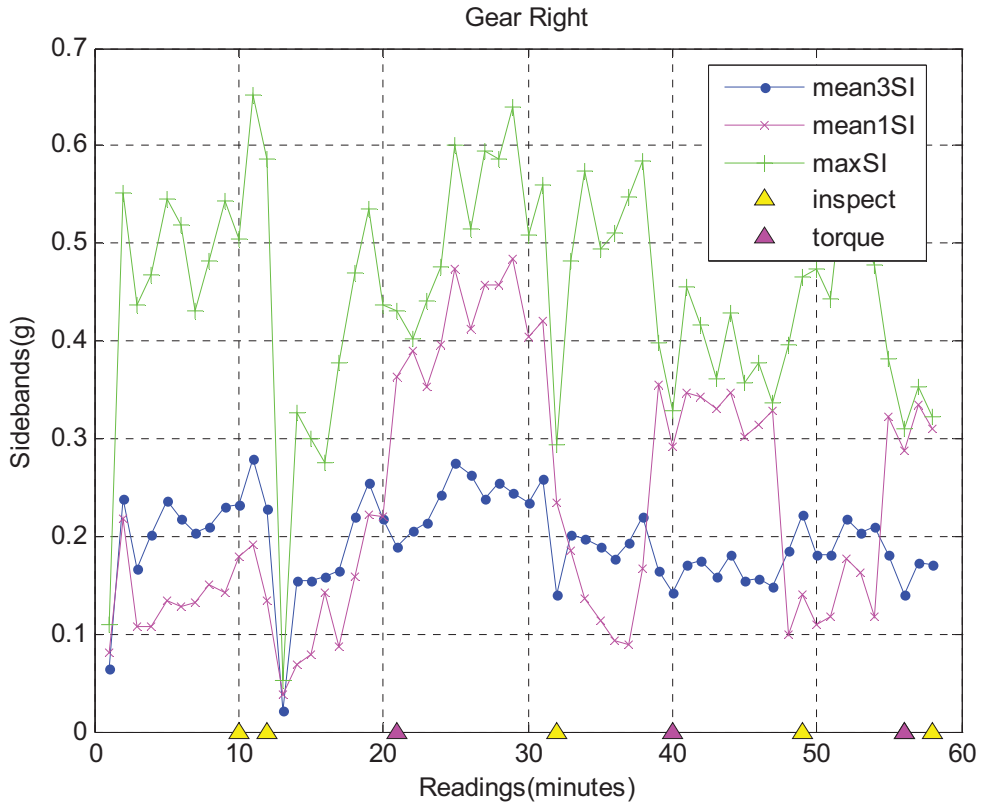

Figure B.2.12.—Test 2 plot of right gear average and maximum sidebands for MSPU.

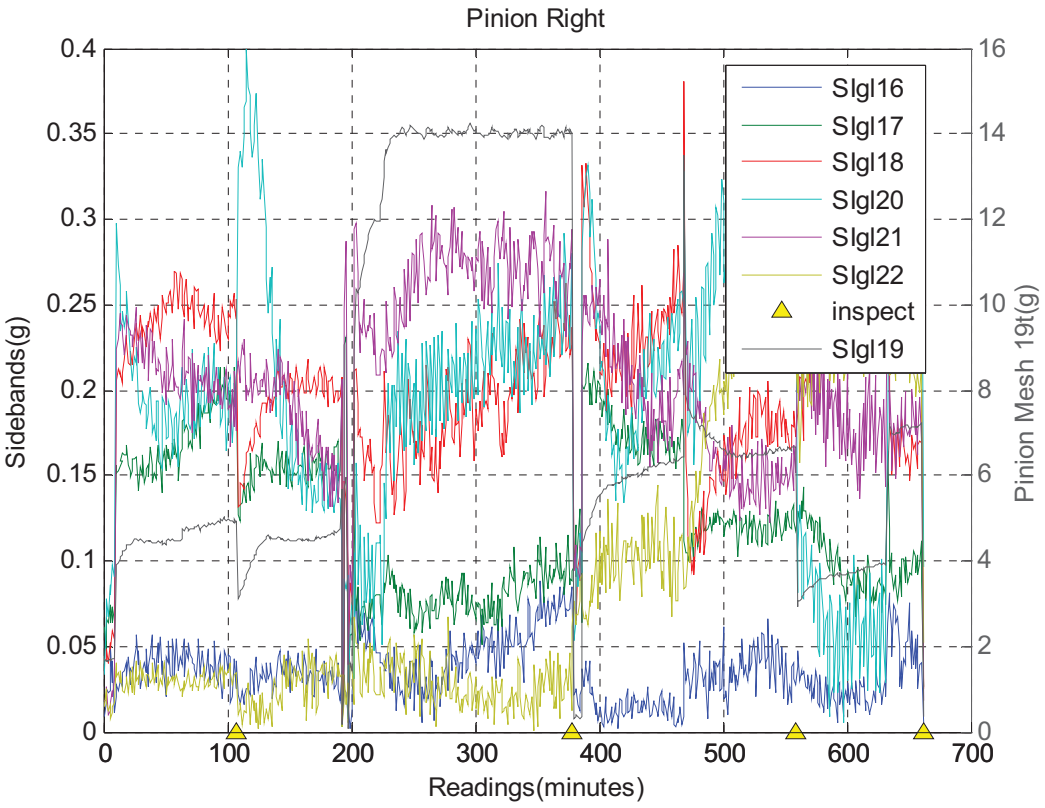

Figure B.2.13.—Test 2 plot of right pinion individual sidebands for MDSS.

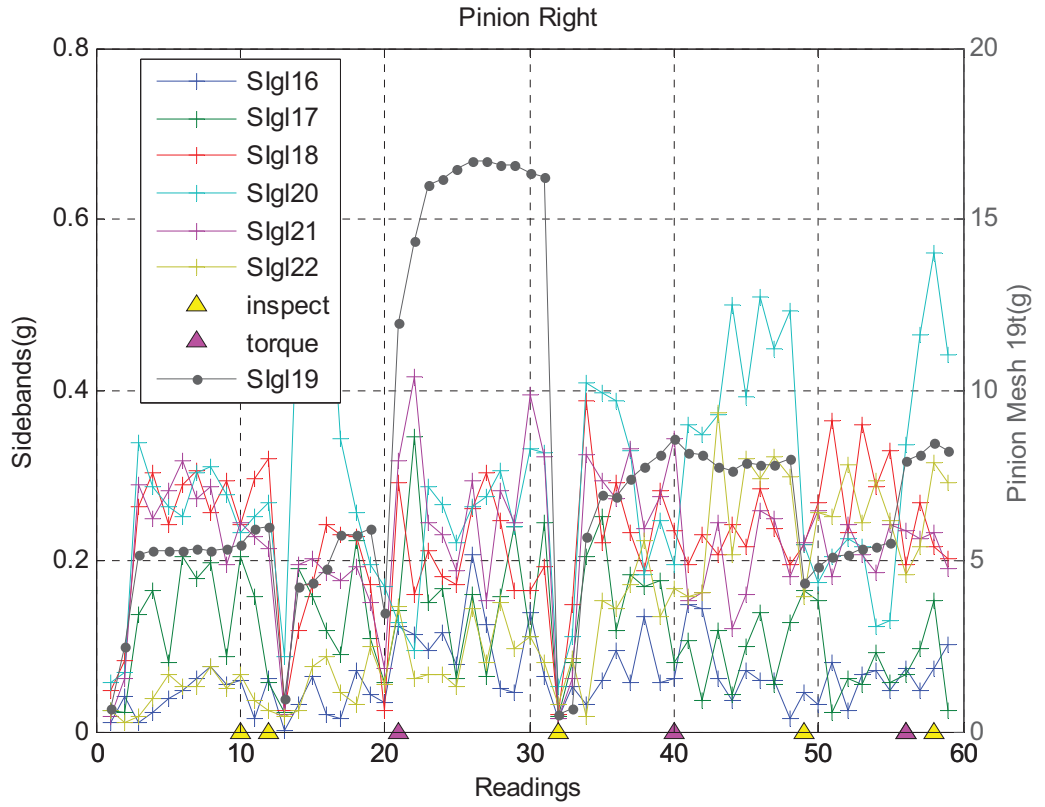

Figure B.2.14.—Test 2 plot of right pinion individual sidebands for MSPU.

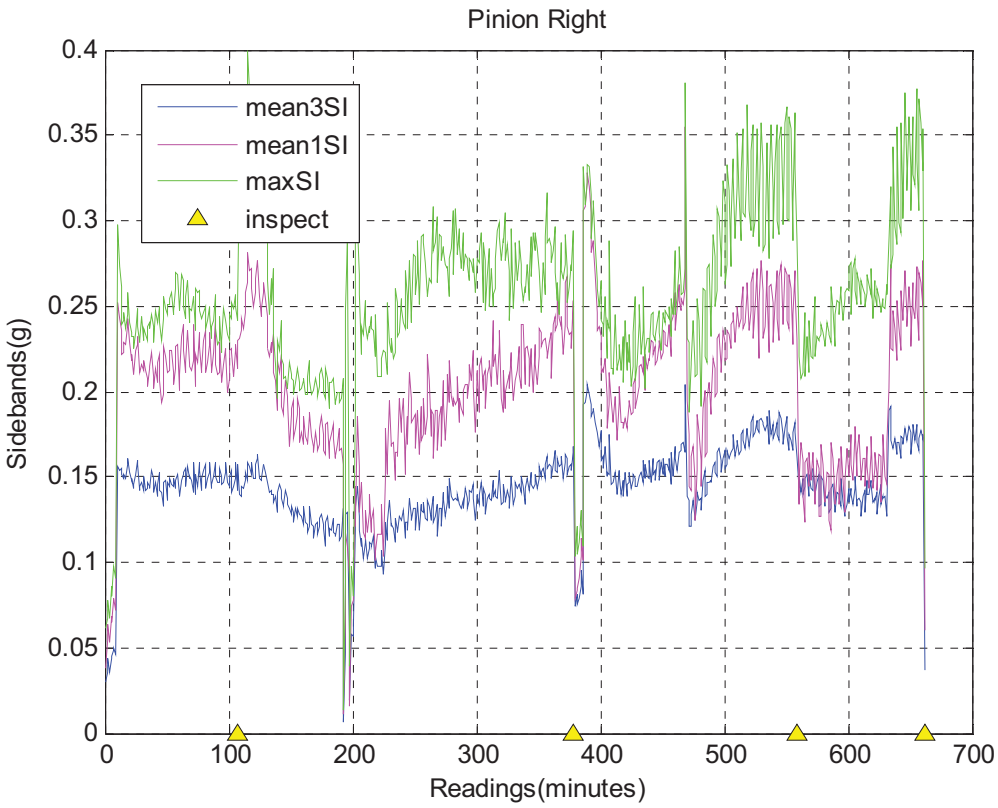

Figure B.2.15.—Test 2 plot of right pinion average and maximum sidebands for MDSS.

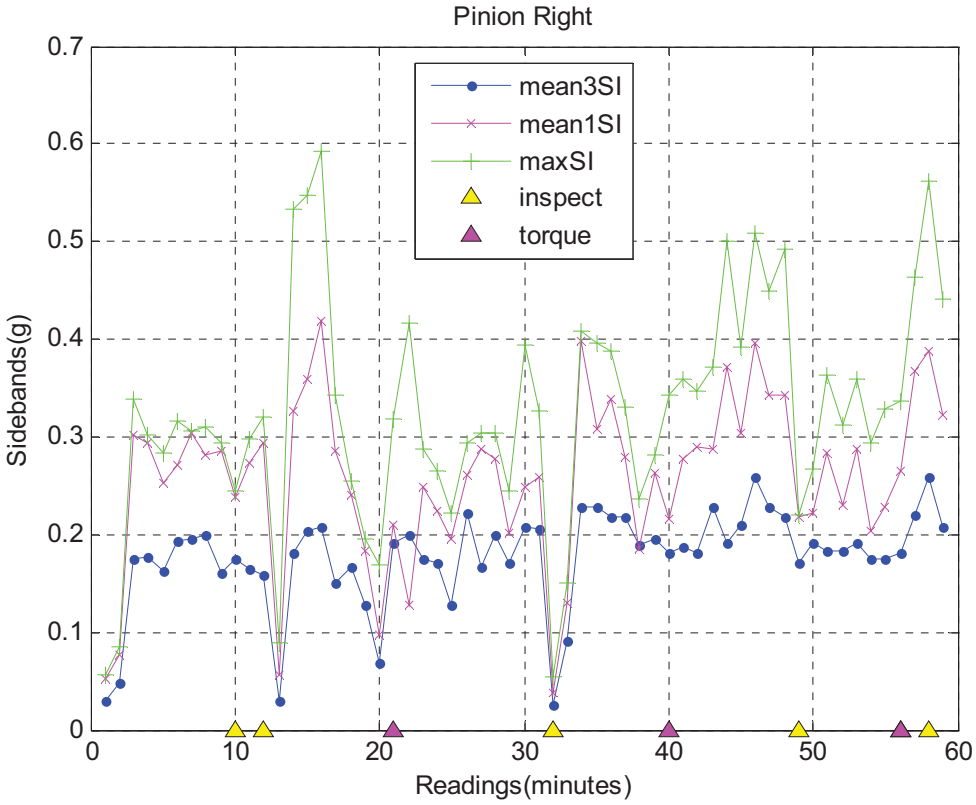

Figure B.2.16.—Test 2 plot of right pinion average and maximum sidebands for MSPU.

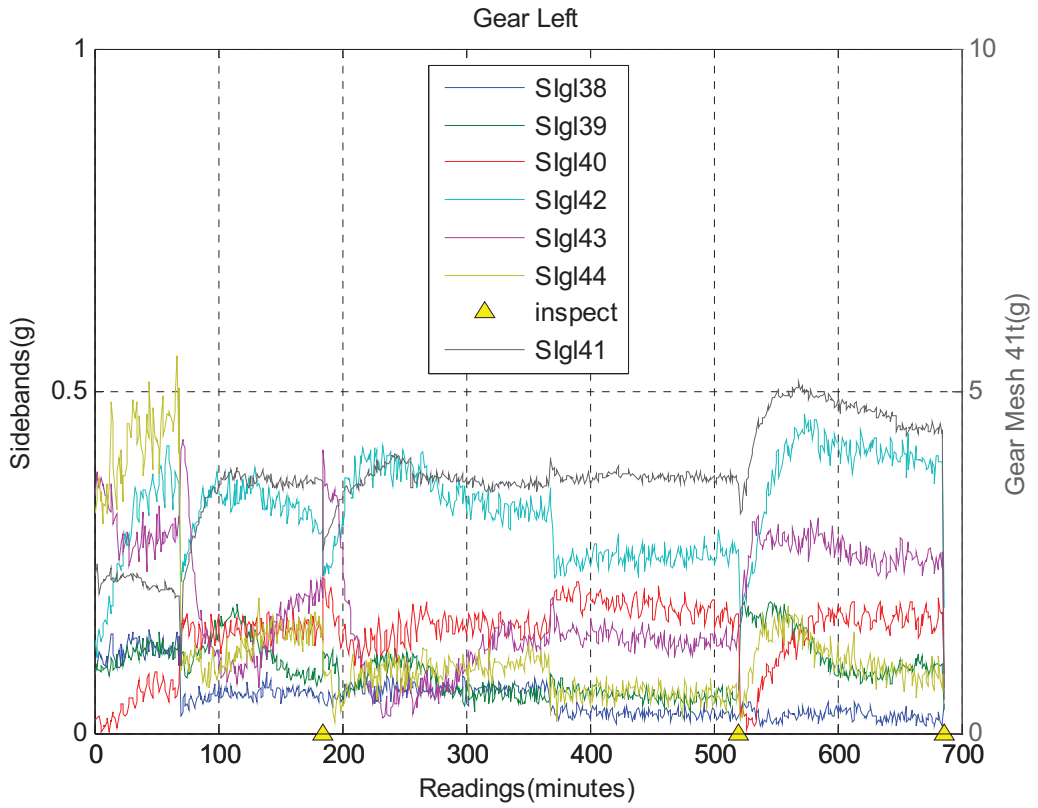

Figure B.3.1.—Test 3 plot of left gear individual sidebands for MDSS.

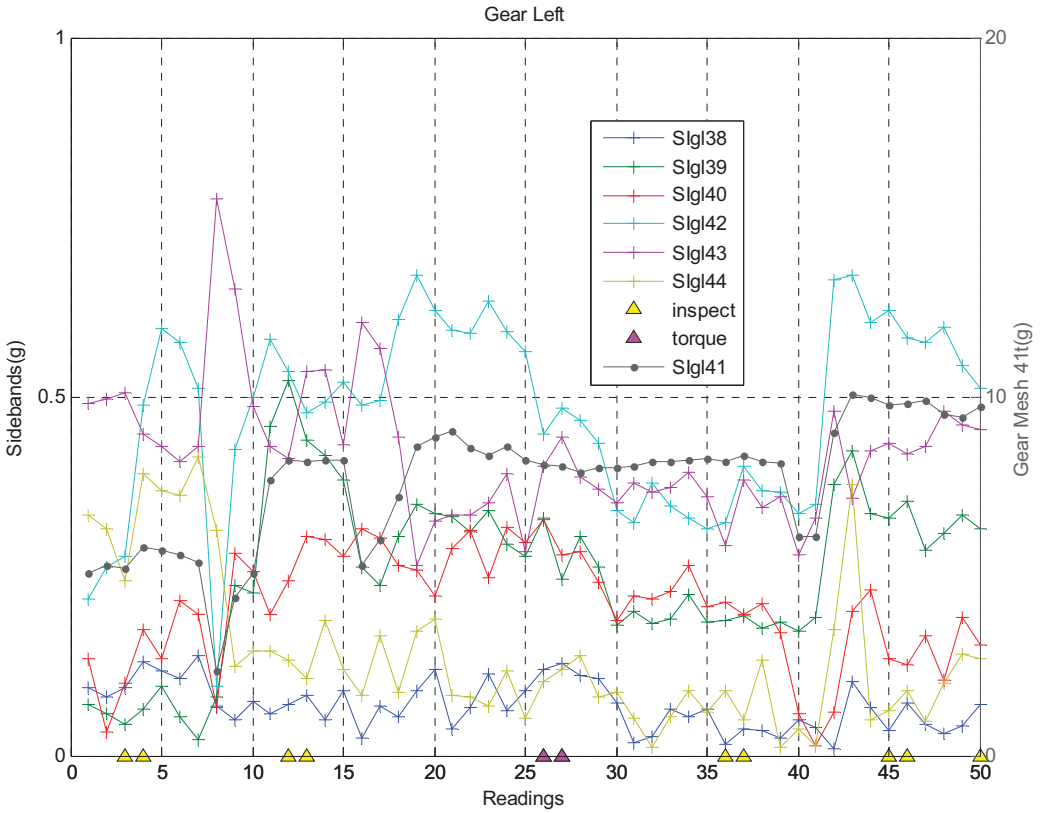

Figure B.3.2.—Test 3 plot of left gear individual sidebands for MSPU.

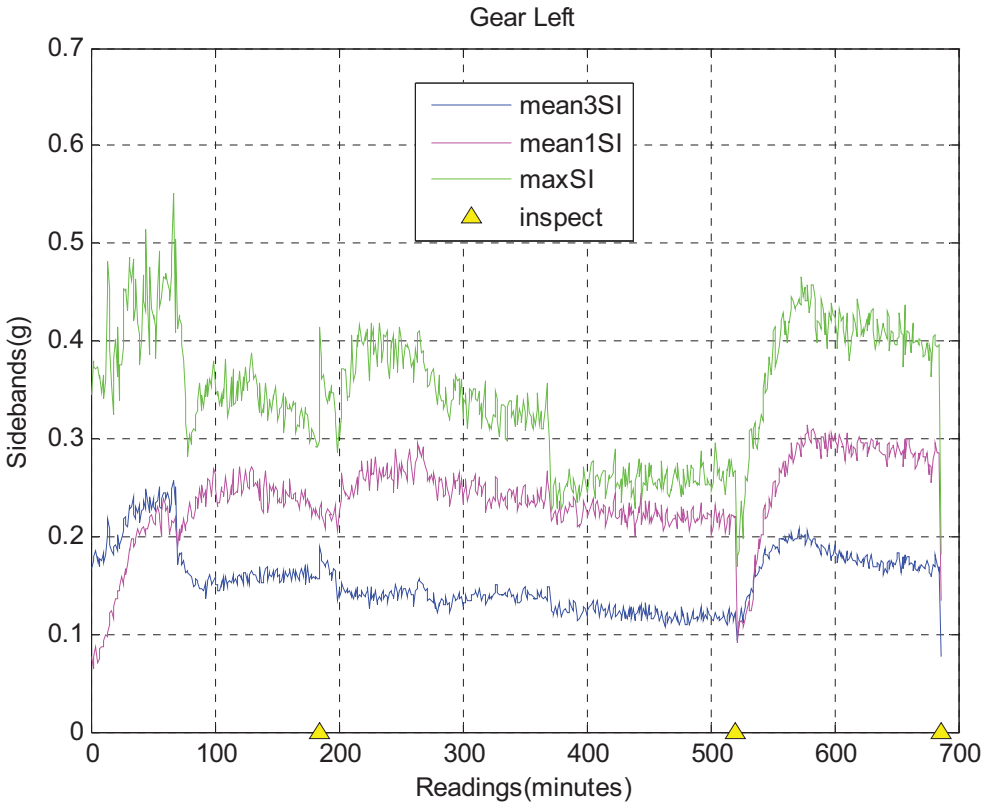

Figure B.3.3.—Test 3 plot of left gear average and maximum sidebands for MDSS.

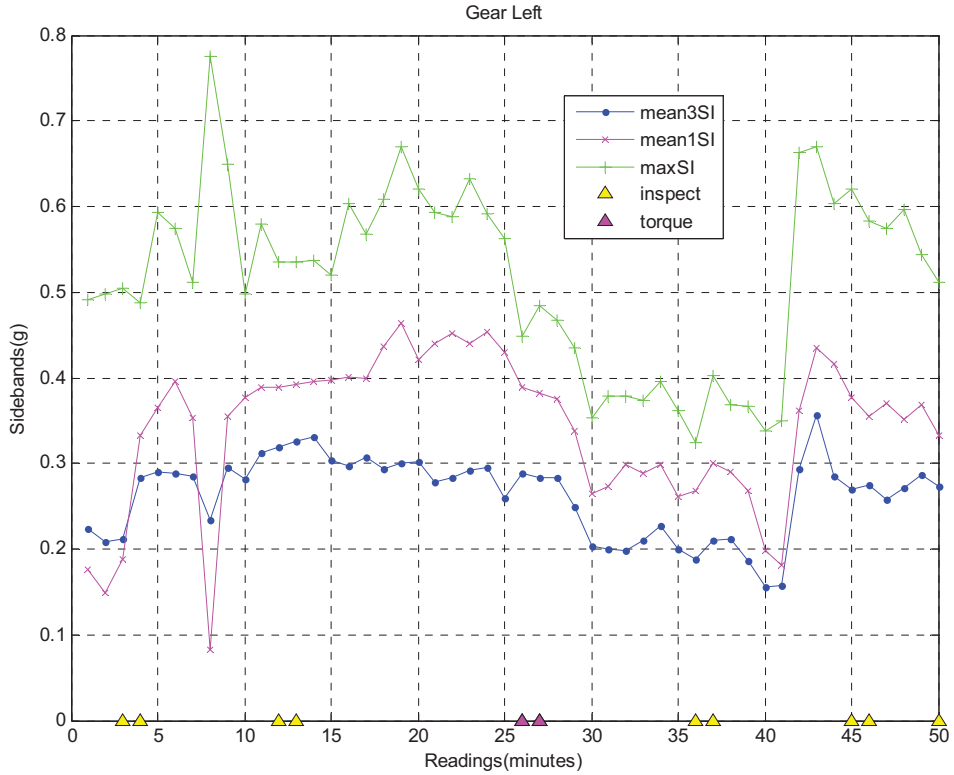

Figure B.3.4.—Test 3 plot of left gear average and maximum sidebands for MSPU.

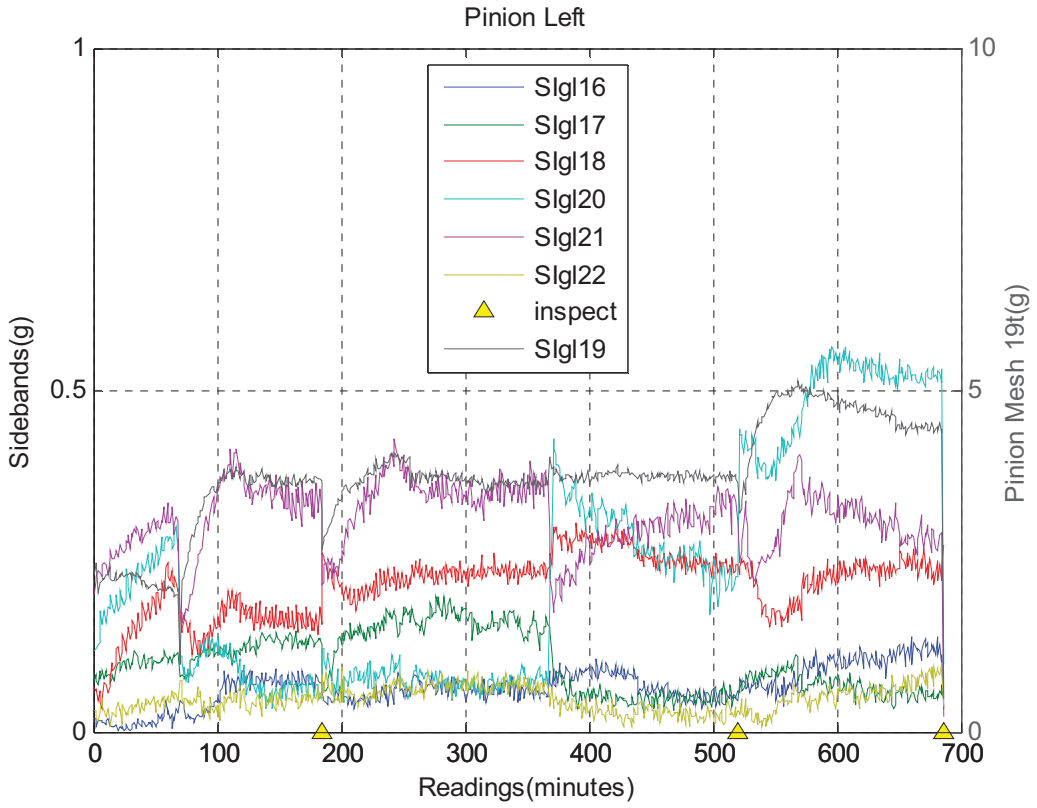

Figure B.3.5.—Test 3 plot of left pinion individual sidebands for MDSS.

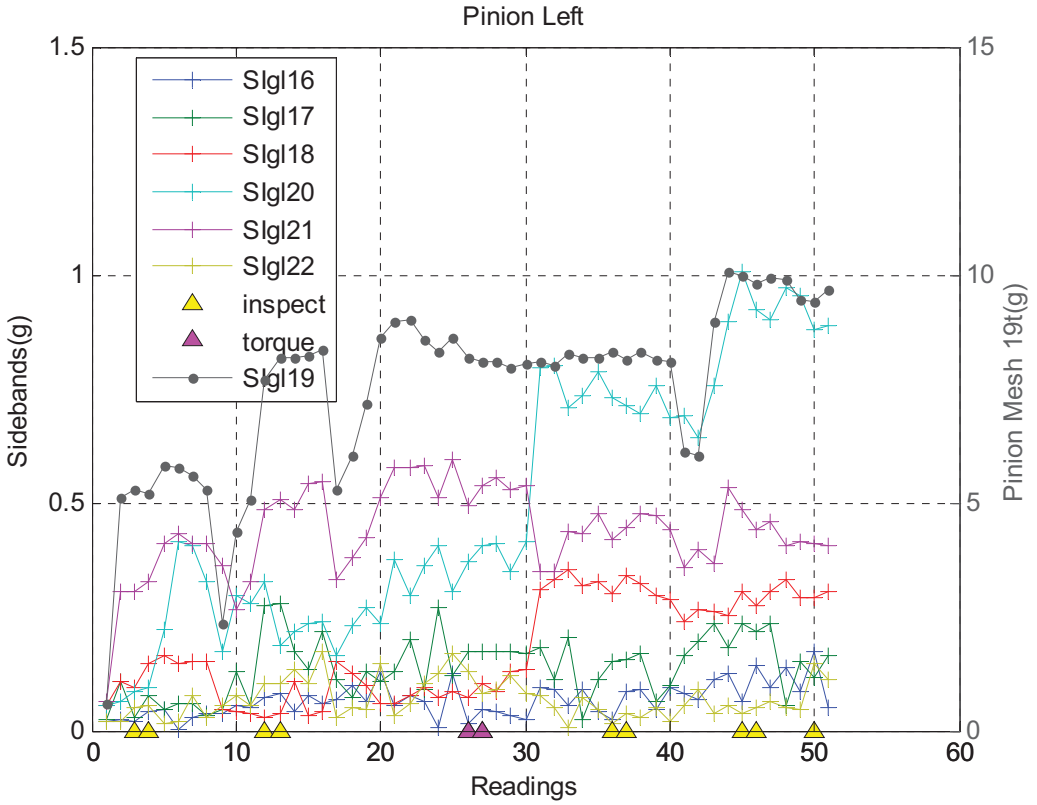

Figure B.3.6.—Test 3 plot of left pinion individual sidebands for MSPU.

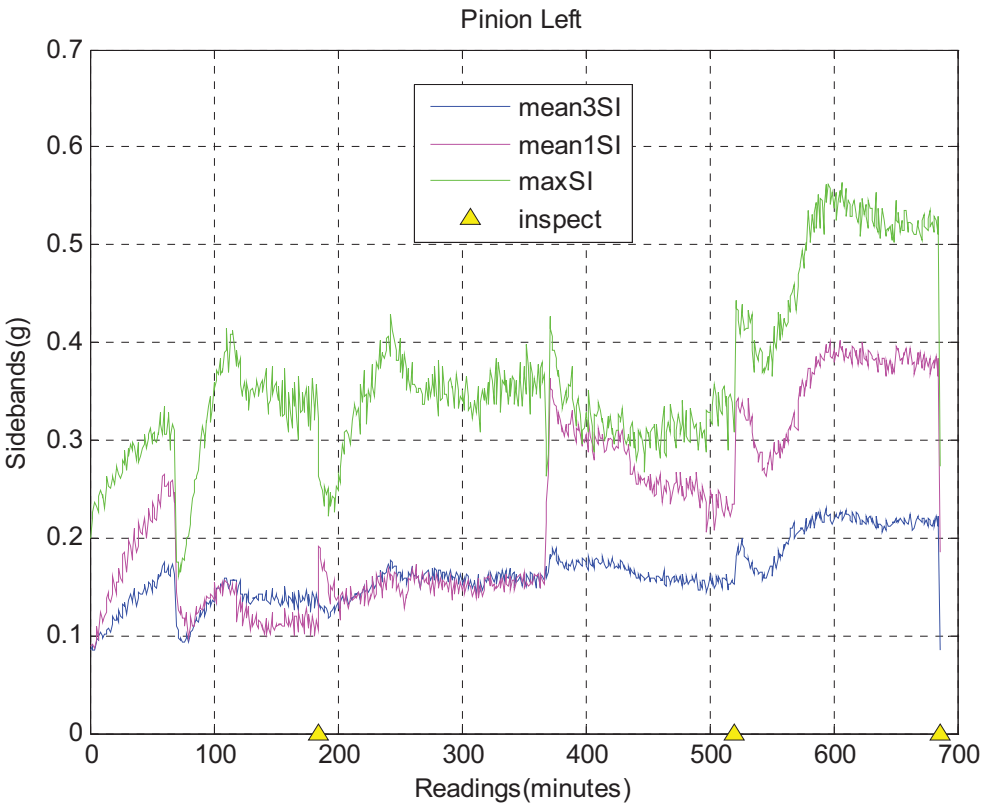

Figure B.3.7.—Test 3 plot of left pinion average and maximum sidebands for MDSS.

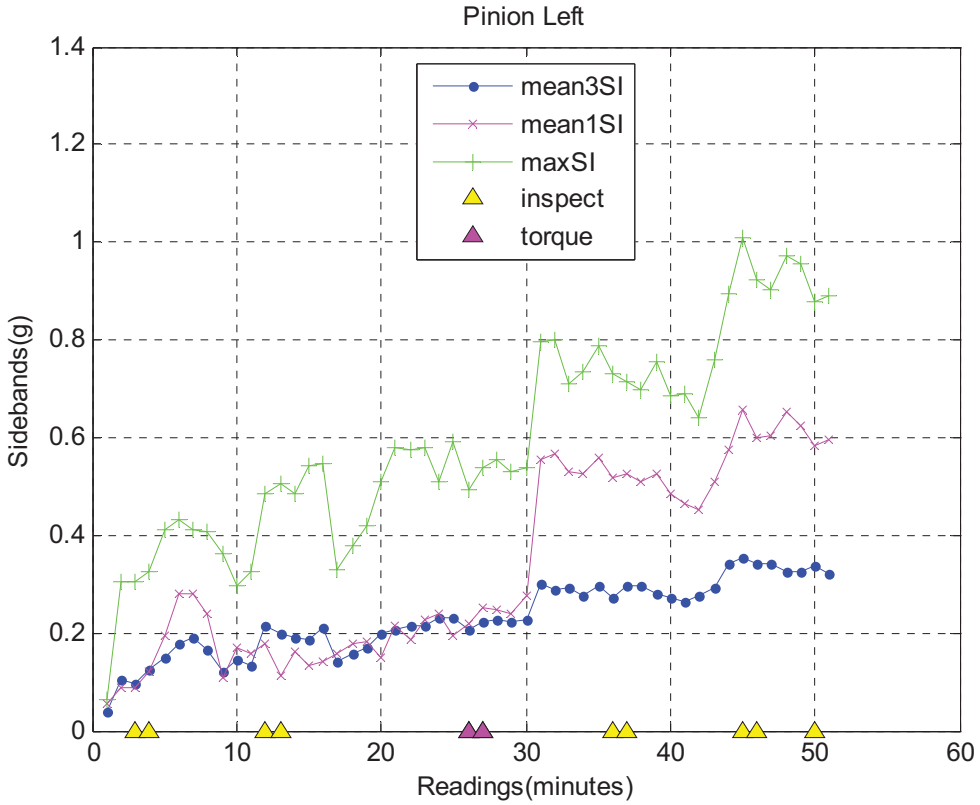

Figure B.3.8.—Test 3 plot of left pinion average and maximum sidebands for MSPU.

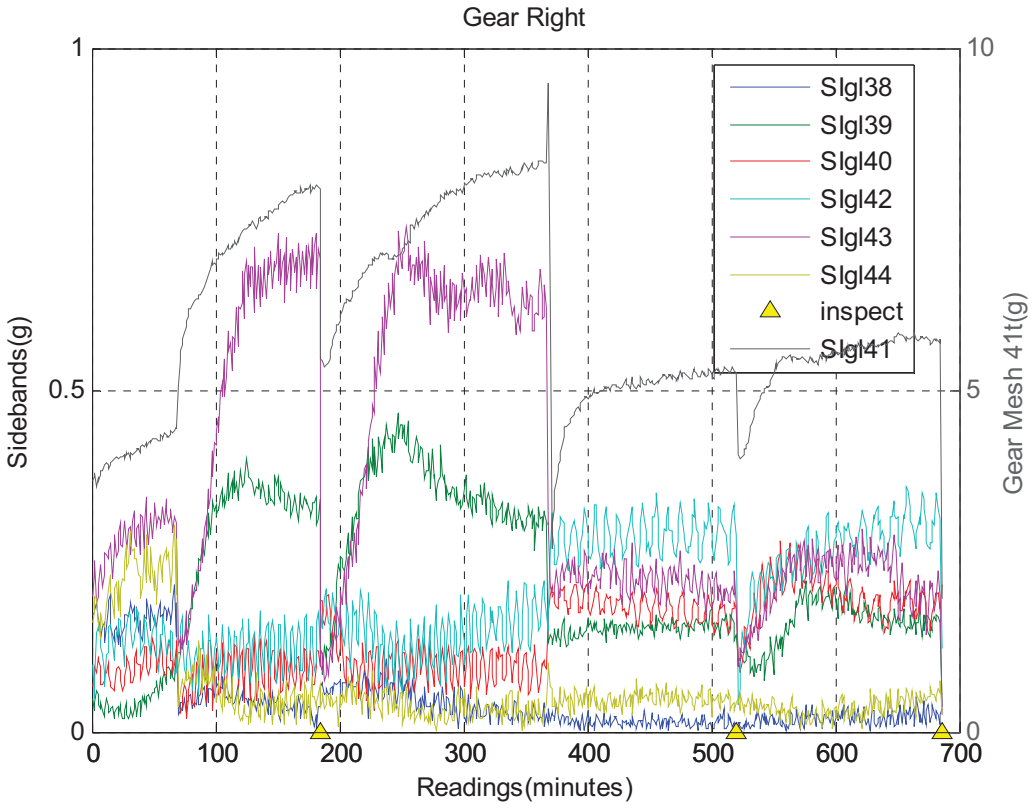

Figure B.3.9.—Test 3 plot of right gear individual sidebands for MDSS.

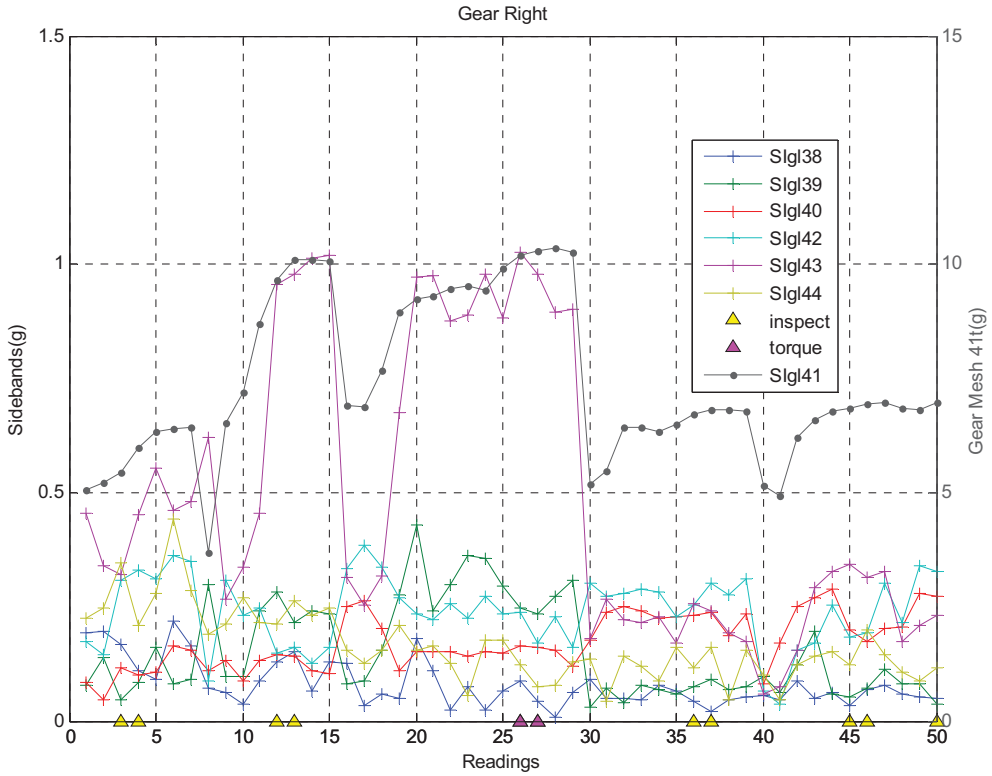

Figure B.3.10.—Test 3 plot of right gear individual sidebands for MSPU.

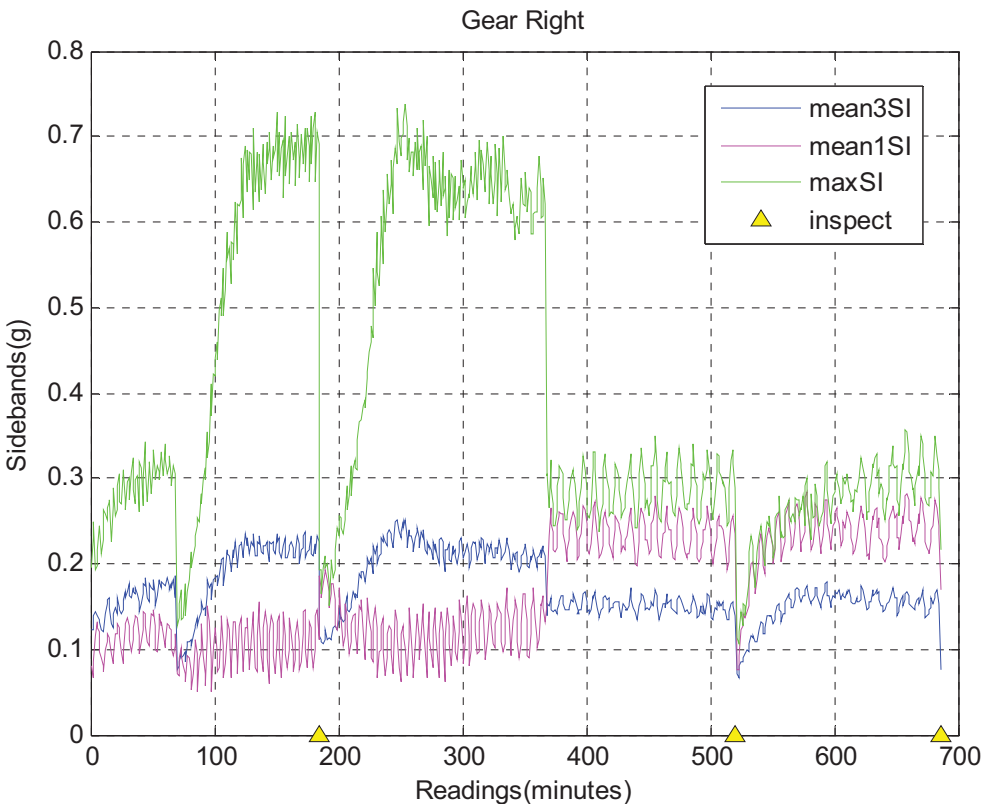

Figure B.3.11.—Test 3 plot of right gear average and maximum sidebands for MDSS.

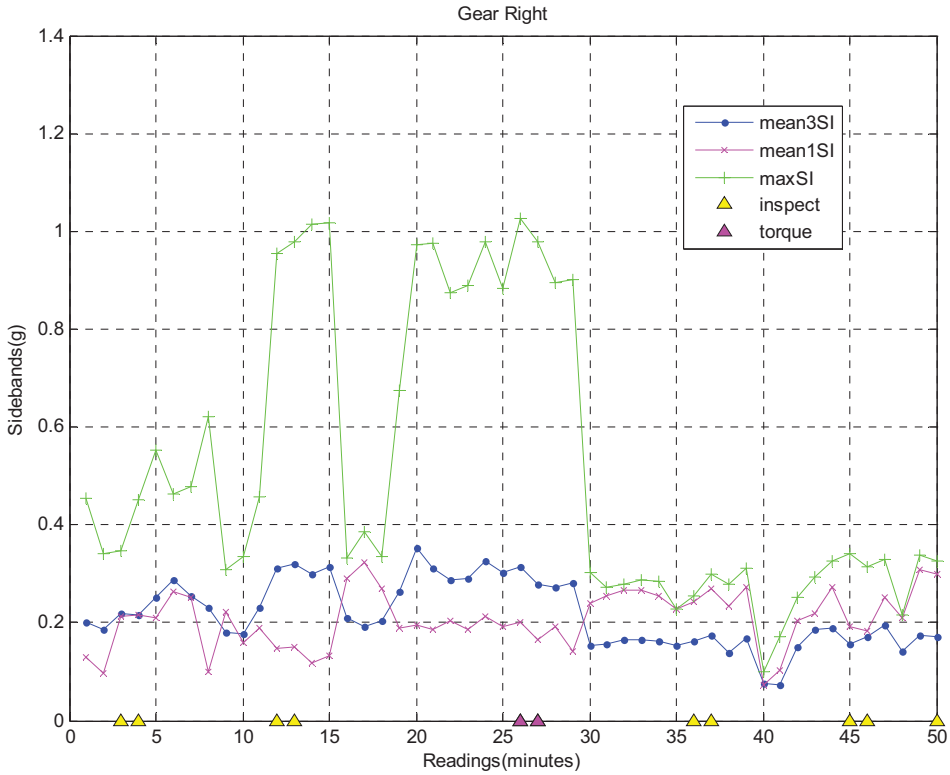

Figure B.3.12.—Test 3 plot of right gear average and maximum sidebands for MSPU.

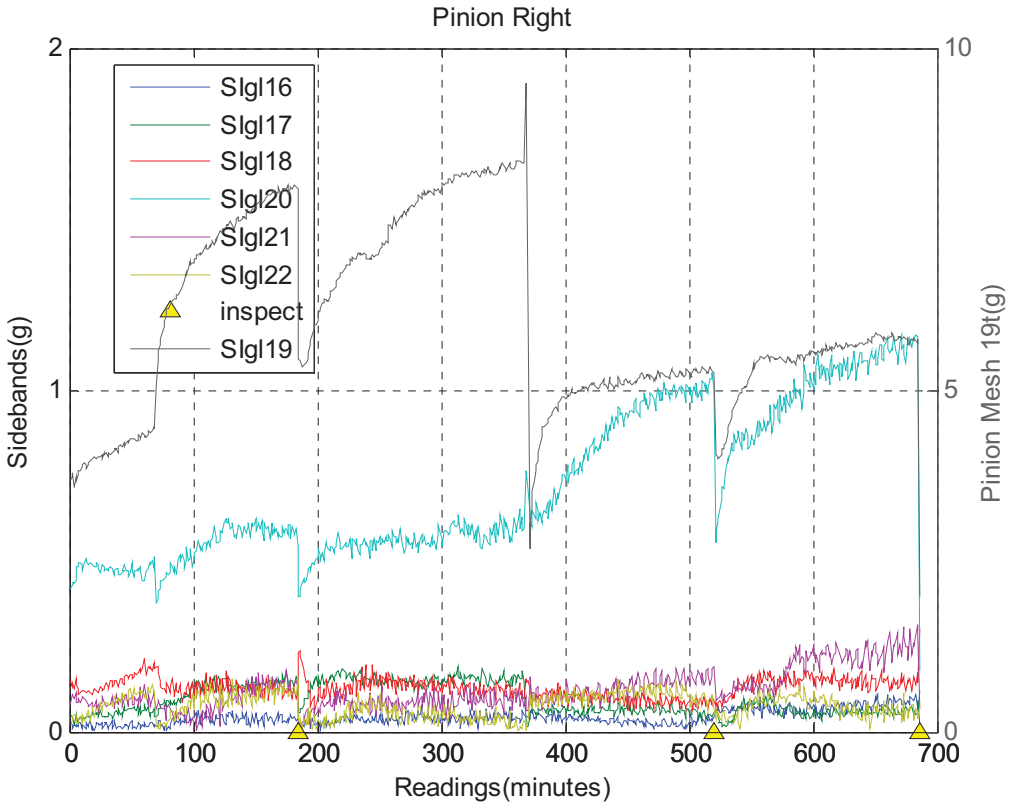

Figure B.3.13.—Test 3 plot of right pinion individual sidebands for MDSS.

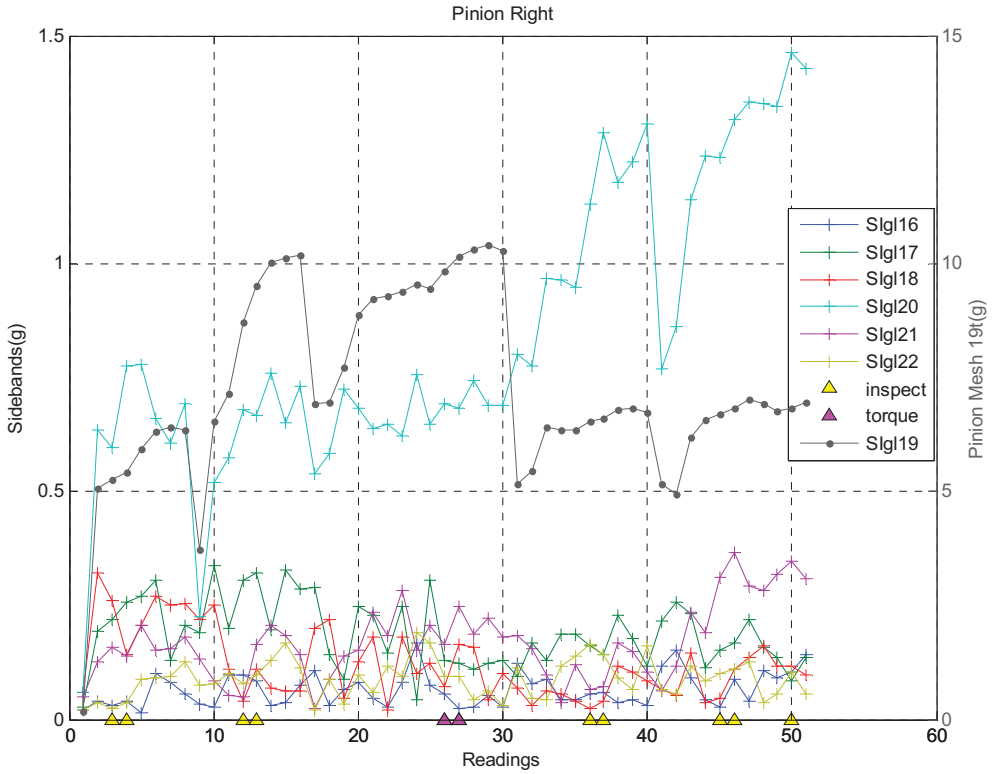

Figure B.3.14.—Test 3 plot of right pinion individual sidebands for MSPU.

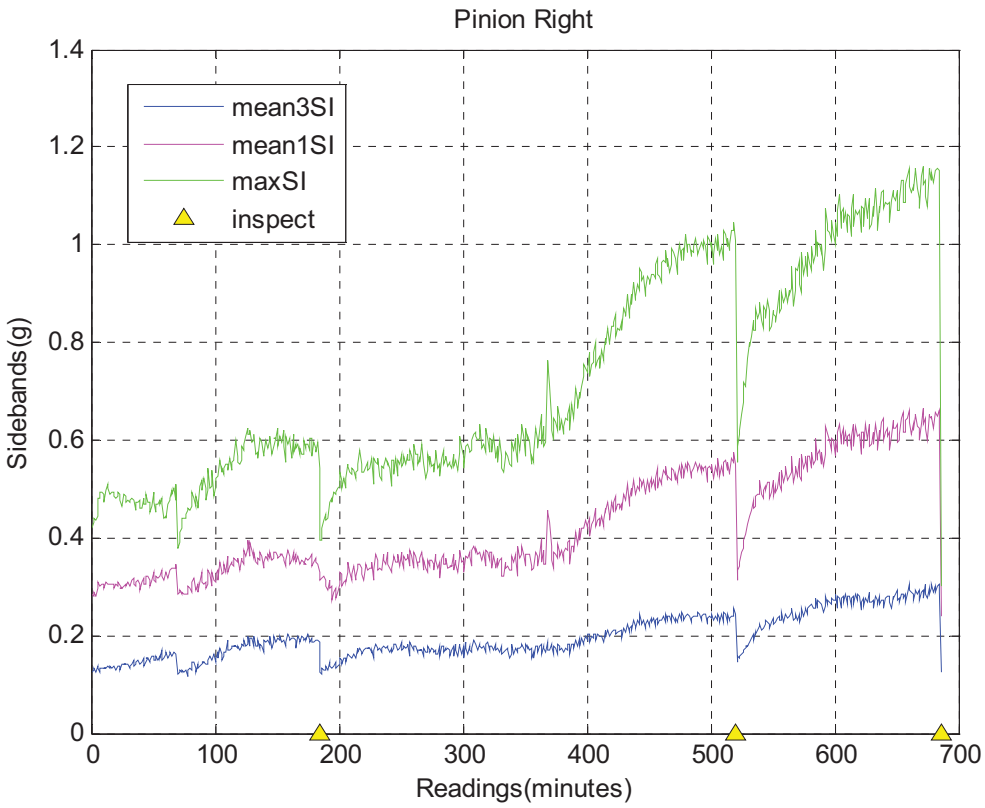

Figure B.3.15.—Test 3 plot of right pinion average and maximum sidebands for MDSS.

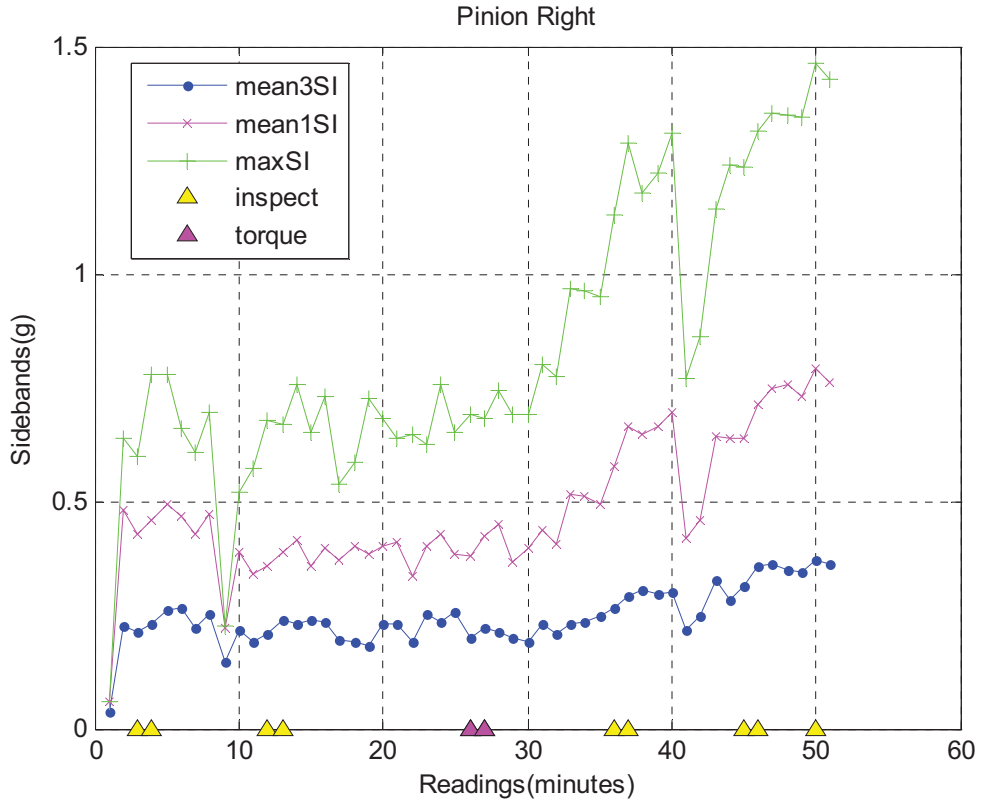

Figure B.3.16.—Test 3 plot of right pinion average and maximum sidebands for MSPU.

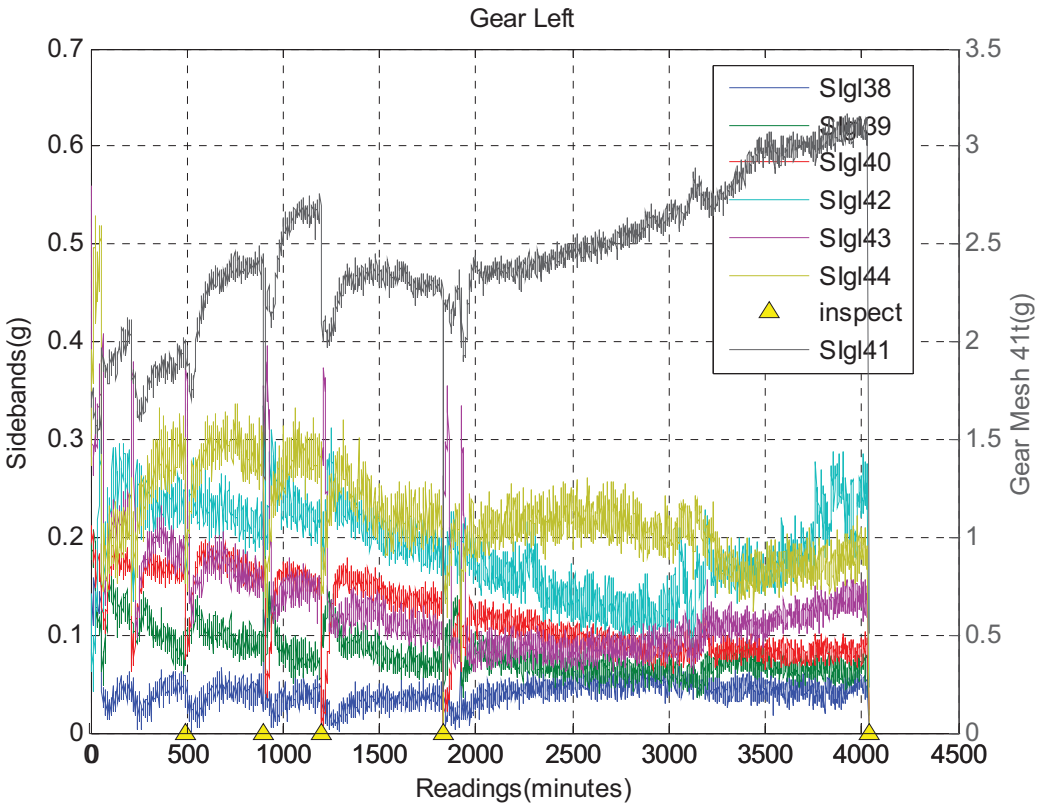

Figure B.4.1.—Test 4 plot of left gear individual sidebands for MDSS.

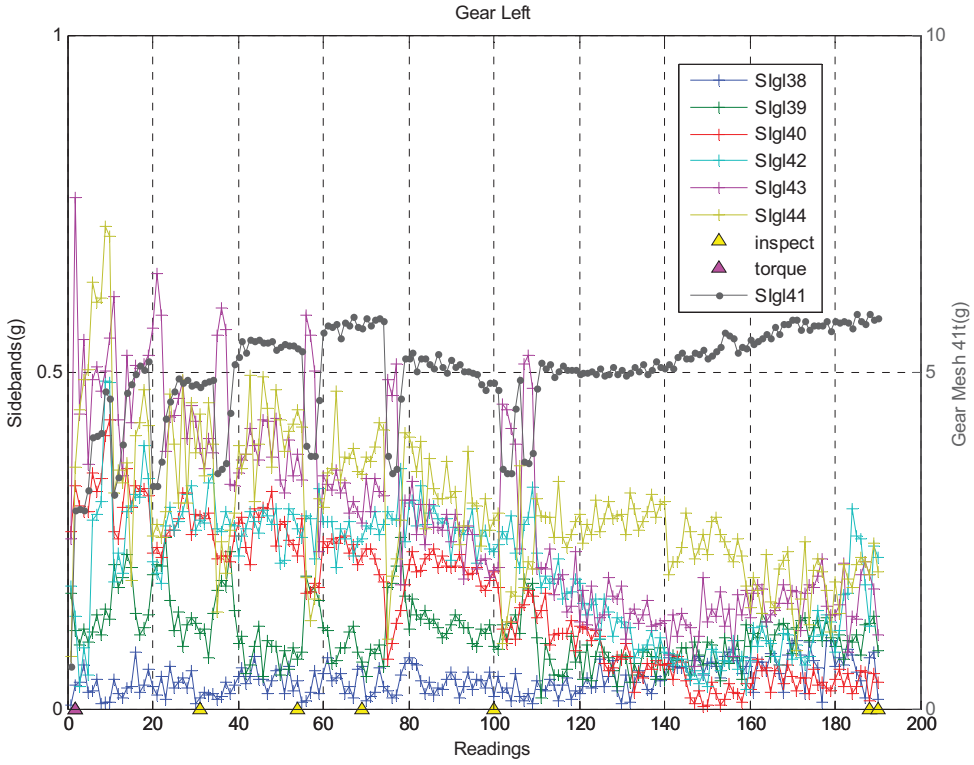

Figure B.4.2.—Test 4 plot of left gear individual sidebands for MSPU.

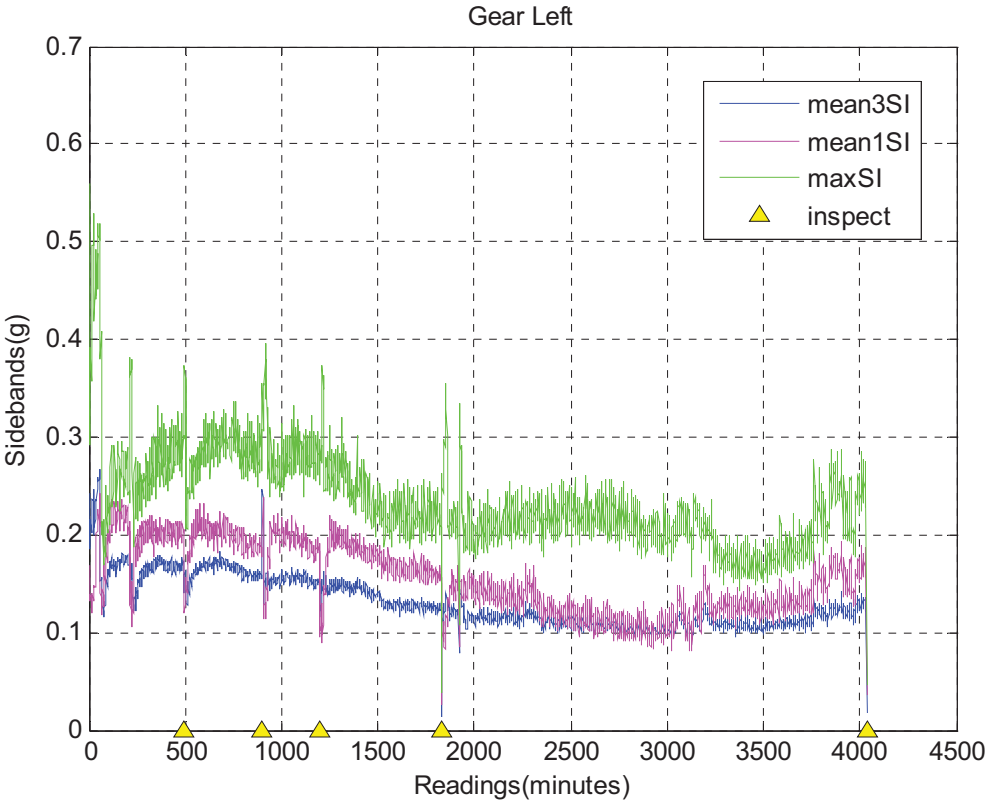

Figure B.4.3.—Test 4 plot of left gear average and maximum sidebands for MDSS.

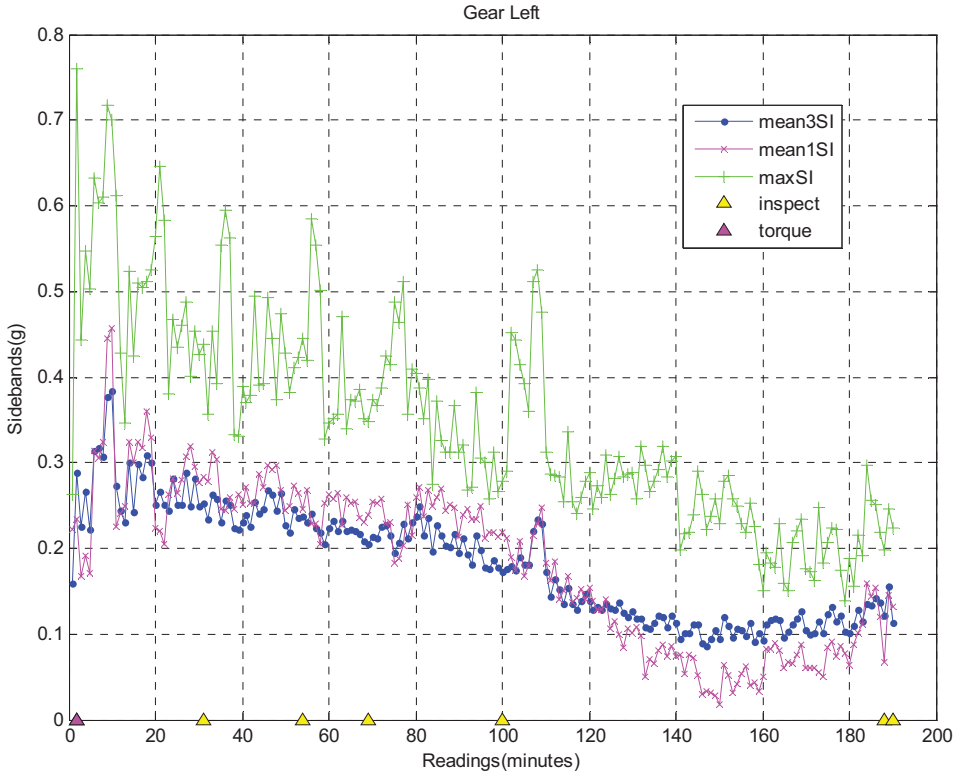

Figure B.4.4.—Test 4 plot of left gear average and maximum sidebands for MSPU.

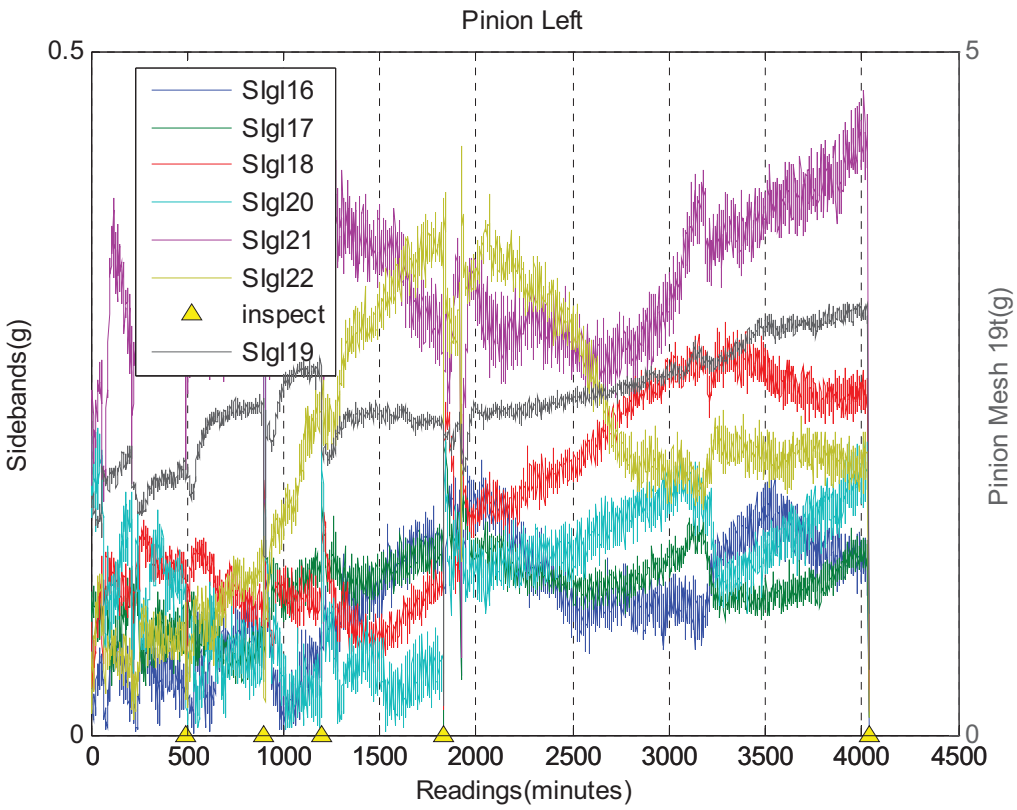

Figure B.4.5.—Test 4 plot of left pinion individual sidebands for MDSS.

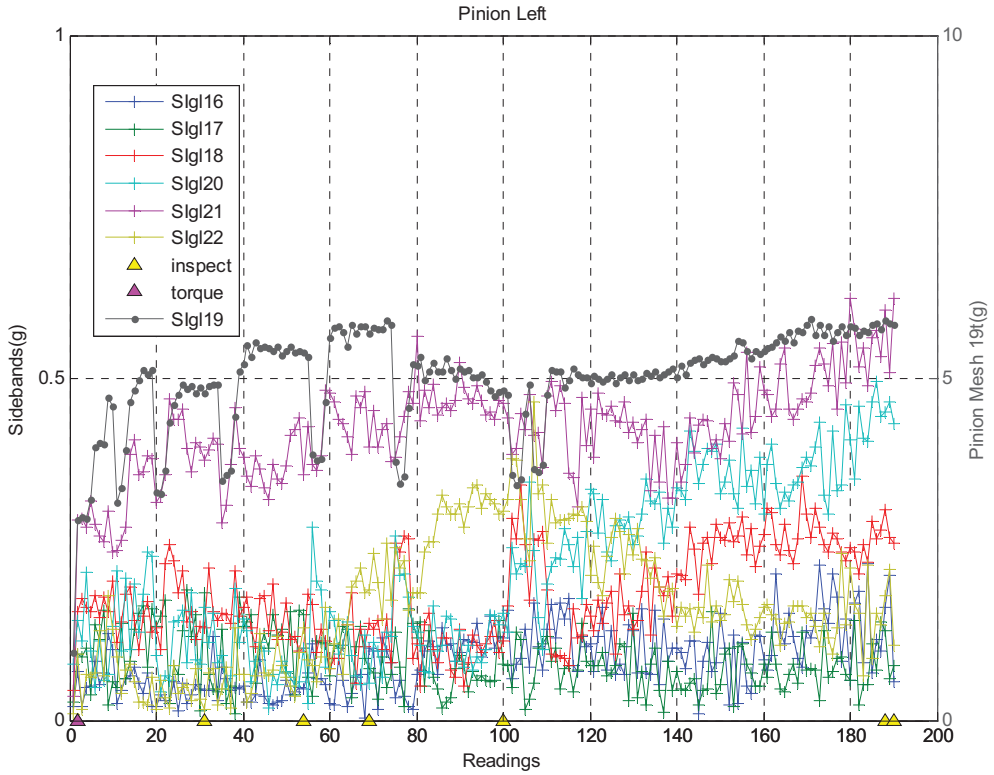

Figure B.4.6.—Test 4 plot of left pinion individual sidebands for MSPU.

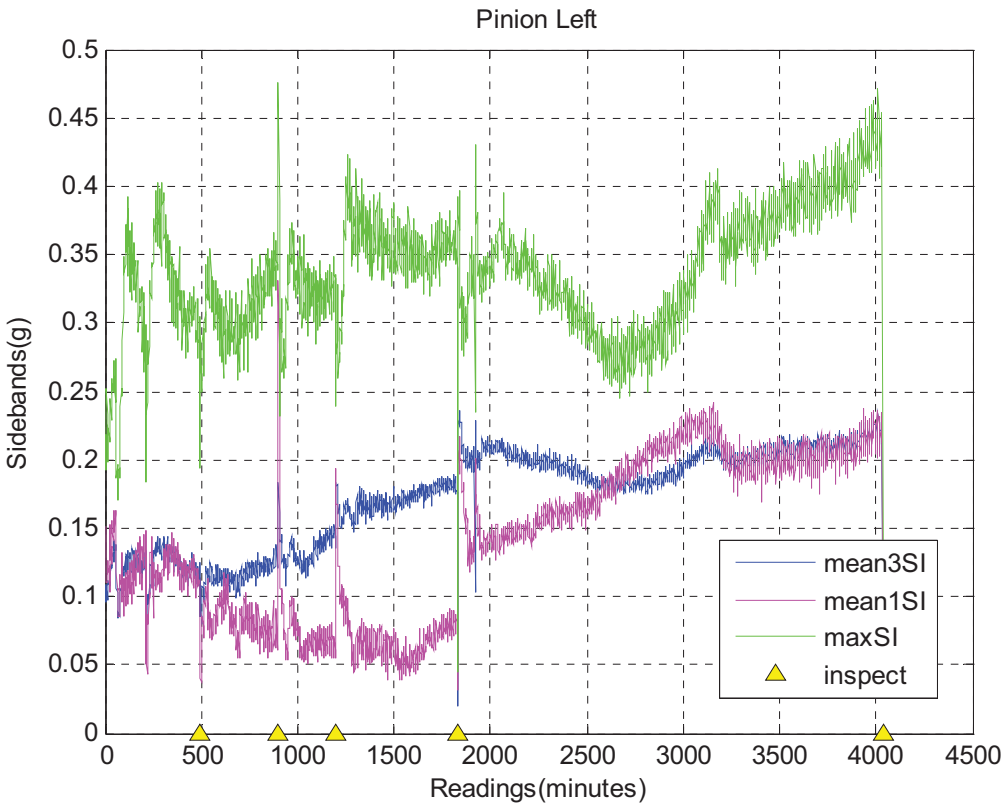

Figure B.4.7.—Test 4 plot of left pinion average and maximum sidebands for MDSS.

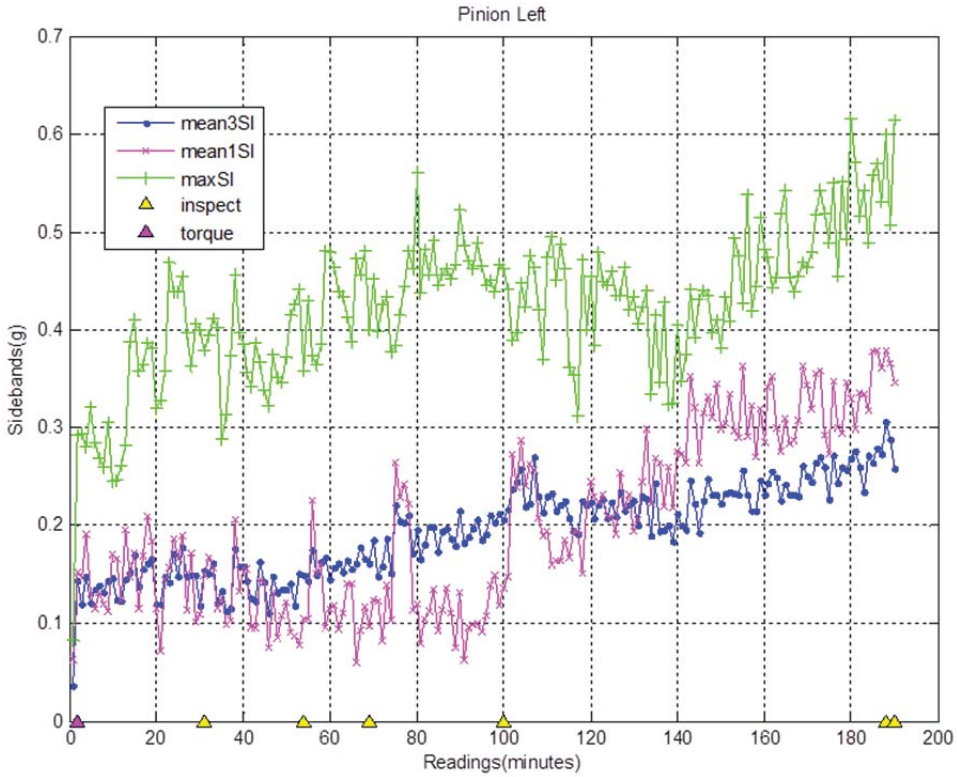

Figure B.4.8.—Test 4 plot of left pinion average and maximum sidebands for MSPU.

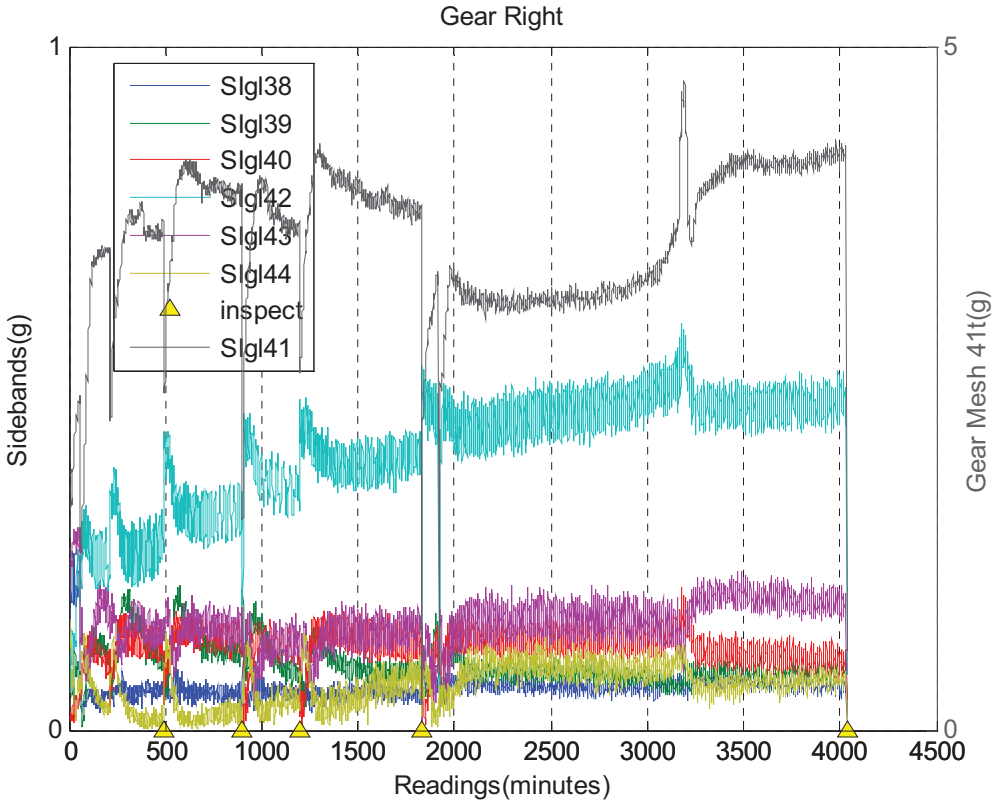

Figure B.4.9.—Test 4 plot of right gear individual sidebands for MDSS.

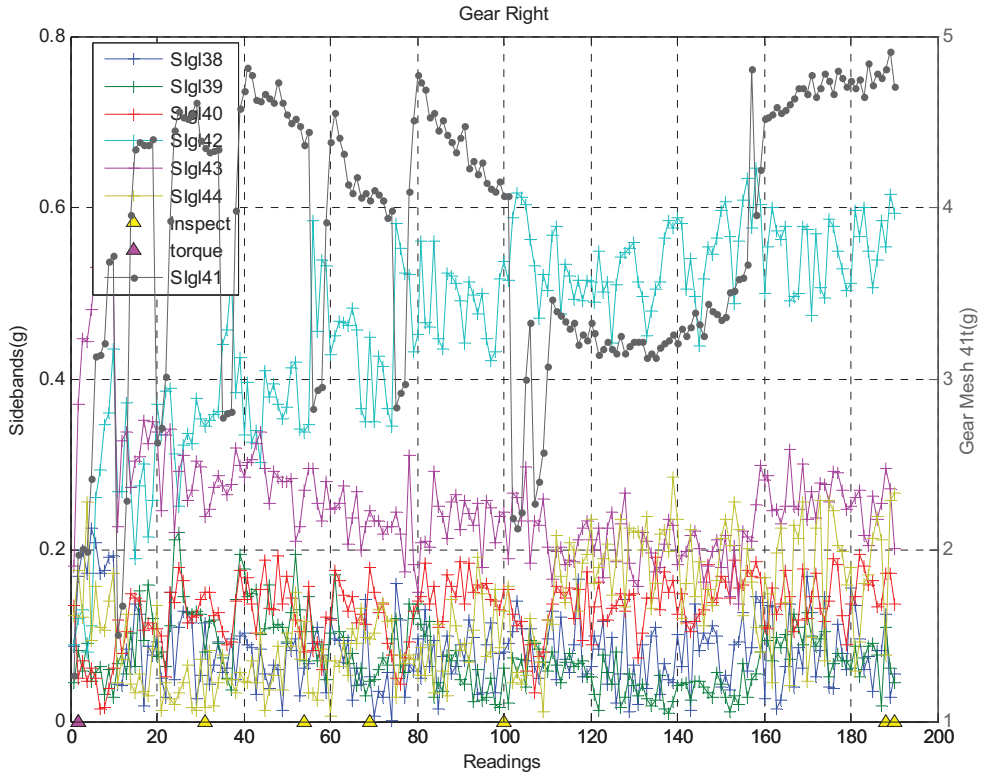

Figure B.4.10.—Test 4 plot of right gear individual sidebands for MSPU.

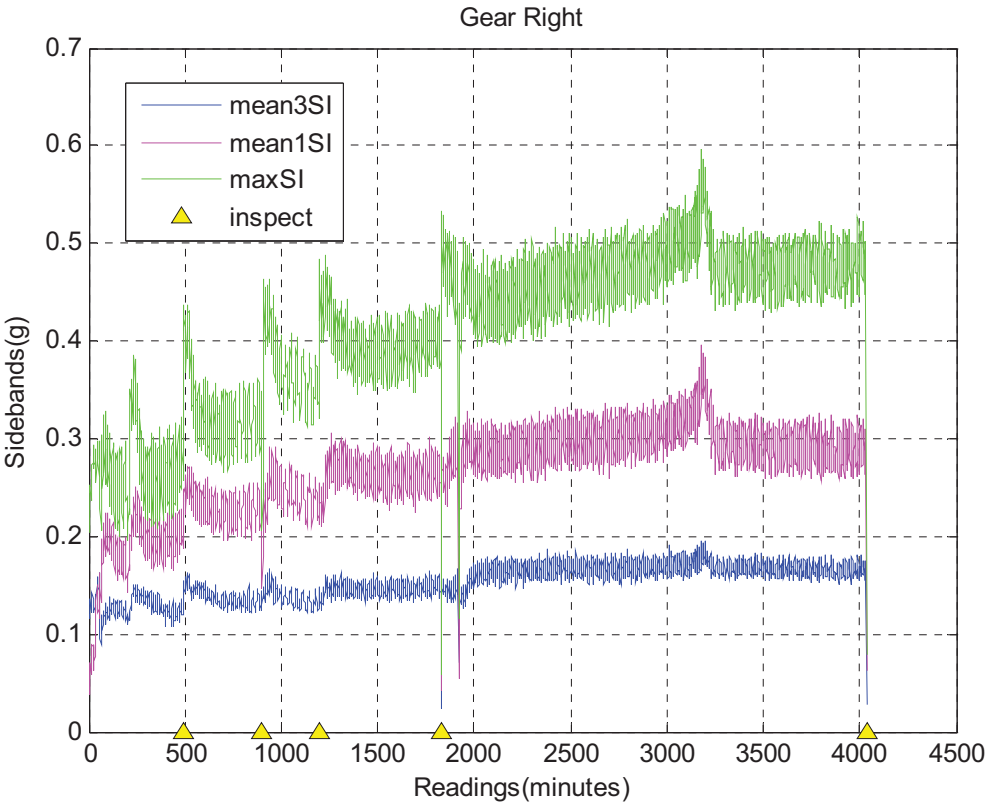

Figure B.4.11.—Test 4 plot of right gear average and maximum sidebands for MDSS.

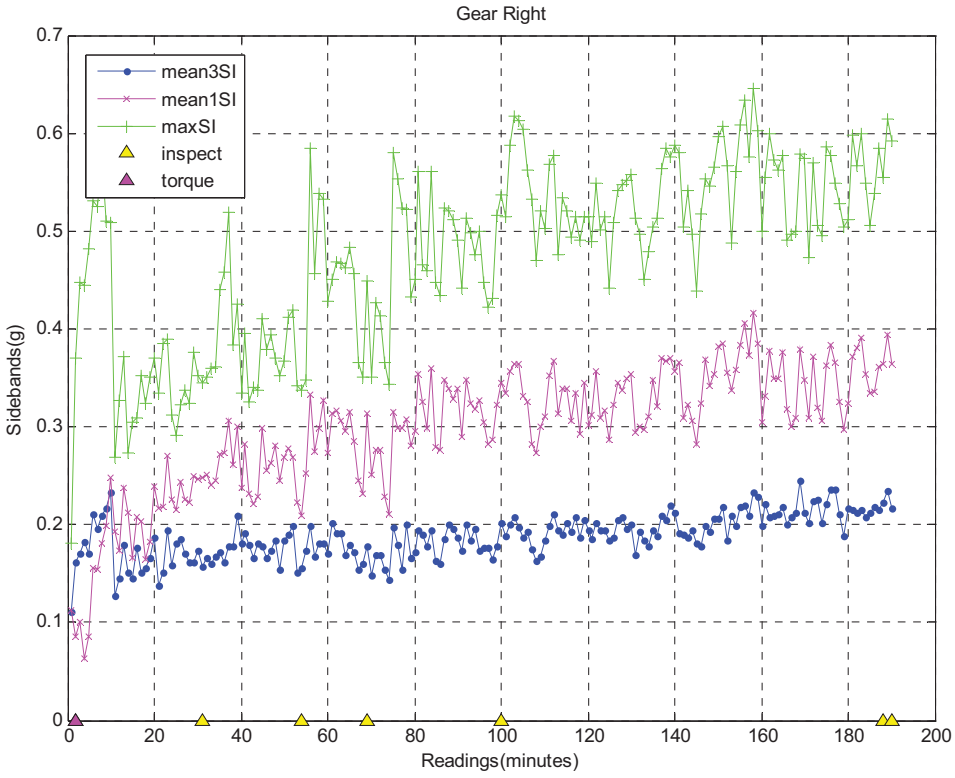

Figure B.4.12.—Test 4 plot of right gear average and maximum sidebands for MSPU.

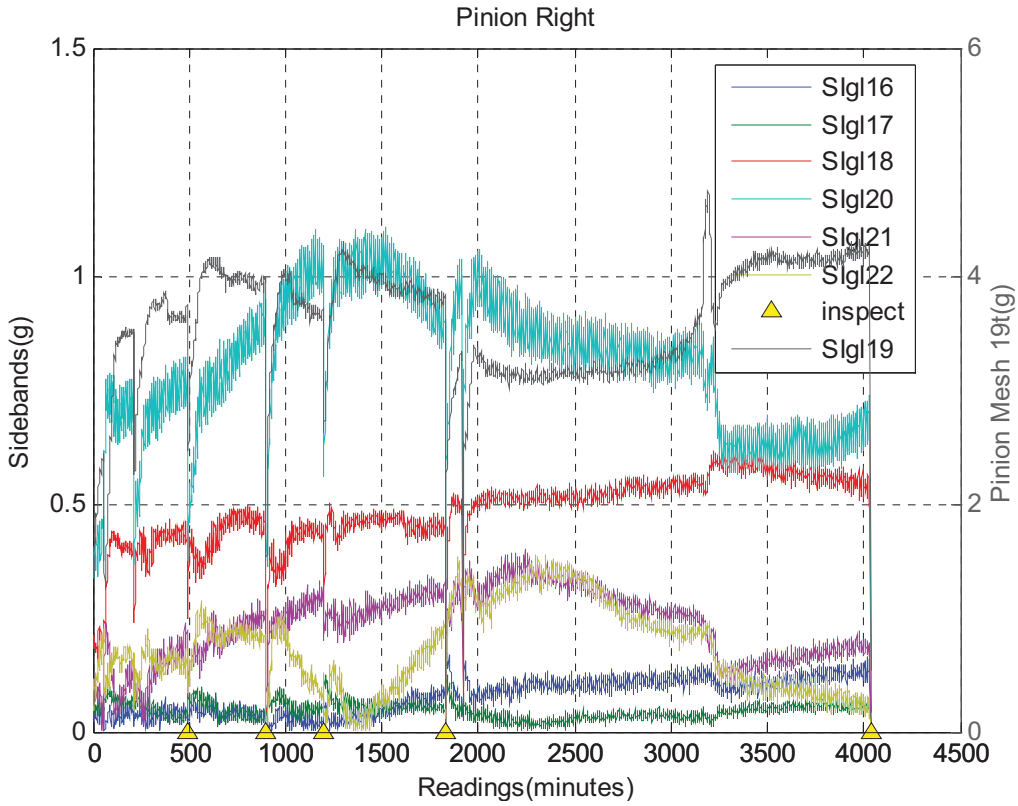

Figure B.4.13.—Test 4 plot of right pinion individual sidebands for MDSS.

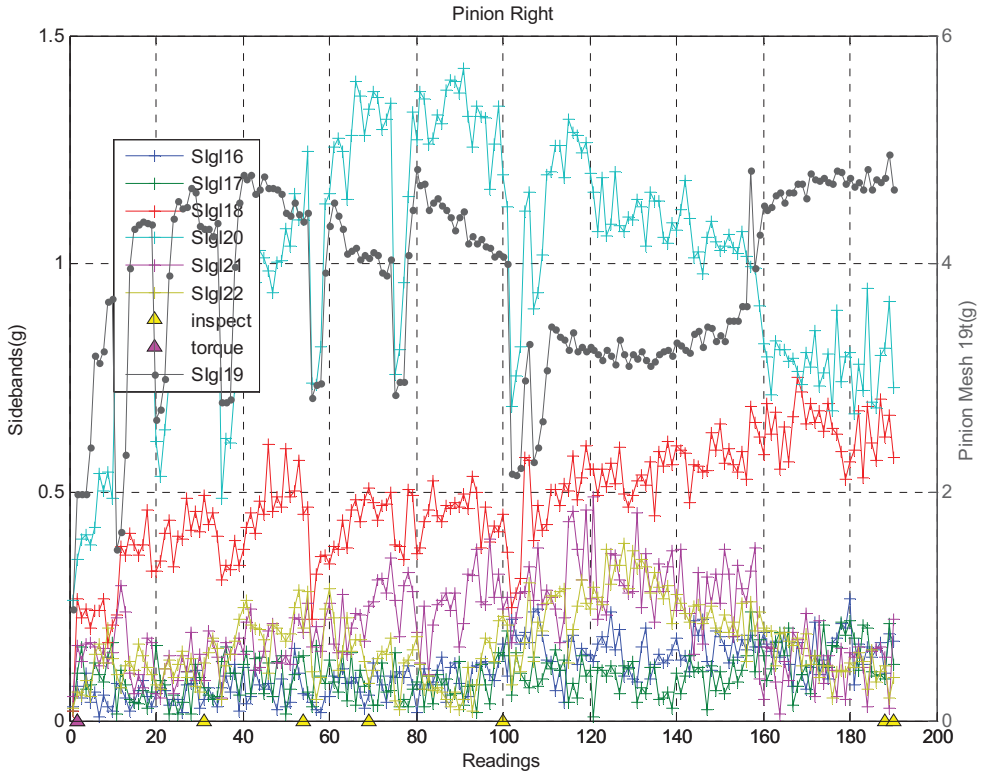

Figure B.4.14.—Test 4 plot of right pinion individual sidebands for MSPU.

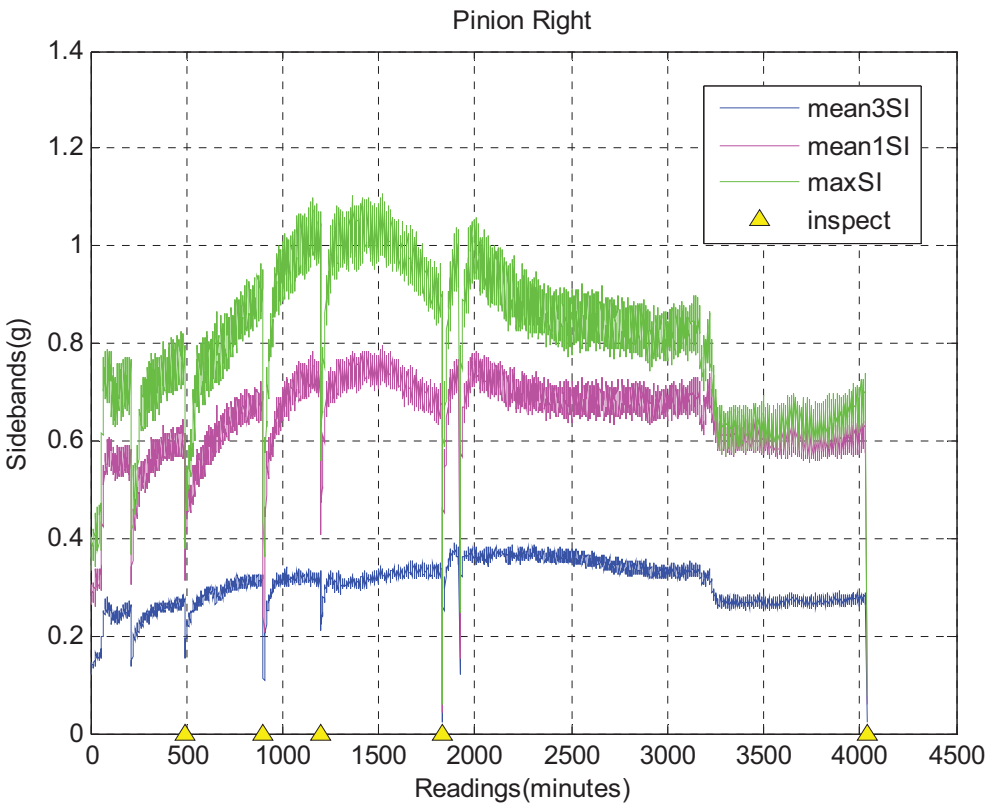

Figure B.4.15.—Test 4 plot of right pinion average and maximum sidebands for MDSS.

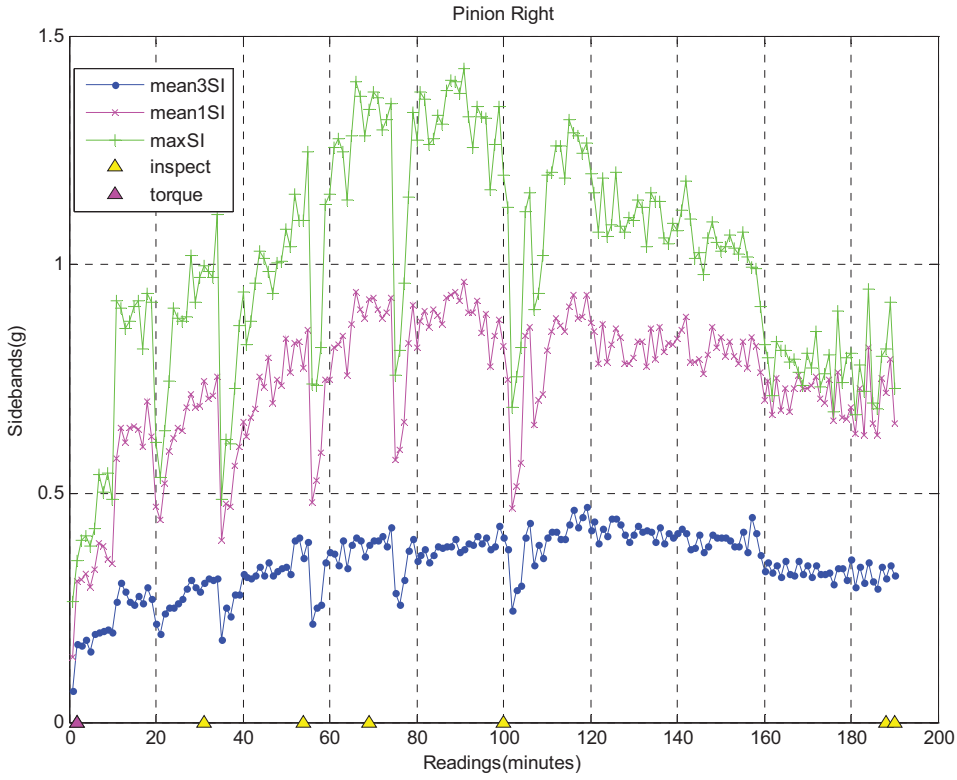

Figure B.4.16.—Test 4 plot of right pinion average and maximum sidebands for MSPU.

Appendix C.—Summary of Test Operational Data Averaged Within Each Inspection Period

Table C.1: Daytronic Operational Parameters

NAME	MEASUREMENT DESCRIPTION
LOI	TC #2, LOI, Left side oil inlet
LOO	TC #3, LOO, Left side oil outlet
Lchg	LOI-LOO
ROI	TC #12, ROI, Right side oil inlet
ROO	TC #13, ROO, Right side oil outlet
Rchg	ROI-ROO
Gear torque	Gear torque
Pinion torque	Pinion torque
Gear rpm	Gear speed
Pinion rpm	Pinion speed
Lpsi	Left side oil inlet pressure
Rpsi	Right side oil inlet pressure

Table C.2: Average Operational Parameter Values for Test 1

Rdg(min)	LOI	LOO	Lchg	ROI	ROO	Rchg	Gear torque	Pinion torque	Gear rpm	Pinion rpm	HP	Lpsi	Rpsi
269	235	184	51	235	183	52	5079	2354	3063	6609	247	79	70
553	247	201	45	247	197	49	7732	3583	3507	7567	430	67	60
1862	245	195	50	245	194	52	7895	3659	3503	7559	439	63	54
4814	246	205	41	246	201	45	7888	3655	3510	7573	439	71	63
6065	250	203	47	250	200	50	7938	3679	3507	7568	442	62	55

Table C.3: Average Operational Parameter Values for Test 2

Rdg(min)	LOI	LOO	Lchg	ROI	ROO	Rchg	Gear torque	Pinion torque	Gear rpm	Pinion rpm	HP	Lpsi	Rpsi
108	248	207	41	248	206	42	3869	1793	3503	7560	215	61	58
379	252	216	35	252	215	36	6439	2984	3469	7486	354	71	65
559	262	210	53	263	210	53	5843	2708	3497	7545	324	42	38
662	251	204	48	252	204	48	4927	2283	3502	7557	274	45	75

Table C.4: Average Operational Parameter Values for Test 3

Rdg(min)	LOI	LOO	Lchg	ROI	ROO	Rchg	Gear torque	Pinion torque	Gear rpm	Pinion rpm	HP	Lpsi	Rpsi
184	250	209	41	251	210	41	4917	2279	3501	7555	273	52	49
520	255	219	36	256	221	35	6836	3168	3500	7553	380	52	55
686	253	216	37	255	218	36	7834	3630	3501	7554	435	52	52

Table C.5: Average Operational Parameter Values for Test 4

Rdg(min)	LOI	LOO	Lchg	ROI	ROO	Rchg	Gear torque	Pinion torque	Gear rpm	Pinion rpm	HP	Lpsi	Rpsi
60	249	207	41	250	210	40	4986	2311	3500	7553	277	54	53
489	254	218	36	255	220	35	5851	2712	3501	7554	325	54	53
901	255	219	36	256	221	35	5808	2691	3501	7554	323	56	53
1196	254	217	36	255	220	35	5827	2700	3501	7554	324	56	53
1829	247	210	37	248	212	36	5950	2757	3501	7555	331	59	58
4034	256	223	33	257	225	32	5954	2759	3500	7553	331	59	56

References

1. Delgado, Irebert; Dempsey, Paula; Antolick, Lance and Wade, Dan: Continued Evaluation of Gear Condition Indicator Performance on Rotorcraft Fleet. Airworthiness, CBM, and HUMS Specialists' Meeting, February 11-13, 2013, Huntsville, Alabama.
2. Evaluation of Gear Condition Indicator Performance on Rotorcraft Fleet, Antolick, Lance; Branning, Jeremy; Dempsey, Paula; Wade, Daniel. 66th American Helicopter Society International Annual Forum 2010, Phoenix, AZ. 11-13 May 2010.
3. Handschuh, R.F.: Thermal Behavior of Spiral Bevel Gears. NASA TM-106518, 1995.
4. Handschuh, R.F.: Testing of Face-Milled Spiral Bevel Gears at High-Speed and Load. NASA/TM—2001-210743, 2001.
5. Feldman, J. and Larsen, C.: Bevel Gear Test Rig Transfer Path Measurements. Etegent Technologies Contract Report prepared for NASA Glenn Research Center. June 2013.
6. Stewart, R.M. 1977. Some useful data analysis techniques for gearbox diagnostics. Machine Health Monitoring Group, Institute of Sound and Vibration Research, University of Southhampton, Report MHM/R/10/77, July 1977.
7. Zakrajsek, J.J. 1989. An investigation of gear mesh failure prediction techniques. NASA TM–102340, AVSCOM TM 89–C-005.
8. Zakrajsek, J.J., Handschuh, R.F., and Decker, H.J. 1994. Application of fault detection techniques to spiral bevel gear fatigue data. Proceedings of the 48th Meeting of the Mechanical Failures Prevention Group. Office of Naval Research, Arlington, Virginia, pp. 93–104.
9. ANSI/AGMA 1010-E95. Appearance of Gear Teeth – Terminology of Wear and Failure.
10. Randall, R.B., "A New Method of Modelling Gear Faults," Journal of Mechanical Design, Vol. 104, pp. 259-267, April 1982.
11. Manson, Graeme. Lecture 5 – Hierarchy of Damage Identification. University of Sheffield. Accessed 04/22/13. http://www.dynamics.group.shef.ac.uk/people/graeme/mec415/Lecture5.pdf.
12. U.S. Army Aeronautical Design Standard for Condition Based Maintenance, ADS79 Handbook. August 2012.
13. Dempsey, P.J. Zakrajsek, J.J., "Minimizing Load Effects on NA4 Gear Vibration Diagnostic Parameter," NASA/TM—2001-210671, February 2001.
14. Mosher, M.M., Pryor, Huff. E.M., "Evaluation of Standard Gear Metrics in Helicopter Flight Operation," Proceedings of the 56th Meeting of the Society for Machinery Failure Prevention Technology, April 15–19, 2002, Virginia Beach, Virginia.
15. Dempsey, P.J., Lewicki, D.G., and Le, D.D., Investigation of Current Methods to Identify Helicopter Gear Health. NASA/TM—2007-214664. Presented at the IEEE Aerospace Conference. Big Sky, Montana, March 3–10, 2007.
16. Dempsey, P.J., Branning, J.S., Wade, D.R. and Bolander, N., Comparison of Test Stand and Helicopter Oil Cooler Bearing Condition Indicators. Proceedings of the American Helicopter Society 66th Annual Forum, Phoenix, Arizona, May 11-13, 2010.

17. Dempsey, P.J., Mosher, M.M. and Huff, E.M., "Threshold Assessment of Gear Diagnostic Tools on Flight and Test Rig Data," NASA/TM—2003-212220, February 2003a.
18. Huff, E.M., Tumer, I.Y., Barszcz, E., Dzwonczyk, M., and McNames, J., An Analysis of Maneuvering Effects on Transmission Vibrations in an AH-1 Cobra Helicopter, J. of American Helicopter Society, Vol. 47, No. 1, 2002.
19. Oza, N.C., Tumer, K., Tumer, I.Y. and Huff, E.M., Classification of Aircraft Maneuvers for Fault Detection, Proceedings of the 4th Intl Workshop on Multiple Classifier Systems, Guildford, Surrey, UK, June 11-13, 2003.
20. Dempsey, P., Handschuh, R. and Delgado, I.: Integrating Condition Indicators and Usage Parameters for Improved Spiral Bevel Gear Health Monitoring. 66th American Helicopter Society International Annual Forum 2013, Phoenix, AZ. 21-23 May 2013.
21. Triola, Mario. Elementary Statistics. 6th edition. Addison-Wesley 1995.